LinCom

FINAL REPORT

AUTOMATIC PHASE CONTROL IN SOLAR POWER SATELLITE SYSTEMS

Prepared for

JOHNSON SPACE CENTER
Houston, TX 77058

Technical Monitor: Jack Seyl

Prepared Under Contract NAS 9-15237

Prepared by

W. C. Lindsey
A. V. Kantak

LINCOM CORPORATION
P. O. Box 2793D
Pasadena, CA 91105

February 15, 1978

TR-7802-0977

LinCom

Page Intentionally Left Blank

Slave (MS), (2) Mutual Synchronous Configuration (MSC), (3) Returnable Timing (RTC), (4) Equational Timing (ETC), (5) Hierarchial Master Slave 1 (HMS1) and 2 (HMS2).

In addition to studing the problem of phase control from the viewpoint of having the PAs operate in unison, the problem of beam steering by the methods of phase conjugation and by Ground Control is addressed. For the phase conjugation method the effects of frequency separation (required to isolate the up and downlink signals) is addressed. The beam pointing error is quantified and evaluated as a function of subarray coordinates, angles of arrival of the transmitted pilot, frequency offset and antenna flexing. A system employing phase conjugation is suggested which corrects for pointing error due to frequency separation. The method of beam steering via ground control is discussed in principle and preliminary comparisons of the phase conjugation method with the ground control method is discussed from the viewpoint of media stability, power robbing, security and jamming. Additional work is currently being performed.

ACKNOWLEDGEMENT

The authors wish to acknowledge the discussions held with Mr. Jack Seyl and Dr. G. D. Arndt of the Johnson Space Center and for providing us with various articles of interest. In addition, the support and encouragement of Mr. R. H. Dietz and Mr. R. O. Piland of the Johnson Space Center is greatly appreciated.

TABLE OF CONTENTS

	Page
SUMMARY	1
1.0 INTRODUCTION	3
2.0 SPSS PHASE CONTROL APPROACHES	8
2.1 SPS Retrodirective Self-Focusing by Phase Conjugation (Ref. 2)	10
2.2 SPS Feedback Control Via Ground Telemetry and Command (Ref. 3)	10
2.3 SPS Hybrid Phase Control Method	13
3.0 FUNDAMENTALS OF REFERENCE PHASE DISTRIBUTION AND CONTROL	15
3.1 Master Slave nonfiguration for Connecting the PCCs	19
3.1.1 Mathematical Model for Master Slave Configuration	19
3.2 Mutual Synchronous Configuration for Connecting the PCCs	22
3.2.1 Mathematical Model for the Mutual Sync Configuration	25
3.2.1.1 A Special Case of Two and Three PCCs	28
3.3 Hierarchial Master-Slave Mutual Sync Configuration	34
3.3.1 Comparison of the Master Slave and Mutual Sync Configurations	34
4.0 DELAY COMPENSATION TECHNIQUES	37
4.1 Returnable Timing Configuration (RTC)	37
4.1.1 Mathematical Model of the Returnable Timing Configuration	38
4.1.1.1 Two PCCs Connected in RTS	40
4.2 Master Slave Returnable Timing System Hybrid Configuration (MSRTC)	43
5.0 COMPARISON OF PHASE CONTROL TECHNIQUES	48

TABLE OF CONTENTS (Continued)

		Page
	5.1 Phase Noise Analysis	53
6.0	SUBARRAY LAYOUT	57
	6.1 The Square Geometry	57
	6.2 Rectangular Geometry	57
7.0	LOCATION OF THE PHASE CONTROL CENTERS ON THE SPS	63
	7.1 Positioning of the PCCs	66
8.0	APPLICATION OF PHASE CONTROL FUNDAMENTALS TO SPS ANTENNA PHASE CONTROL	69
	8.1 Master Slave Phase Control	69
	8.2 Hierarchial Master Slave Phase Control on Groups of Four	69
	8.3 Hierarchial Master Slave Phase Control in Groups of 4^n	72
	8.4 Master Slave Returnable Timing System Hybrid Configuration	74
9.0	SYMMETRY REQUIREMENT AND PHASE BUILD UP	78
10.0	PHASING OF THE POWER AMPLIFIERS	86
11.0	ANTENNA BEAM STEERING	95
	11.1 On-Board Phase Control and Beam Steering via Phase Conjugation	95
	11.1.1 Frequency Separation and Beam Pointing	97
	11.1.2 Calculations of Phase Shifts Necessary	102
	11.1.3 Effect on Pointing Due to Measurement Error in the Position	104
	11.2 SPS Beam Forming and Steering via Ground Station	109
12.0	POWER TRANSMISSION EFFICIENCY CALCULATION	118
	12.1 Problem Formulation	118
	12.2 Two Frequency Technique for Retrofire Arrays	124
	REFERENCES	125

AUTOMATIC PHASE CONTROL IN SOLAR POWER SATELLITE SYSTEMS

W. C. Lindsey
A. V. Kantak

SUMMARY

This final report presents the results found during a nine month study of the SPS Phase Control problem. Various approaches to the problem of generating, maintaining and distributing a coherent, reference phase signal over a large area are suggested, mathematically modeled and analyzed with respect to their ability to minimize: phase build-up, beam diffusion and beam steering phase jitter, cable length and maximize power transfer efficiency. In addition, phase control configurations are suggested which alleviate the need for layout symmetry.

In order to minimize the required cable length, phase build-up, beam diffusion and phase jitter, Phase Control Centers (PCCs) are introduced and special layouts (including the square, hexagonal and rectangular) are suggested. For the current design, it is shown that 1364 PCCs are required plus one master PCC. This leads to the philosophy of using the reference phase generated at each Terminal PCC to phase control the power amplifiers (PAs) located in the individual subarrays.

Configurations for interconnecting the PCCs and the PAs are suggested so as to minimize cable length, phase build-up, beam diffusion and phase jitter. The phase control configurations suggested, mathematically modeled and analyzed include: (1) Master

Slave (MS), (2) Mutual Synchronous Configuration (MSC), (3) Returnable Timing (RTC), (4) Equational Timing (ETC), (5) Hierarchial Master Slave 1 (HMS1) and 2 (HMS2).

In addition to studing the problem of phase control from the viewpoint of having the PAs operate in unison, the problem of beam steering by the methods of phase conjugation and by Ground Control is addressed. For the phase conjugation method the effects of frequency separation (required to isolate the up and downlink signals) is addressed. The beam pointing error is quantified and evaluated as a function of subarray coordinates, angles of arrival of the transmitted pilot, frequency offset and antenna flexing. A system employing phase conjugation is suggested which corrects for pointing error due to frequency separation. The method of beam steering via ground control is discussed in principle and preliminary comparisons of the phase conjugation method with the ground control method is discussed from the viewpoint of media stability, power robbing, security and jamming. Additional work is currently being performed.

1. INTRODUCTION

This interim report presents the results obtained during the six months study associated with the Solar Power Satellite System (SPSS) Phase Control and Beam Pointing Problems. In accordance with previous documentation,the SPSS consists of a geosynchronous satellite at an altitude of 37000 km., the main purpose of which is to collect the solar power, condition it for transmission and then transmit it to the ground. Design of the SPSS can be divided into three major areas (see Figure 1):

(1) Design of the Power Conversion System to convert the solar power into electrical power,

(2) Design of the Power Transmission System which beams the power down to the ground via microwave transmission, and

(3) Design of the Ground Based Rectenna System which collects the microwave power radiated from the Solar Power Satellite (SPS) and conditions it for distribution.

Currently the transmitting antenna on the SPS is conceived to be a phased array having an area of a 1 km. diameter circle. It consists of slotted waveguide subarrays which are fed by the power amplifier tubes. The radiated beam is phase controlled so as to direct the beam to the ground based receiving antenna (rectenna).

This study is concerned with problems associated with the design of the Power Transmission System using mathematical modeling and analytical simulation techniques. The central design problem which this study addresses is that of Phase Control, i.e., controlling the

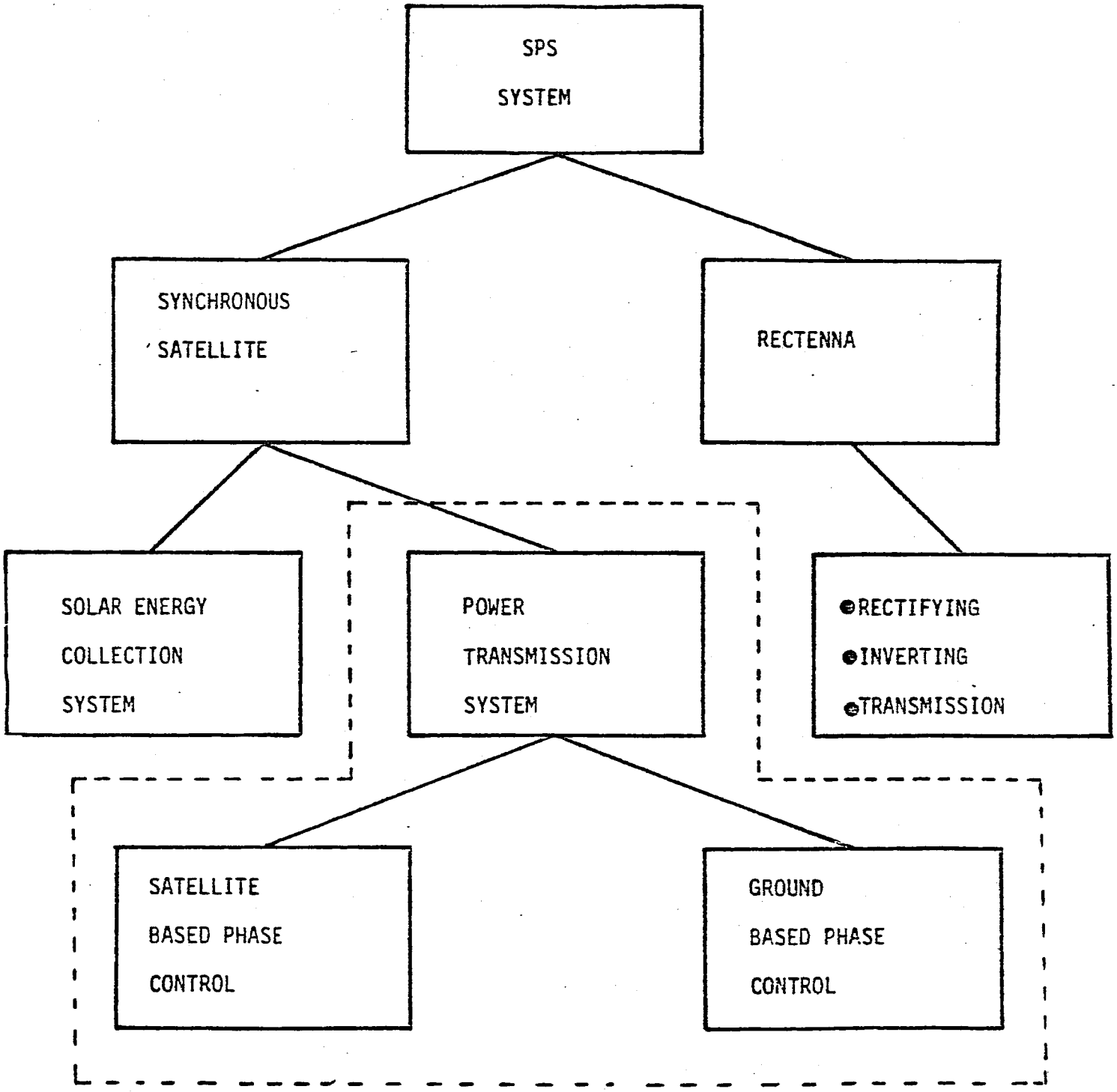

Figure 1. SPS System.

phase of the power amplifier output signals over the large transmitting antenna so that a coherent beam is formed and properly pointing toward the rectenna. LinCom believes that the phase control problem is best addressed by subdividing it into three problem areas. These include:

(1) Design of the Reference Phase Control Distribution System.

(2) Phase Control of the Power Amplifiers.

(3) Beam Steering Control.

A tight (coherent) phase control in each of these areas is essential because the phase errors introduced contribute individually to deflection of the transmitted beam from the intended target (the ground based rectenna) and thereby reduces the power transmission efficiency. There is, however, another reason for tight (coherent) phase control and that is the phase jitter present in the reference phase distribution system (due to ionospheric effects, oscillator instabilities, and the power amplifier phase control system, etc.) results in lower main beam gain and increased beamwidth conseqeuntly lowering the power transmission efficiency.

Phase Control, as applied to the SPS antenna, is considerably different from existing antenna phasing problems because of the huge size of the antenna, the number of power amplifiers involved, and the complete automation desired in its operation. To date, it appears that phase control has not been demonstrated when several thousnad power amplifiers are required to operate in unison.

In this study various techniques for generating,distributing and maintaining a constant phase and frequency reference over a large area and for controlling the phases of the power amplifiers are postulated and studied. They include systems employing: (1) A Master Slave Configuration, (2) Mutual Synchronous Configuration, (3) Returnable Phase (Timing) Configurations, (4) Equational Phase (Timing) Configuration and (5) Hybrid Configurations. Except for the master slave case, the configurations are designed to introduce coupling between the oscillations being distributed so that a highly stable and coherent transmitted beam is achieved. In addition, these phase control configurations are designed to reduce the phase noise in the oscillation sidebands through spectral line narrowing due to the nonlinear coupled oscillations generated with close frequencies (Ref. 1). Distribution of reactively coupled oscillations over a large aperture is accompanied by phase jumps due to various system noise components and disturbances. Such phase jumps lead to the problem of interruptions or failures in the distributed phase reference causing the spectral line of the transmitted signal to be degraded through the process of phase diffusion. Analysis of the spectrum can be found from the solution of a set of coupled nonlinear stochastic integro-differential equations. Section 4 of this report introduces, describes and develops mathematical models for the various techniques of distributing a constant phase characteristic over the aperture of a large antenna.

To minimize cable length requirements , phase error build-up, beam phase jitter and diffusion, LinCom's proposed solution to be phase control problem requires the introduction

of Phase Control Centers (PCCs) geometrically distributed over the transmitting antenna aperture. In order to minimize the cable length required to interconnect the phase control centers, it is found that the transmitting antenna will consist of approximately 1365 PCCs. Layout of these phase control centers is also treated in this report. It is also shown that PCC layout is intimately connected with the shape of the antenna. This layout determines the amount of cable length required. Three different PCC layouts are considered in Section 7. They are the rectangular, square and hexagonal layouts. The same section also discusses the symmetry requirements for the reduction of cable length necessary for a constant reference phase distribution system. Finally, a phase control method which does not depend upon the individual phase-center locations is suggested.

In Section 10, the important problem of phase build-up is addressed quantitatively. LinCom believes that phase build-up and beam jitter are extremely important since the power transmission efficiency is highly dependent on these performance degrading effects. Therefore, considerable energy has been devoted to mathematically characterizing phase build-up and relating it to power transmission efficiency. Further work is proceeding in this area.

The next problem addressed in this report is that of beam steering or pointing. Once a constant phase reference is distributed over the entire aperture of the antenna and the power amplifiers phased, beam pointing can be accomplished by one of three methods. These are: (1) On-board phase control

for beam steering using the retrodirective active phased array concept (Ref.2,3), (2) SPS beam forming and steering via ground control (Ref.4), and (3) A hybrid of methods one and two. The retrodirective method requires that a pilot tone be transmitted from the center of the antenna on the ground. With this approach the problem of isolating the up-link from the down link manifests itself. Section 11 discusses this problem and investigates ways of alleviating it. On the other hand, the ground based phase control scheme needs a large amount of sensors distributed over the rectenna area and it also needs equipment for processing the signals. Section 11 also describes the method of operation of this system and a mild comparison of this scheme with the retrodirective scheme is made.

2.0 SPSS PHASE CONTROL APPROACHES

Three approaches to SPSS phase control have been considered, see Fig. 2. These include:

(1) Phase Control via Satellite Processing.

(2) Phase Control via Ground Station Processing.

(3) Phase Control via Hybrid of Above Two Approaches.

In any of the approaches it is desirable to form a narrow microwave beam and accurately point it to the receiving rectenna. To form this narrow beam we need not only to distribute a constant phase and frequency but also to maintain and control the phases of the power amplifiers. The signal, radiated by each transmitting element, has a phase that is the function of the phase distributed by the phase distribution system and the phase of the power amplifier feeding a particular element. If we

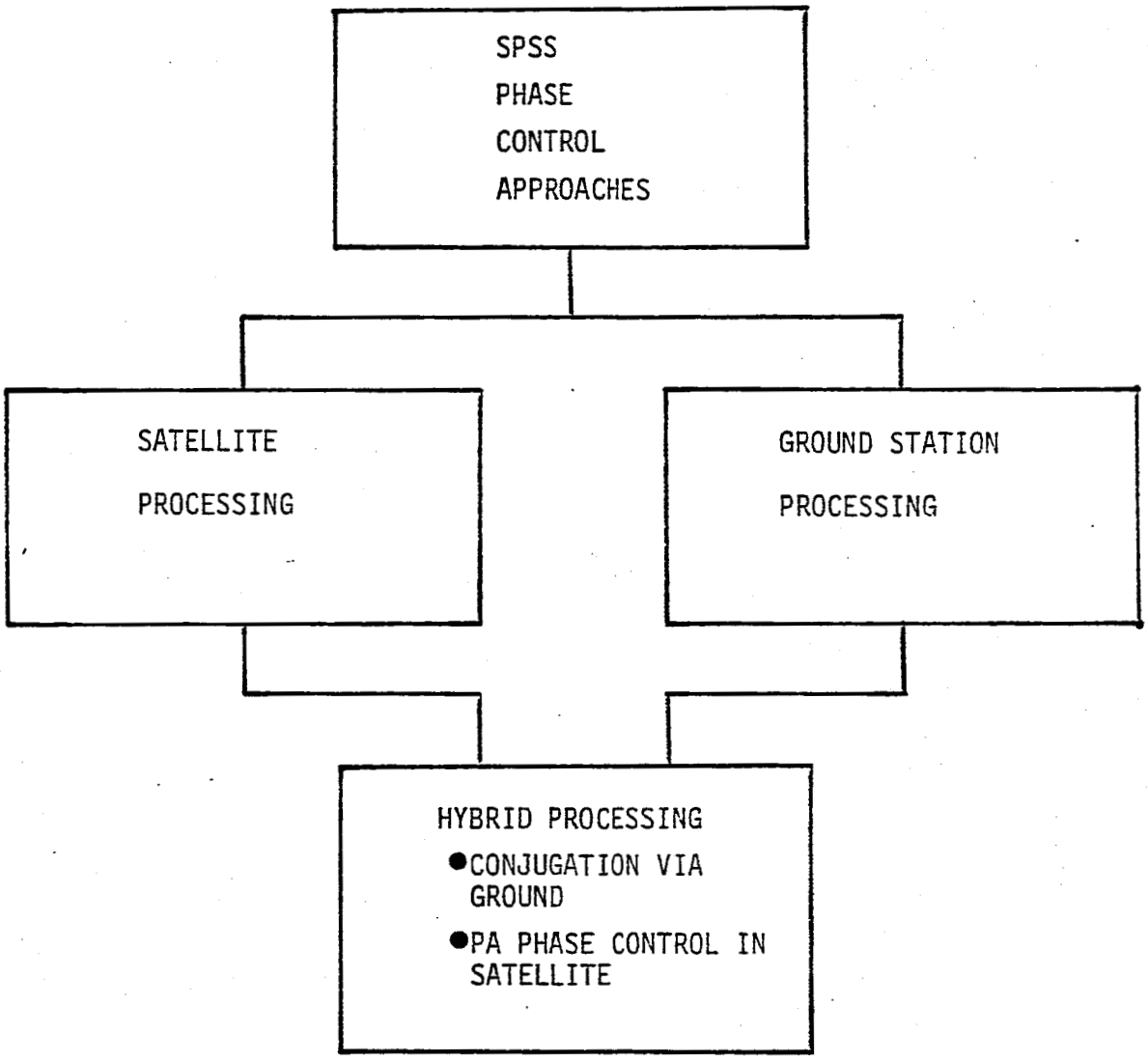

Figure 2. Conceptual Approach to SPS Phase Control.

model each signal as a vector having magnitude and phase, then the purpose of the phase distribution system is to phase align all the signal vectors and point the resultant vector to the center of the rectenna. In what follows we qualitatively discuss three approaches of distributing a constant phase reference and use this reference to control the power amplifier output phases.

2.1 SPS Retrodirective Self-Focusing by Phase Conjugation

The retrodirective self focusing feature of the antenna can be implemented using two different techniques: (1) The single frequency technique and (2) the two frequency technique.

2.1.1 Single Frequency Retrodirective Self Focusing Technique

In this approach, a pilot signal from the rectenna center illuminates the SPS transmitting antenna. The pilot phase received by the central subarray of the SPS antenna is distributed via the reference phase distribution/power amplifier control system to the phase conjugation circuits. The purpose of the phase conjugation circuits is to conjugate the phase of the incoming pilot signal received by eahc radiating element. By the property of retrodirectivity, the radiated signal will be reflected back to the rectenna. This approach is plagued with the problem of frequency separation, i.e., the isolation of the uplink from the downlink signal thus introducing the beam squint problem. This beam squint problem basically is the deflection of the radiated power beam from the pilot source direction which introduces a loss in power transmission efficiency. The solution to this problem is to introduce proper phase shifts in the currents feeding the radiating elementsof the antenna. Section 11 discusses this problem and also gives a solution. The solution mainly consists of having an onboard computer to compute the phase shifts necessary for the currents feeding each element or a group of elements. The main problem with this system is that depending upon the angle of arrival of the pilot beam, the phase shifts necessary to correct for the beam deflection due to frequency separation become so small (of the order

of several minutes of arc) that the system is not practical to implement with current phase shifter technology. The two frequency approach described below circumvents this difficulty.

2.1.2 Two Frequency Retrodirective Self Focusing

In this system, suggested by LinCom, the uplink pilot signal consists of two tones,one at $\Delta\omega$ radians/sec above the nominal pilot tone at ω_0 and the other $\Delta\omega$ below the nominal tone at ω_0. The phases of these two tones are sensed at the SPS antenna elements. The phases are averaged and then the conjugate of this averaged phase is used to radiate the power beam at the frequency ω_0. This radiated beam will always find the rectenna without fail as predicted by the retrodirective antenna theory. Even though the signal processing equipment increases when compared to the single frequency method, the need for the on-board computator is avoided and furthermore, there are no phase shifters necessary for the operation of the system.

Figure 3a describes the essentials of the single frequency scheme while Figure 3b depicts the two frequency scheme in terms of functional block diagram.

2.2 SPS Feedback Control Via Ground Telemetry and Command (Ref. 3)

In this approach, phase control of the transmitting antenna is transferred to the ground, see Fig. 4. On the rectenna site a huge number of sensors are distributed. Each sensor senses the incoming signal and sends it to the signal processor unit. This

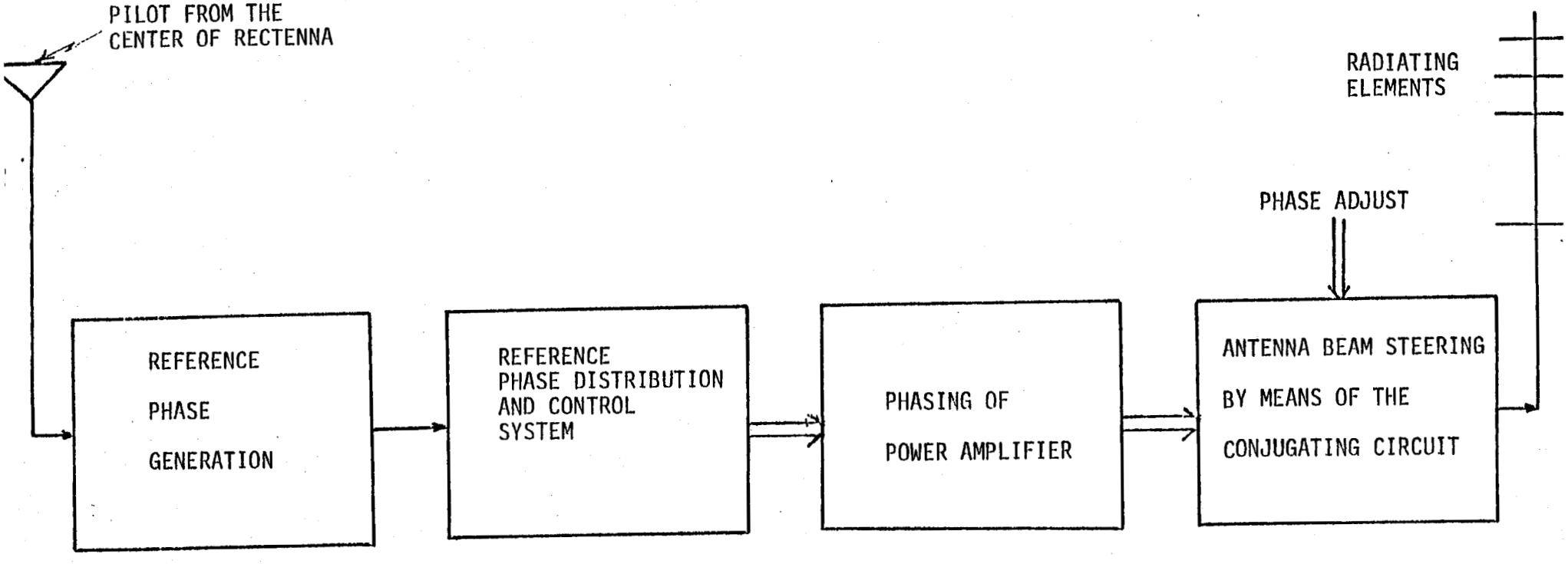

Figure 3a. SPS Retrodirective Self Focusing by Phase Conjugation (Single Frequency Scheme).

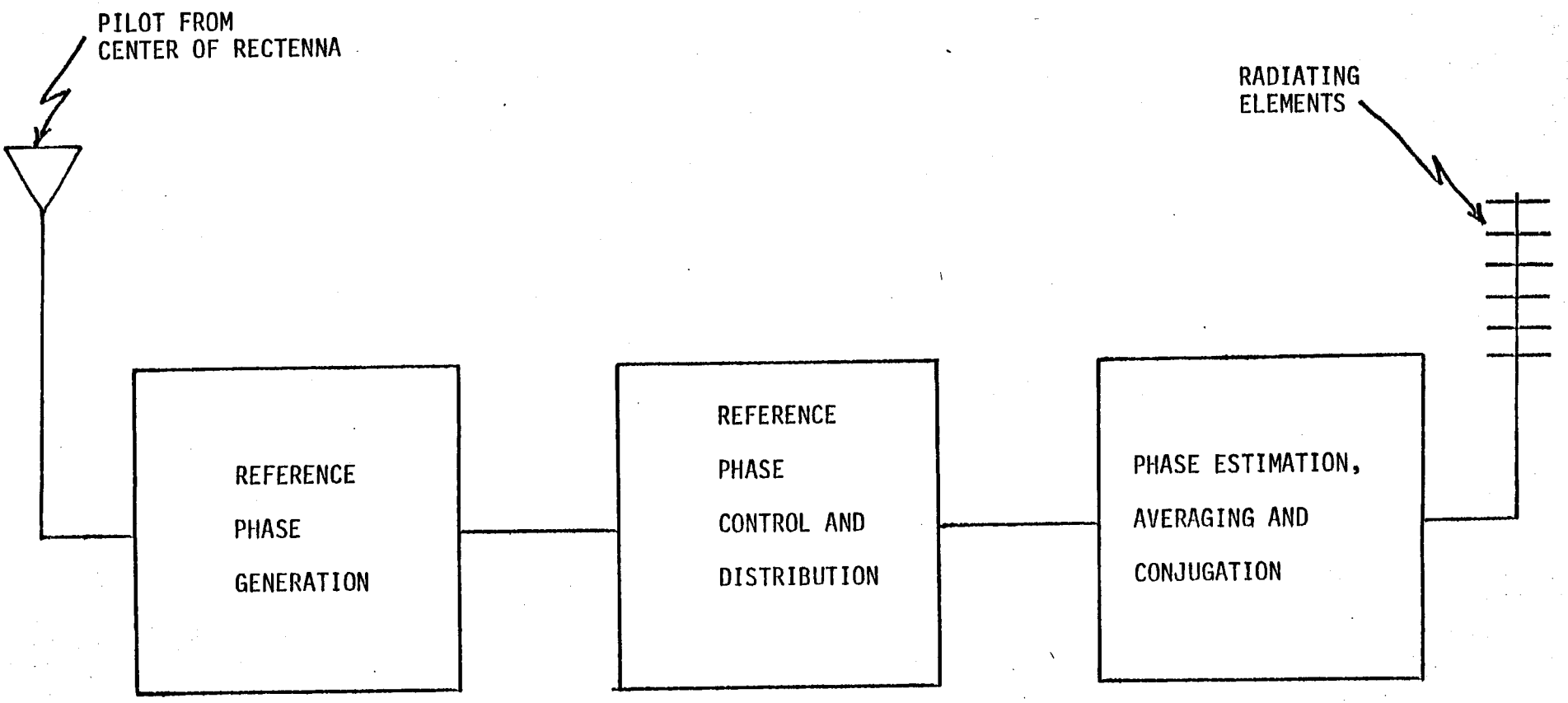

Figure 3b. SPS Retrodirective Self Focusing by Phase Conjugation. (Two Frequency Method)

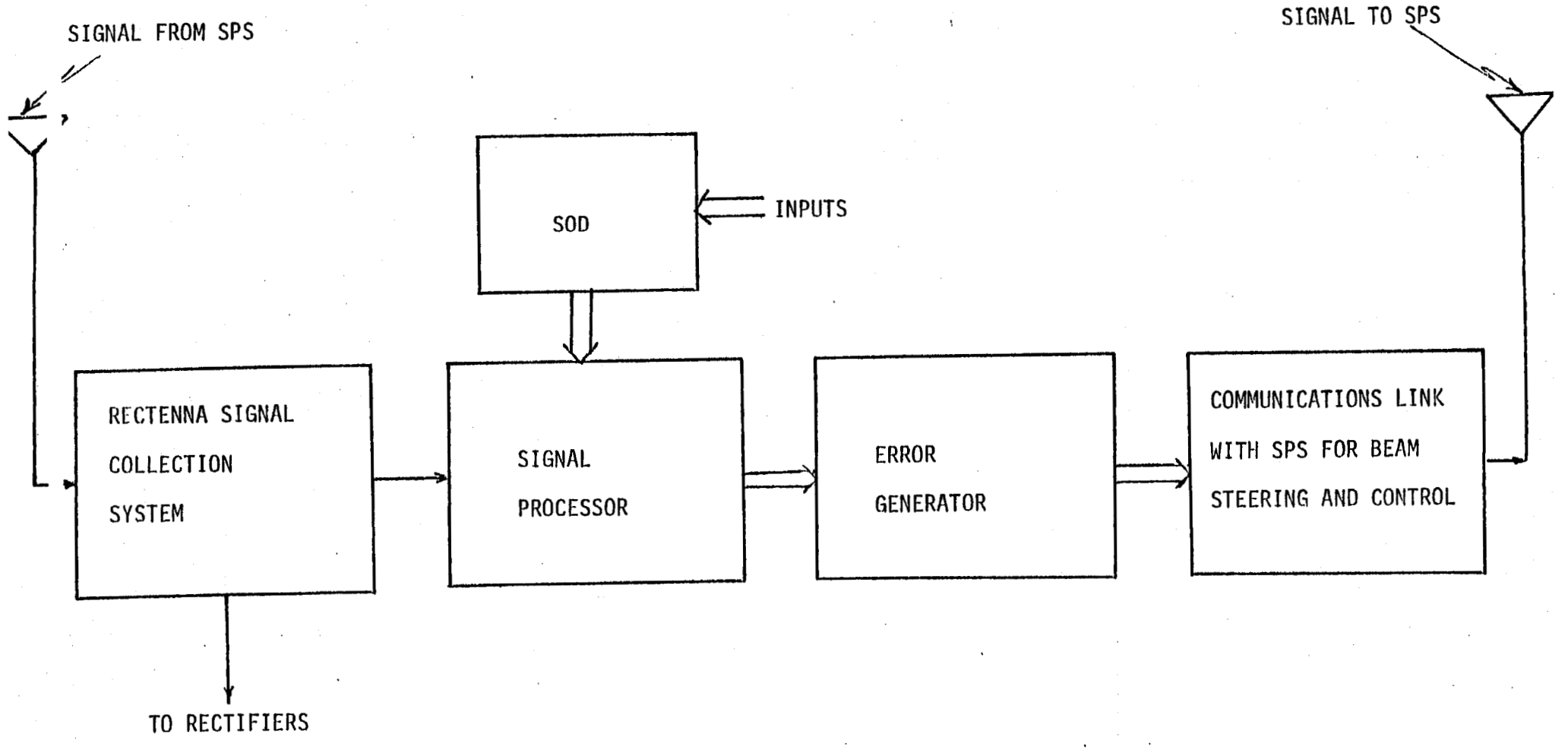

Figure 4. SPS Feedback Control Via Ground Telemetry and Command.

signal processor unit has input from the Satellite Orbit Determination computer (SOD). These inputs basically are the position coordinates of the satellite. The SOD has inputs from a properly designed ranging system. Figure 4 shows the system in block diagram form. The output of the signal processor unit is fed to the error generator unit. This unit produces the beam pointing error for each subarray in the transmitting antenna. These error values of each subarray are transmitted to the satellite via a separate communications link. The satellite feeds the proper correction voltage to each subarray which steers the beam to the correct direction. This method is fully automatic and hence no matter what causes the error in pointing the beam, the error is automatically nulled. This scheme, though more complex than the one discussed above, offers a way of securing the power transfer. All the control equipment is on the ground; hence, this configurationis easier to maintain.

2.3 SPS Hybrid Phase Control Method

This method is a hybrid of the single frequency method using retrodirective principle and the SPS feedback control via ground telemetry and command method. This method combines the good points of both the methods, i.e., it uses the retrodirective principle for automatic direction finding while all the errors in beam pointing, e.g., due to frequency separation, oscillator instability, the random errors generated by the thermal gradients and the antenna structure flexing, etc., are taken care of by the ground control processing.

Basic to all the above phase control methods is the problem of distributing and maintaining a constant phase across the aperature of the antenna and using this to shape the power amplifier outputs. In what follows, a phase control theory is presented for its application to the SPS phase control problem.

3.0 FUNDAMENTALS OF REFERENCE PHASE DISTRIBUTION AND CONTROL

The distribution of a constant phase and frequency over the entire aperture of the SPS antenna can be achieved by introducing phase control centers (PCCs) and interconnecting these centers in such a manner as to minimize cable length, phase build-up, beam phase jitter and diffusion and meet the performance and system reliability requirements. There are several ways of connecting these PCCs each giving rise to a different configuration. Configurations and their connections investigated herein include:

(1) Master Slave Configuration,

(2) Mutual Synchronous Configuration,

(3) Hierarchial Master Slave Mutual Sync Configuration,

(4) Returnable Timing Configuration

(5) Hybrid Master Slave Returnable Timing Configuration.

Each of these configurations will be described and a mathematical model characterizing the behavior and performance will be presented.* These models will be useful in performing comparisons studies and in the simulation of a baseline SPS phase control system. Before proceeding with the investigation of the configurations listed above, we should mention that the PCCs can be connected in various ways. Figure 5 illustrates alternate ways in which the PCCs can be connected. PCC connectivity is intimately related to the performance achievable by the phase control configuration and the length of cable required in its mechanization. As illustrated, PCCs can be singly, doubly, partially or fully connected.

*These five configurations are equally applicable to the power amplifier phase control problem.

Figure 5. Concept of Phase Control Center Connectivity.

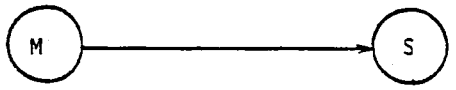

SINGLY CONNECTED
(MASTER SLAVE)

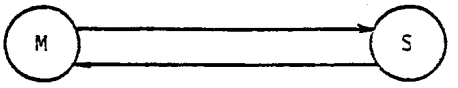

FULLY CONNECTED

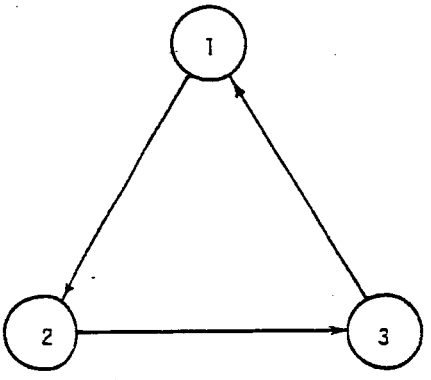

SINGLY CONNECTED

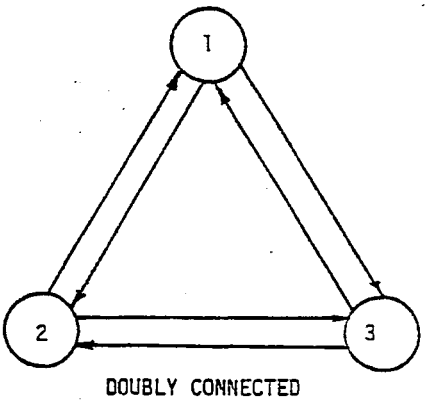

DOUBLY CONNECTED

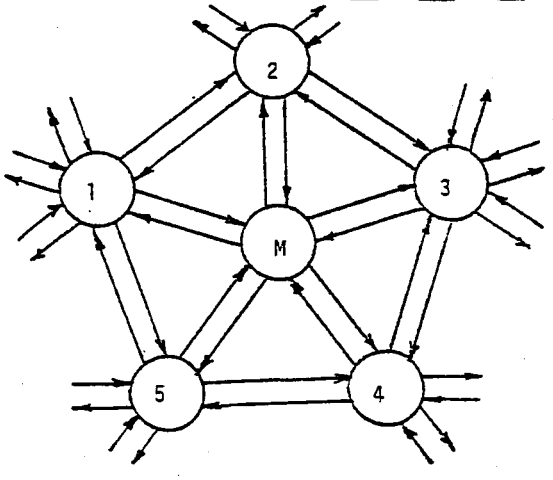

PARTIALLY CONNECTED

3.1 Master Slave Configuration for Connecting the PCCs

The master slave configuration consists of a master PCC located at the center of the antenna, see Fig. 6. This master PCC phase locks to the pilot signal received from the rectenna. The output of the master PCC is sent to the first level of slave PCCs. These slave PCCs in turn phase lock to the master PCC output and their outputs are fed to the second level of PCCs. Phase locking to the incoming signals at the second level of PCCs produces signals for transmission to the third level of PCCs. Phase locking at the third level of PCCs to the signals received from the second level of PCCs produces signals for transmission to the fourth level of PCCs. This master-to-slave-to-slave-to-slave transmission and phase locking at each level, is continued until a phase reference is distributed for use over the entire antenna aperture.

3.1.1 Mathematical Model of Master Slave Configuration

We begin by defining the phase characteristics of each PCC. Let $\Phi_M(t)$ represent the total phase of the master PCC, $\Phi_{ij}(t)$ represent the total phase of the $j^{\underline{th}}$ PCC in the $i^{\underline{th}}$ level of hierarchy of PCCs, d_{ij} represent the radian delay between the $i^{\underline{th}}$ level PCC and $j^{\underline{th}}$ level PCC under consideration, ω_{ij} represent the natural frequency of the $j^{\underline{th}}$ PCC in the $i^{\underline{th}}$ level of the PCC hierarchy, and $g_{ij}(\cdot)$ is the phase detector characteristic of the $j^{\underline{th}}$ PCC in the $i^{\underline{th}}$ level. With all these quantities we can write down the equation of operation for the first level of PCC slaves, i.e.,

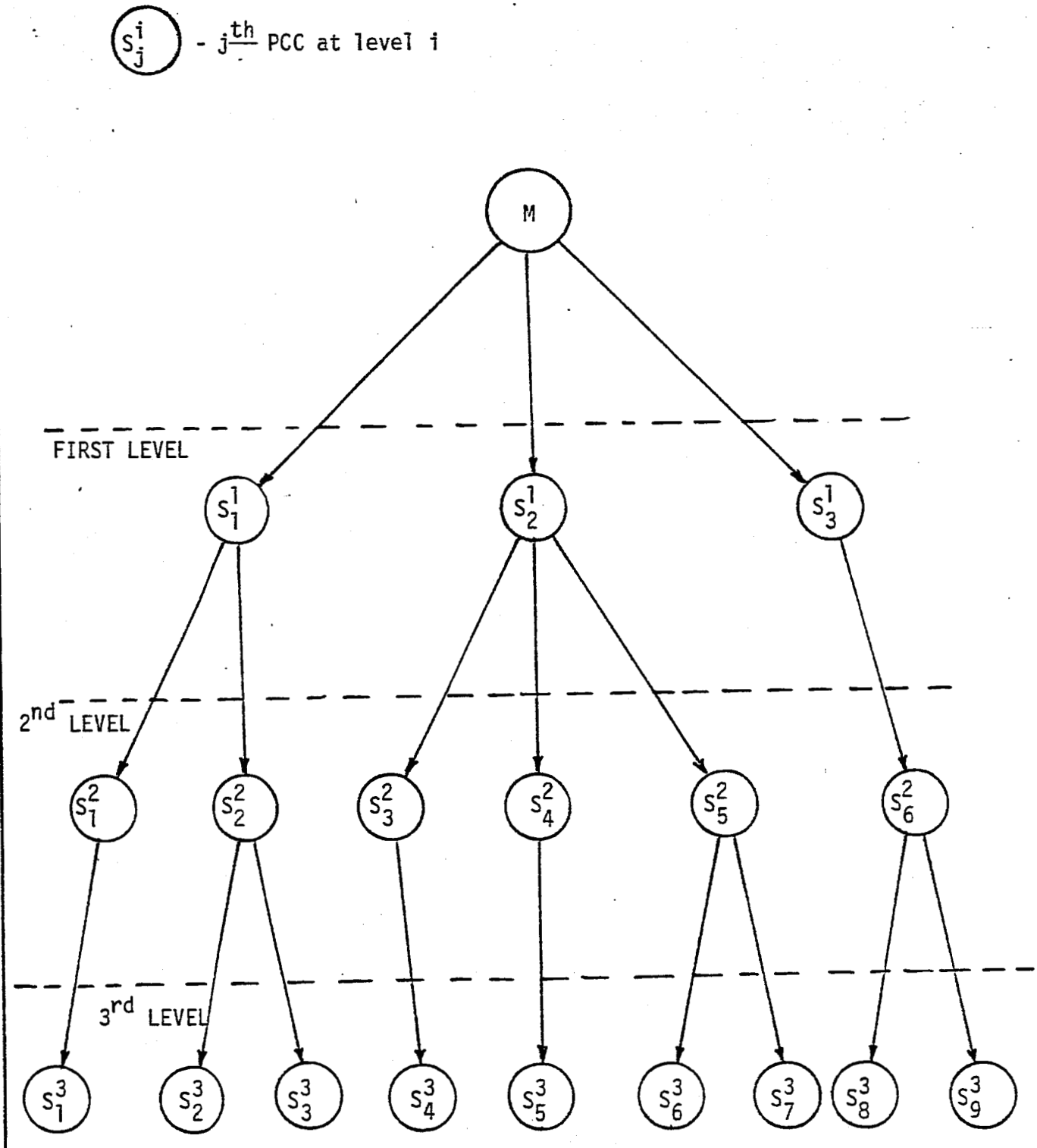

Figure 6. Connectivity of the Master Slave Configuration.

$$\dot{\Phi}_{1j} = \omega_{ij} + G_{1j}g_{1j}(\Phi_M - \Phi_{1j} - d_{jM}) \quad j=1,\ldots,N \qquad (3.1.1\text{-}1)$$

where the over dot represents differentiation with time, G_{1j} is the gain of the signal transmission path at the $j^{\underline{th}}$ PCC of $1^{\underline{st}}$ level of PCC slaves. In the steady state one can solve this to yield

$$\Phi_{1j} = \Phi_M - d_{jM} - g^{-1}\left(\frac{\omega_M - \omega_{1j}}{G_{1j}}\right) \qquad (3.1.1\text{-}2)$$

Continuing this procedure, we can obtain the total phase of any slave PCC at any level. As an example, we write down the phase of $1^{\underline{st}}$ PCC at $K^{\underline{th}}$ PCC level, i.e.,

$$\Phi_{k1} = \Phi_M - \sum_{i=1}^{k} d_{i,i-1} - \sum_{i=1}^{k} g^{-1}\left(\frac{\omega_{i-1,1} - \omega_{i1}}{G_{i1}G_{i-1,1}}\right) \qquad (3.1.1\text{-}3)$$

with $d_{10} = d_{1M}$ and $\omega_{01} = \omega_M$. We can use (3.1.1-2) repeatedly to determine the phase of any PCC in any particular level keeping track of which slave oscillator acts as the master to the slave in the lower level. Using the same equation one can write down the steady state phase difference between any two slave oscillators in the hierarchy. As an example we will write down the phase difference between the $i^{\underline{th}}$ and $j^{\underline{th}}$ PCC on the $1^{\underline{st}}$ level. Using (3.1.1-2) we have

$$\Phi_{1j} - \Phi_{1i} = d_{iM} - d_{jM} + g^{-1}\left(\frac{\omega_M - \omega_{1i}}{G_{1i}}\right) - g^{-1}\left(\frac{\omega_M - \omega_{1j}}{G_{1j}}\right) \qquad (3.1.1\text{-}4)$$

If we design such that the nominal frequency is the same at all PCCs, i.e., $\omega_M = \omega_{1i} = \omega_{1j}$, then we get the phase build up

between the $i^{\underline{th}}$ and $j^{\underline{th}}$ PCC at level one, viz.,

$$\Phi_{1j} - \Phi_{1i} = d_{iM} - d_{jM} \qquad (3.1.1\text{-}5)$$

Thus (3.1.1-5) gives in the differential phase or <u>phase build up</u> between the two PCCs. It can be seen that the primary cause of this phase build up is the path delays between PCCs. Thus the phase build up is present in the master slave configuration if the lengths of the connecting cables between any two successive levels of slaves is not exactly the same. This differential delay is also dependent on the frequency used between PCC levels. Figure 7 shows the phase build up at the first level of slaves for different frequencies. As an example of the frequency dependence, for 2 cm. differential cable length we have about 58° of phase build up at 2.48 GHz and 1.68° at 70 MHz. Thus to control phase build up we must reduce differential cable length between any two successive levels of slaves.

3.2 <u>Mutual Synchronous Configuration for Connecting the PCCs</u>

In the mutual synchronous configuration, there is no master PCC but each PCC in the configuration adjusts its own frequency and phase so as to reduce the error between itself and a weighted average of the total phases of the rest of the PCCs in the configuration. Assuming that there are N PCCs in the configuration and that they are fully connected, i.e., each PCC in the configuration is connected to every other PCC in the configuration, there are (N-1) incoming signals received at each PCC and the same number of transmitted signal paths. Figure 8 illustrates typical connections for the case of two and three PCCs.

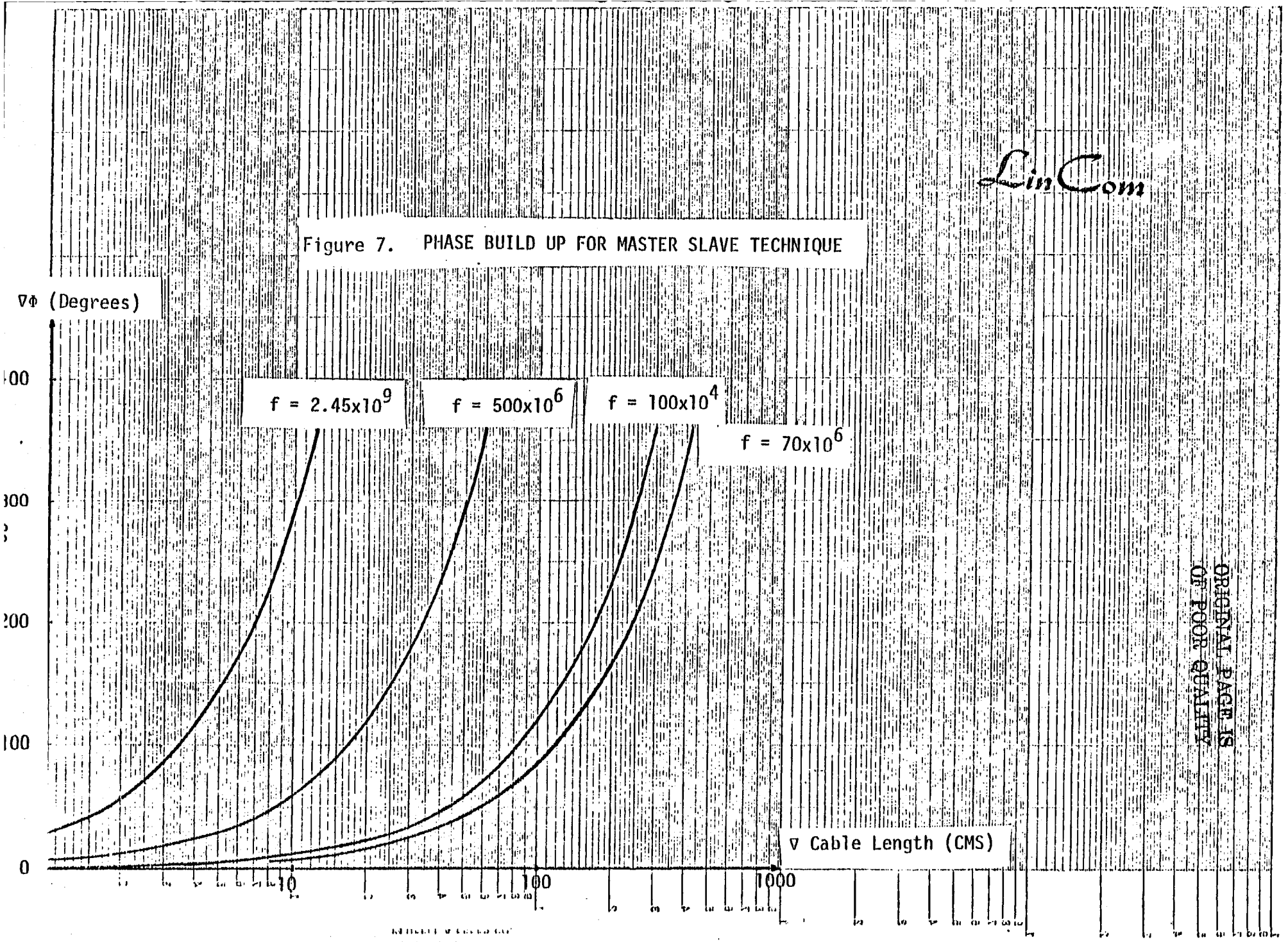

Figure 7. PHASE BUILD UP FOR MASTER SLAVE TECHNIQUE

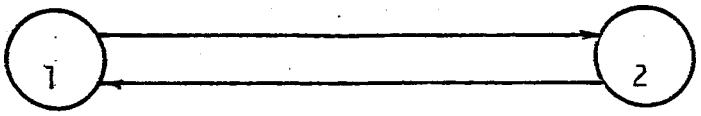

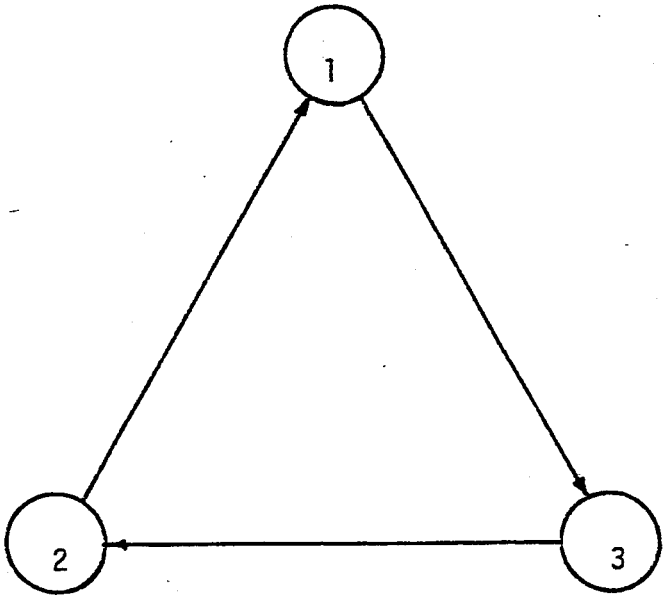

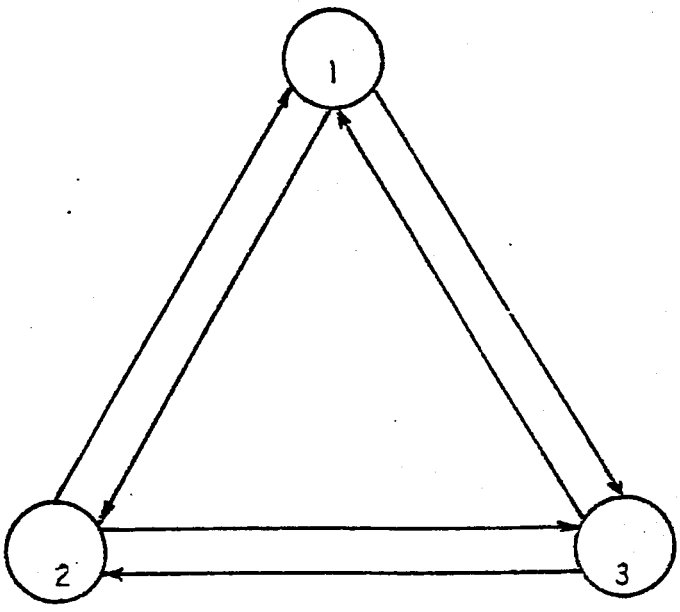

Figure 8. Connection for Mutual Sync Configuration.

3.2.1 Mathematic Model for the Mutual Sync Configuration

Using the total phase of the PCCs in the configuration as independent variables, the mathematical model can be described in terms of the nonlinear vector differential equation.

$$\dot{\underline{\Phi}} = \underline{C} + F \cdot \underline{g(\Phi)} \qquad (3.2.1\text{-}1)$$

Here we have suppressed time and $\underline{\Phi} = [\Phi_1, \Phi_2, \ldots, \Phi_N]^T$ represents the vector of total phases of the PCCs. This is an Nx1 vector, $\underline{C} = [C_1, C_2, \ldots, C_N]^T$ is an Nx1 vector of nominal PCC frequencies, $\underline{g(\Phi)}$ is a N(N-1)x1 vector of PCC phase detector characteristics which depends upon the path delays, total phases, etc., and F is the NxN(N-1) connection matrix defined by

$$F = \frac{1}{(N-1)} \begin{bmatrix} F_1B_{12} & 0 \ldots & F_1B_{1N} & 0 & 0 \ldots 0 & \ldots 0 & 0 & \ldots 0 \\ 0 & 0 \ldots & 0 & F_2B_{21} & \ldots F_2B_{21} \ldots & 0 & 0 & \ldots 0 \\ \vdots & \vdots & \vdots & \vdots & \vdots & & & \\ 0 & 0 & 0 & 0 & 0 & \ldots F_nB_{N1} & \ldots & F_NB_{NN-1} \end{bmatrix} \qquad (3.2.1\text{-}2)$$

where F_i characterizes the filter processing in the i^{th} PCC, and B_{ij} is the total gain associated with the j^{th} input at the i^{th} PCC.

The mathematical model described above is for a fully connected PCC configuration. It should be noted that each element in the matrix F represents a connection and the subscript on B, say B_{ij}, tells us that the information flows from j^{th} PCC to i^{th} PCC. Now suppose that the configuration of PCCs is not fully connected, i.e., say the i^{th} PCC has M incoming signals with $1 \leq M \leq (N-1)$, then (3.2.1-1) still models the system

but with the following changes. By breaking the connection from $j^{\underline{th}}$ PCC to $i^{\underline{th}}$ PCC in the vector $g(\underline{\Phi})$, the element $g_{ij}(\cdot)$ may be set to zero without reducing the dimensionality of $g(\underline{\Phi})$. Also the factor $1/(N-1)$ does not appear in front of the F matrix but the $i^{\underline{th}}$ row is divided by the number M. Thus matrix F could be interpreted as a particular kind of a connection matrix.

If we assume that $B_i = B_0$ and $F_i = F_0$ for all $i = 1,2,\ldots,N$, then

$$F=\frac{F_0B_0}{(N-1)}\begin{bmatrix} 1 & 1 & \ldots & 1 & 0 & 0 & \ldots & 0 & \ldots & 0 & 0 & \ldots & 0 \\ 0 & 0 & \ldots & 0 & 1 & 1 & \ldots & 1 & \ldots & 0 & 0 & \ldots & 0 \\ \vdots & & & \vdots & \vdots & \vdots & & \vdots & & & & & \\ 0 & 0 & \ldots & 0 & 0 & 0 & \ldots & 0 & \ldots & 1 & 1 & \ldots & 1 \end{bmatrix} \qquad (3.2.1\text{-}3)$$

and if we define the vector

$$\underline{0} = [0 \;\; 0 \ldots 0] \text{ a } 1x(N-1) \text{ vector}$$

and the vector

$$\underline{1} = [1 \;\; 1 \ldots 1] \text{ a } 1x(N-1) \text{ vector}$$

(3.2-3) reduces to

$$F = \frac{F_0B_0}{(N-1)}\begin{bmatrix} \underline{1} & \underline{0} & \ldots & \underline{0} \\ \underline{0} & \underline{1} & \ldots & \underline{0} \\ \vdots & \vdots & & \vdots \\ \underline{0} & \underline{0} & \ldots & \underline{1} \end{bmatrix} \qquad (3.2.1\text{-}4)$$

As an example of the connection matrix, we can apply (3.2.1-4) to the PCC connections given in Fig. 8. As the

first example, consider two fully connected PCCs; here the F matrix would be a 2x2 matrix, i.e.,

$$F = F_0 B \begin{bmatrix} \underline{1} & \underline{0} \\ \underline{0} & \underline{1} \end{bmatrix} \text{ where } \underline{1} = 1 \text{ and } \underline{0} = 0$$

Now consider the ring of three PCCs shown in Fig. 8. Here F is the 3x3 matrix

$$F = F_0 B \begin{bmatrix} \underline{1} & \underline{0} & \underline{0} \\ \underline{0} & \underline{1} & \underline{0} \\ \underline{0} & \underline{0} & \underline{1} \end{bmatrix} \qquad \begin{aligned} \underline{1} &= [1 \quad 0] \\ \underline{0} &= [0 \quad 0] \end{aligned}$$

For a fully connected system of three PCCs, see Fig. 8,

$$F = \frac{F_0 B}{2} \begin{bmatrix} \underline{1} & \underline{0} & \underline{0} \\ \underline{0} & \underline{1} & \underline{0} \\ \underline{0} & \underline{0} & \underline{1} \end{bmatrix} \qquad \begin{aligned} \underline{1} &= [1 \quad 1] \\ \underline{0} &= [0 \quad 0] \end{aligned}$$

In the general case of N PCCs, (3.2.1-4) characterizes the connection matrix. For the case of the SPS antenna phasing system, the dimensionality of F is on the order of 1000. The steady state frequency ω_s of a fully connected set of PCCs is of interest (assuming it exists). It can be shown that ω_s depends upon the nominal frequencies ω_i of the PCCs, the equivalent gain B_e, and path delays through the equation

$$\omega_s = \frac{1}{N} \sum_{i=1}^{N} \omega_i - \frac{B_e}{N(N-1)} \sum_{\substack{i=1 \\ i \neq j}}^{N} \sum_{j=1}^{N} d_{ij} \qquad (3.2.1\text{-}5)$$

If $\omega_i = \omega_0$ for $i = 1,\ldots,N$ then

$$\omega_s = \omega_0 - \frac{B_e}{N(N-1)} \sum_{\substack{i=1 \\ i\neq j}}^{N} \sum_{j=1}^{N} d_{ij} \qquad (3.2.1\text{-}6)$$

which says ω_s is dependent upon the delay variations.

In addition, in the steady state we can show that the phase build up is given by

$$\Phi_i - \Phi_j = -\frac{1}{N}(D_i - D_j) \qquad (3.2.1\text{-}7)$$

where

$$D_i \triangleq \sum_{\substack{j=1 \\ j\neq i}}^{N} d_{ij}$$

If $d_{ij} = d_{ji}$, then the phase developed by the individual PCCs is identical. To clarify the concept of mutual synchronization, we will consider two and three PCCs fully connected.

3.2.1.1 A Special Case of Two and Three PCCs

Figure 9 shows the connections for the two PCC mechanized in the form of phase-locked loops. The equations describing the behavior of the coupled configuration are nonlinear differential equations. Using the total phases as the independent variables we can write

$$\frac{d\Phi_1}{d\tau} = \frac{\omega_1}{B_1} + \sin(\Phi_2 - \Phi_1 - d_{12})$$

$$\frac{d\Phi_2}{d\tau} = \frac{\omega_2}{B_1} + \frac{B_2}{B_1}\sin(\Phi_1 - \Phi_2 - d_{21}) \qquad (3.2.1.1\text{-}1)$$

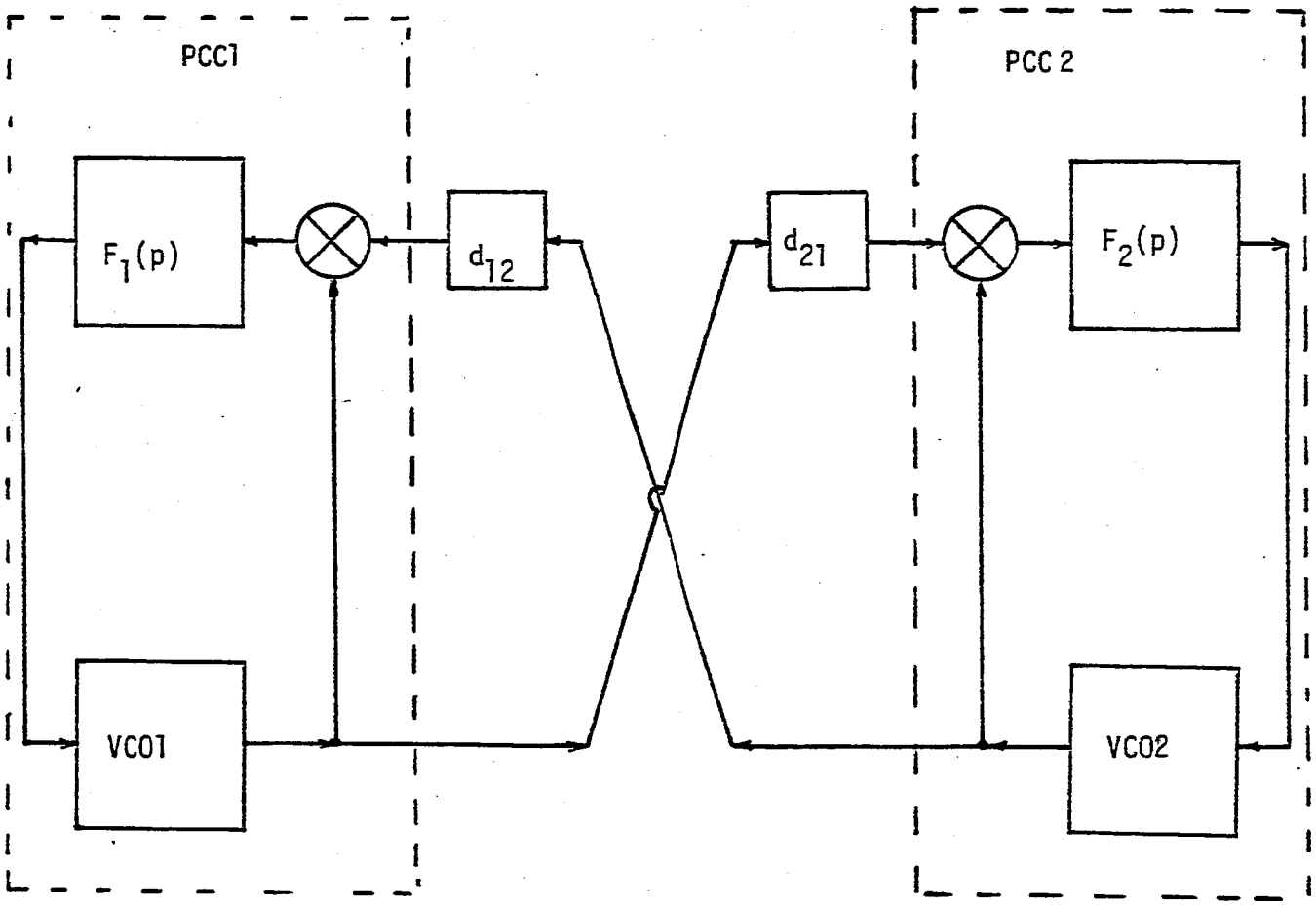

Figure 9. Two PCCs Fully Connected.

where ω_1 and ω_2 are the nominal frequencies of the PCCs 1 and 2. d_{12} and d_{21} are the delays associated with the connecting links. With $\alpha = B_2/B_1$ these equations could be solved to yield

$$\Phi_2-\Phi_1 \triangleq \nabla\Phi = \tan^{-1}\left[\frac{\sin d_{12} - \alpha \sin d_{21}}{\cos d_{12} + \alpha \cos d_{21}}\right] + \sin^{-1}\left[\frac{\omega_2-\omega_1}{R}\right] \qquad (3.2.1.1\text{-}2)$$

where

$$R = [1 + 2\alpha \cos(d_{12}+d_{21}) + \alpha^2]^{1/2}$$

With $\alpha = 1$ i.e. $B_1 = B_2$ we get

$$\nabla\Phi = \frac{d_{12}-d_{21}}{2} \qquad (3.2.1.1\text{-}3)$$

and

$$\omega_r = \omega_1 - B_1 \sin\left(\frac{d_{12}+d_{21}}{2}\right) \qquad (3.2.1.1\text{-}4)$$

Figure 10 to Figure 12 show the behavior of the system for the different values of the parameters of the systems. Fig. 11 is the plot of normalized $(\omega_s-\omega_1)$ and $(\omega_s-\omega_2)$ vs. the normalized frequency offset $(\omega_2-\omega_1)/B_1$. The delays are $d_{12} = 10°$ $(d_{21} = 20°)$ with the parameter being the gain ratio . Figure 12 is a similar plot with $d_{12} = d_{21} = 0°$. These straight lines pass through the orgin, indicating that if the initial frequency offset is zero, i.e. $\omega_1 = \omega_2$ then the steady state frequency $\omega_s = \omega_1 = \omega_2$. Also note that the lines for $\frac{K_2}{K_1}=1$ are symmetric about the axis and they have a slope of 0.5 suggesting that $\omega_s = (\omega_1+\omega_2)/2$. Now in Fig. 11 $d_{12} = 10°$ and $d_{21} = 20°$ and in this case the steady state frequency does depend upon the delays. As an example of the usefulness of these curves, we consider an example, with $\omega_1 = 10$ MHz and $\omega_2 = 11$ MHz, $B_1 = B_2 = 10^6$,

Figure 10. PHASE ERROR TRAJECTORY AT NODE ONE FOR VARIOUS DAMPINGS & DELAYS

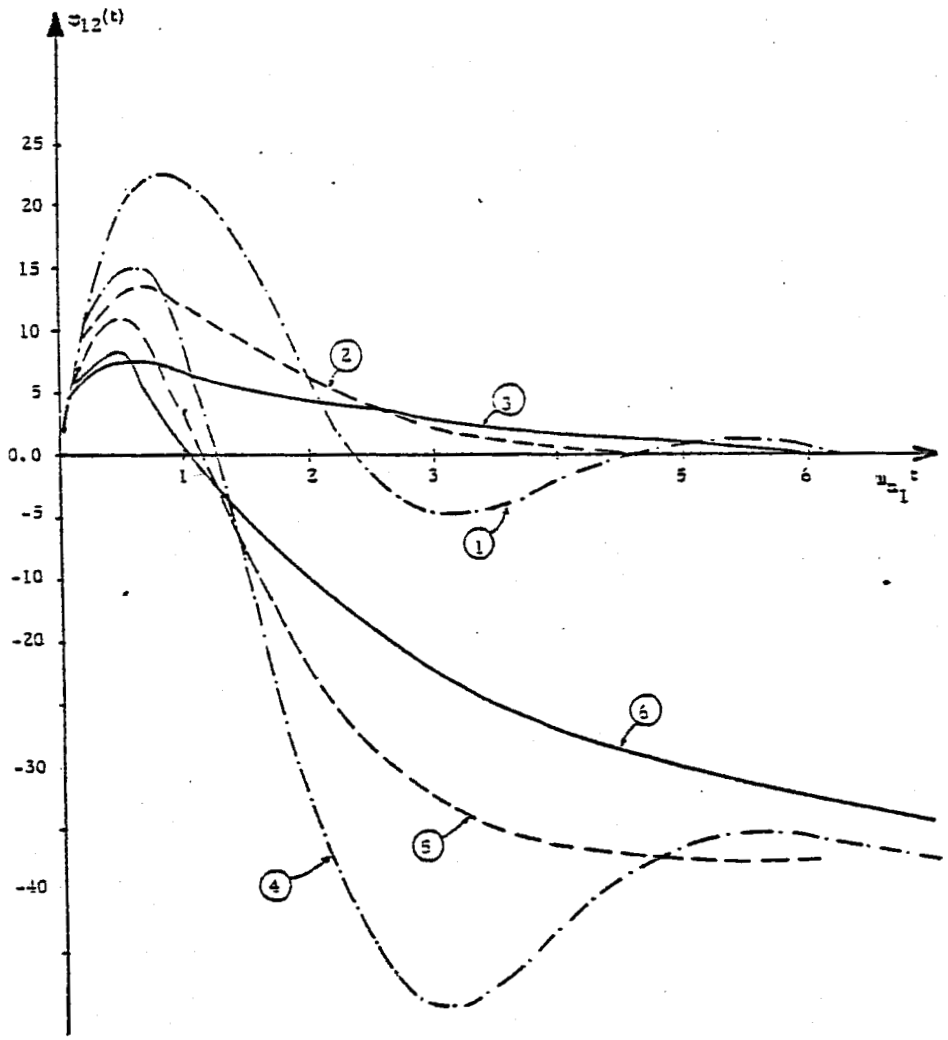

Figure 11.

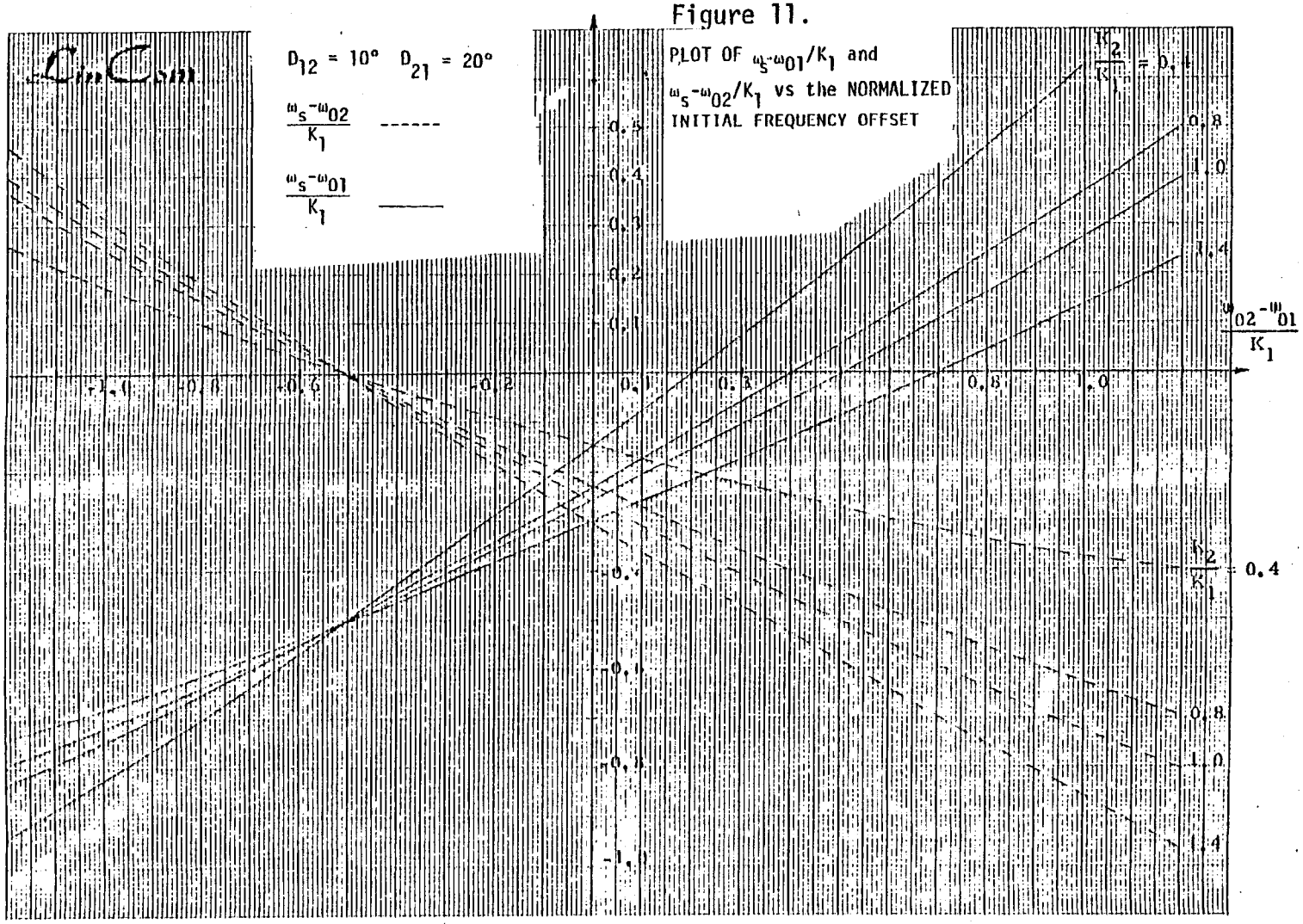

$d_{12} = 10°$ and $d_{21} = 20°$, the plot will give us a steady state frequency of 10.27 MHz. Suppose we desire a steady state frequency of 10.5 MHz. In this case the curves could be used to give the $B_1 = 1.667 \times 10^6$ and $B_2 = 0.6668 \times 10^6$ as one possible solution. The same example with $d_{12} = d_{21} = 0$ gives $\omega_s = 10.5$ MHz and $\omega_s = 10.4$ MHz could be obtained by $B_1 = 2 \times 10^6$ and $B_2 = 2.8 \times 10^5$. The main thing to note here is that if the delays are not zero then the frequency is affected by them.

Figure 13 shows the connection diagram for a fully connected configuration containing three PCCs. This is basically the same as the two PCC case except for the averaging network added at each of the PCCs. Here the performance of the configuration depends upon the path delays.

3.3 Hierarchial Master-Slave Mutual Sync Configuration

This configuration is basically the same as the master-slave configuration described in Section 3.1, but at each level of PCC hierarchy, the mutual synchronous configuration is superimposed on groups of PCCs at each level. This configuration is termed Hierarchial Master Slave Mutual Sync I. When we connect all the PCCs at any level of hierarchy in a mutual synchronous configuration, we get the Hierarchial Master Slave Mutual Sync II. This technique is of great interest in what follows.

3.3.1 Comparison of the Master Slave and Mutual Sync Configurations

The equation for phase build up between any two PCCs at the N level of slave in a master slave configuration is given by

$$\nabla\Phi_{ij} = D_i - D_j \qquad (3.3.1\text{-}1)$$

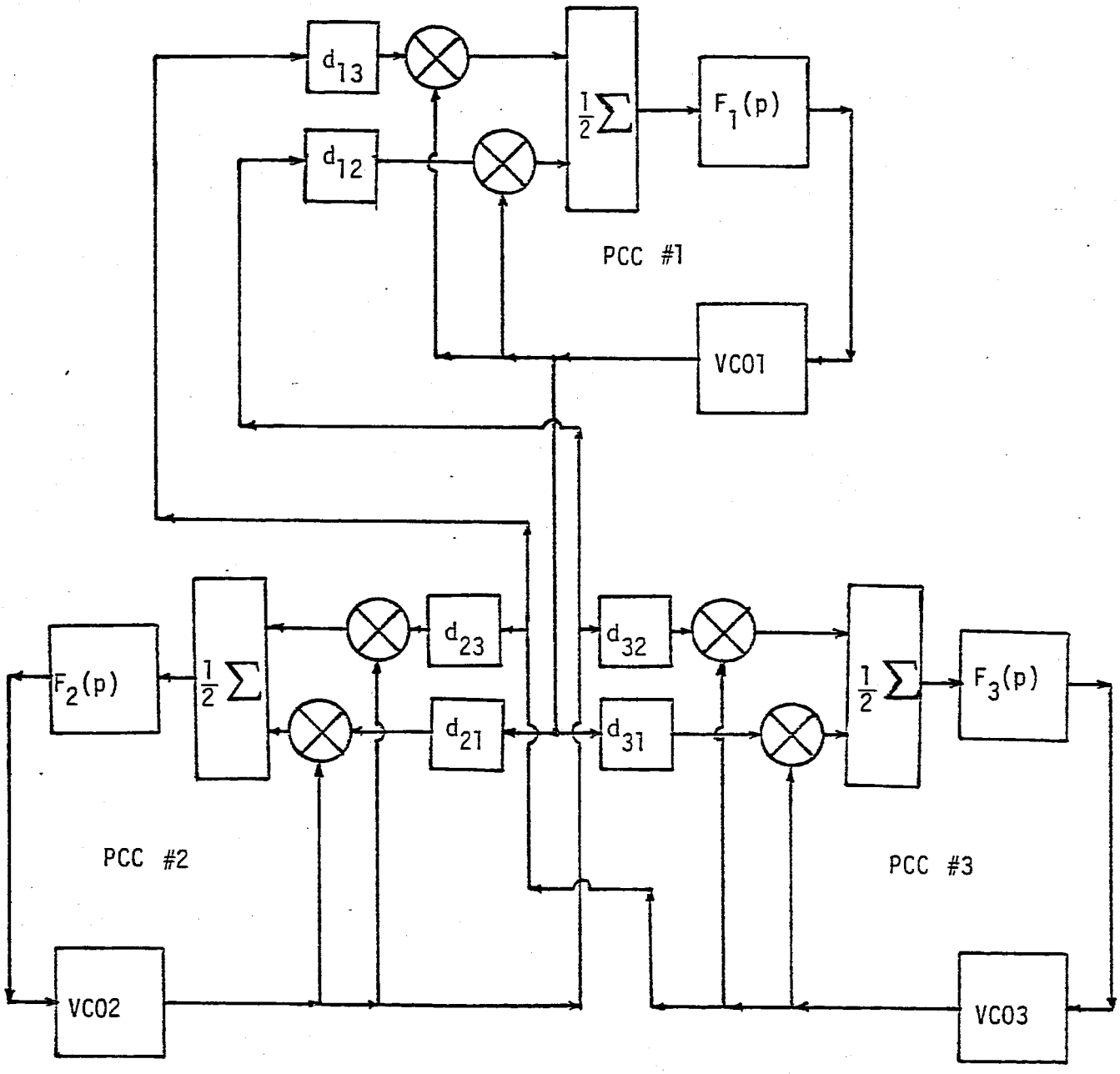

Figure 13. Mutual Synchronization Connection for Three PCCs.

where D_i is the sum of delays due to links between the master and the $i^{\underline{th}}$ slave at $N^{\underline{th}}$ level. On the other hand, for the mutual sync configuration it can be shown that

$$\nabla\phi_{ij} = \frac{1}{M}(D_i - D_j) \qquad (3.3.1\text{-}2)$$

where M is the number of PCCs connected in a mutual sync configuration at the $N^{\underline{th}}$ level. Comparing the phase build up as expressed by (3.3.1-1) and (3.3.1-2) we can see that the performance of the mutual synch configuration is N times better.

This improvement in the phase build up is tradeoff against the cost of cable weight. Hence, an effort to strike a balance between the phase build up and the cable weight results into what we have termed Hierarchial Master Slave Mutual Sync Configuration. In this configuration, the mutual synchronous connection is imposed at different levels of the Master Slave Configuration, see Fig. 27. Even this arrangement may require the use of a large amount of cable. Here we mutually synchronize groups of four PCCs at each level of slaves in the Master-Slave configuration. This arrangement is inferior in the phase build up when compared to total mutual synchronous system but it gains quite a bit in saving the cable length. Since this system is being proposed for the SPS antenna, cable weight is an important factor.

4. DELAY COMPENSATION TECHNIQUES

We have seen in the previous sections that the delay parameter associated with the linkage path is of utmost importance in determining the steady state behavior of the phase control system. We have also seen that the phase build up is directly proportional to the differential path delays. Since the linkage paths are absolutely essential, some way of compensating for the delays is required. The delays also enter into the equation which specifies the steady state frequency. The delay parameter depends upon the temperature variation, flexing of antenna structure, etc. thus indicating that the performance of the antenna depends upon these quantities. Thus it is desirable to make the phase control system performance delay independent. This can be done using the Equational Timing Configuration (ETC) or the Returnable Timing Configuration (RTC). Both of these methods of phase control are similar in principle; they differ only in the way they are connected. Hence, in what follows we discuss RTC in greater detail and we will make reference to ETC when the performance is significantly different.

4.1 Returnable Timing Configuration (RTC)

The RTC belongs to the category of single ended phase control systems in the sense that all the phase measurements affecting the PCCs control signal are done at the same PCC. However, there are signals appearing at each PCC which to some extent reflect the phase relationship between the signals received at other PCCs.

The main idea in this method is that at every PCC the

signal received is used and is also sent back to the transmitting PCC, see Fig. 14. The connections made at each PCC makes it possible to compensate for path delays. In this case we can also have the concept of fully connected and partially connected configurations. We will consider the fully connected RTC of N PCCs for the following analysis.

4.1.1 Mathematical Model of the Returnable Timing Configuration

It is quite easy to write down the nonlinear matrix differential equation for this configuration because it is closely related to the mutual synch configuration. The mathematical model for this configuration is described by

$$\underline{\dot{\Phi}} = \underline{C} + F' \cdot \underline{g(\Phi)} + \tilde{F} \cdot \underline{\tilde{g}(\Phi)} \qquad (4.1.1\text{-}1)$$

where $\underline{\Phi}$, $\underline{C}$, and $\underline{g(\Phi)}$ are described in Section 3. The matrix F' is the same as matrix F described in Section 3 but the factor $1/N\text{-}1$ is replaced by $1/(N\text{-}1)(\tilde{a}+1)$. The matrix F is the same as F' but with B_{ij} replaced by $\tilde{B}_{ij}$. The factor $\tilde{a} = 0$ if $\tilde{B}_{ij} = 0$ for all i and j otherwise $\tilde{a} = 1$. It should be noted that the quantities with $\sim$ represent the corresponding quantities with the return path. We can see from (4.1.1-1) that if all the $\tilde{B}_{ij} = 0$ then (4.1.1-1) becomes (3.2.1-1).

Figure 14 illustrates PCCs connected in the RTC mechanization. The first case uses two PCCs connected in the RTC. For this connection the F and $\tilde{F}$ matrix reduce to

$$F = \frac{F_0 B_0}{2}\begin{bmatrix} \underline{1} & \underline{0} \\ \underline{0} & \underline{1} \end{bmatrix} \text{ and } \tilde{F} = \frac{F_0 \tilde{B}_0}{2}\begin{bmatrix} \underline{1} & \underline{0} \\ \underline{0} & \underline{1} \end{bmatrix}$$

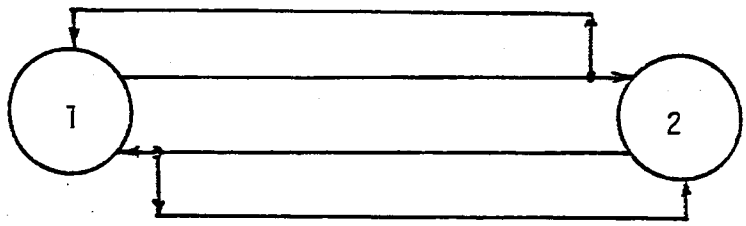

(a) Two PCC Configuration

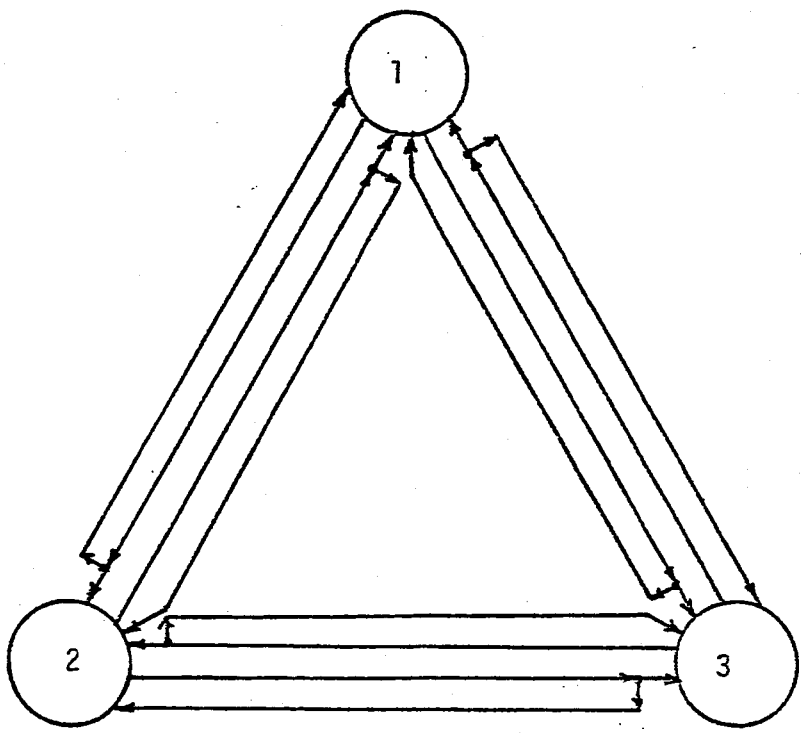

(b) Three PCC Configuration

Figure 14. Connection of PCCs in the RTS Configuration.

where $\underline{1} = 1$ and $\underline{0} = 0$ in this case. Fig. 14b illustrates the case of three PCCs. Here the F and $\tilde{F}$ matrices are defined by

$$F = \frac{F_0 B_0}{4}\begin{bmatrix} \underline{1} & \underline{0} & \underline{0} \\ \underline{0} & \underline{1} & \underline{0} \\ \underline{0} & \underline{0} & \underline{1} \end{bmatrix} \quad \text{and} \quad \tilde{F} = \frac{F_0 B_0}{4}\begin{bmatrix} \underline{1} & \underline{0} & \underline{0} \\ \underline{0} & \underline{1} & \underline{0} \\ \underline{0} & \underline{0} & \underline{1} \end{bmatrix}$$

where $\underline{1} = [1 \quad 1]$ and $\underline{0} = [0 \quad 0]$.

In the steady state, the steady state frequency can be shown to be given by

$$\omega_s = \frac{\sum_{i=1}^{N} \left(\frac{\omega_i}{B_i}\right)}{\sum_{i=1}^{N} \frac{1}{B_i} + \frac{1}{(N-1)(\tilde{a}+1)} \sum_{\substack{i,j=1 \\ i\neq j}}^{N} (\tau_{ji} - \tilde{\tau}_{ji})} \qquad (4.1.1\text{-}2)$$

where $B_i = B_{ij}$ for all $j = 1,\ldots,N$ and τ_{ji} and $\tilde{\tau}_{ji}$ are the path time delays encountered by signals between the $i^{\underline{th}}$ PCC and $j^{\underline{th}}$ PCC, by the forward path and the return path respectively. Assuming a fully connected configuration $\tilde{a} = 1$, and the return path time delay $\tilde{\tau}_{ji}$ can be written in terms of the forward path time delay through

$$\tilde{\tau}_{ji} = \tau_{ji} + \Delta \cdot \tau_{ji} \qquad (4.1.1\text{-}3)$$

$$\omega_s = \frac{\sum_{i=1}^{N} \left(\frac{\omega_i}{B_i}\right)}{\sum_{i=1}^{N} \left(\frac{1}{B_i}\right) + \frac{\Delta}{2(N-1)} \sum_{\substack{i,j=1 \\ i\neq i}}^{N} \tau_{ji}} \qquad (4.1.1\text{-}4)$$

Equation (4.1.1-4) shows that if Δ is small and N is large, the uncompensated delays do not affect the steady state frequency of the system. Furthermore if Δ is small, N is large, and with $B_i = B$ for all i, then

$$\omega_s \cong \frac{1}{N}\sum_{i=1}^{N} \omega_i \qquad (4.1.1\text{-}5)$$

To understand the RTC better we now consider a special case where two PCCs are to be connected in the RTC.

4.1.1.1 Two PCCs Connected in the RTC

Here N=2 and (4.1.1-1) reduces to (Fig. 15 shows the connections)

$$\begin{aligned}\dot{\Phi}_1 &= \omega_1 + B_1 \sin(\nabla\Phi - d_{12}) + \tilde{B}_1 \sin(\nabla\Phi - d_{12} + d_{21} + \tilde{d}_{12}) \\ \dot{\Phi}_2 &= \omega_2 + B_2 \sin(-\nabla\Phi - d_{21}) + \tilde{B}_2 \sin(-\nabla\Phi - d_{21} + d_{12} + \tilde{d}_{21})\end{aligned} \qquad (4.1.1.1\text{-}1)$$

where $\nabla\Phi$ is the phase build up between the PCCs. It is this $\nabla\Phi$ that will affect the beam pointing error of the antenna. Near the steady state, in a perfectly compensated system and with $B_1 = \tilde{B}_1$, $B_2 = \tilde{B}_2$, the phase difference becomes equal to

$$\nabla\Phi = \frac{d_{12} - d_{21}}{2} \qquad (4.1.1.1\text{-}2)$$

and the steady state frequency reduces to

$$\omega_s = \frac{1}{2}(\omega_1 + \omega_2)$$

Thus we see from the above equation that this configuration

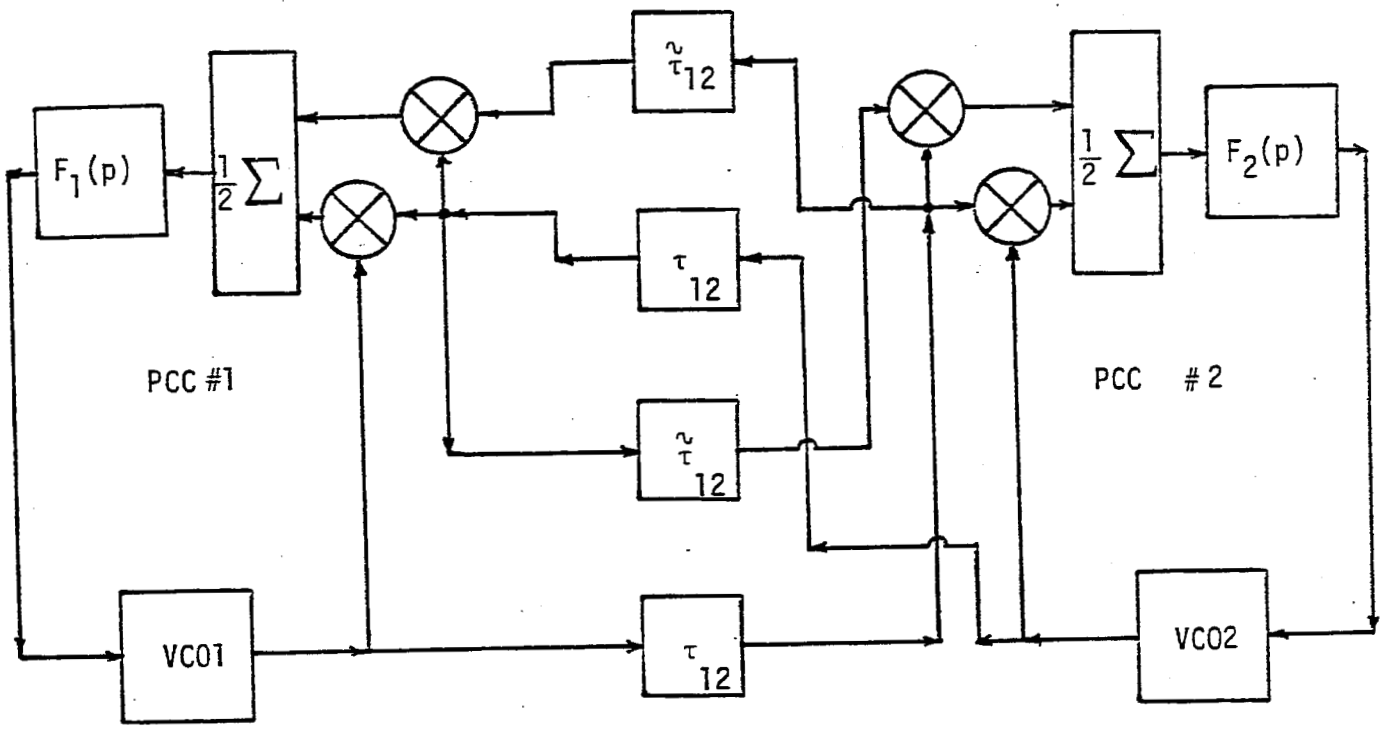

Figure 15. Returnable Timing Configuration.

compensates for the path delays as far as the steady state frequency of the configuration is concerned but the differential path delay still enters into the phase build up (see eq. (4.1.1.1-2)). Figure 16 shows the phase build up for N=2 case.

4.2 Master Slave Returnable Timing System Hybrid Configuration (MSRTC)

The Master Slave configuration has the advantage of minimum cable length requriement whereas the RTS has the steady state frequency independent of the system delays. The RTS also has the advantage of minimum phase build up. The MSRTC hybrid combines the advantages of MS and RTS. It also has one additional rather important advantage, i.e., the phase at any particular PCC is the same as the phase at any other PCC in the entire configuration. This perfect delay compensation is obtained by processing the signal and in no way depends upon the shape of the antenna or the phasing system layout.

Figure 16 describes the MSRTS basic building block. The signal s(t) is the pilot signal from the rectenna site. We assume that

$$s(t) \triangleq A \cos(\omega_0 t + \theta_0) \qquad (1)$$

where

ω_0 = master signal frequency (pilot signal frequency)

θ_0 = the phase associated with the master signal (pilot signal phase received at the center element of the antenna).

We want the frequency ω_0 and the phase θ_0 to be distributed over the aperture of the antenna.

Point Q in the figure given above is the far end of the cable connecting the local [illegible] next [illegible]

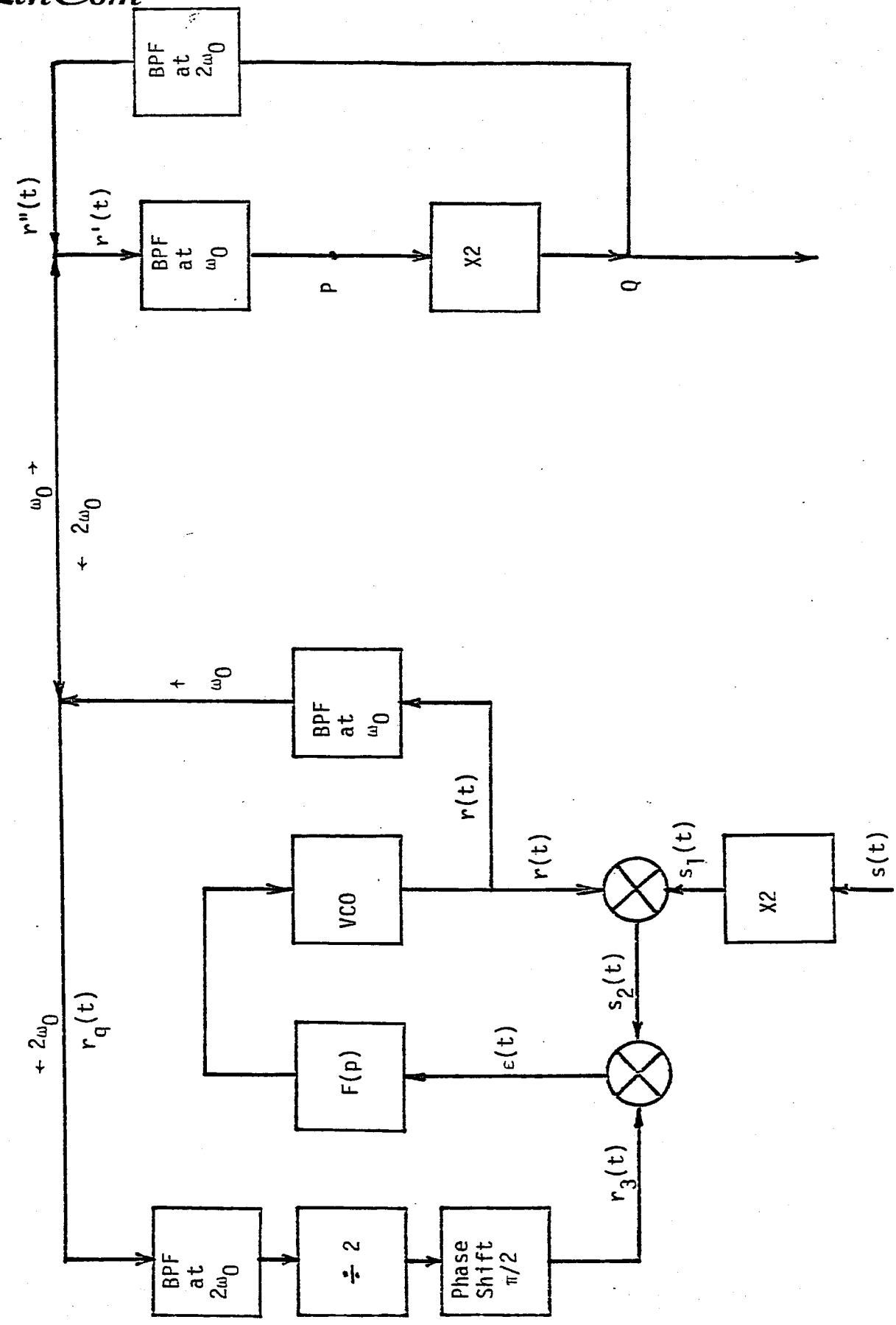

Figure 16. Building Block for MSRTS.

of this system is to reproduce (send) the signal $s_1(t)$ at the point Q or equivalently, signal s(t) at the point P.

Now

$$s_1(t) = A\cos(2\omega_0 t + 2\theta_0) \tag{2}$$

VCO output reference signal r(t)

$$r(t) \triangleq K'\cos(\omega_0 t + \theta(t)) \tag{3}$$

i.e., we have assumed that the local VCO has the same nominal frequency as the signal s(t)

$$s_2(t) = \text{lower side band of } [s_1(t)r(t)]$$

$$s_2(t) = AK'\cos(\omega_0 t + 2\theta_0 - \theta(t)) \tag{4}$$

Now

$$r(t) = K'\cos(\omega_0 t + \theta(t))$$

$$r'(t) = K'\cos(\omega_0 t + \theta(t) - d_{21})$$

$$r''(t) = K'\cos(2\omega_0 t + 2\theta(t) - 2d_{21})$$

$$r_q(t) = K'\cos(2\omega_0 t + 2\theta(t) - 2d_{21} - d_{12})$$

$$r_3(t) = K'\sin(\omega_0 t + \theta(t) - d_{21} - d_{12}/2) \tag{5}$$

Lower side band of $\varepsilon(t)$:

$$\varepsilon(t) = A\tilde{K}\sin(2\theta_0 - 2\theta(t) + d_{21} + d_{12}/2) \tag{6}$$

$$Z(t) = F(p)\varepsilon(t)$$

and

$$\theta(t) = \frac{K_V Z(t)}{p} = \frac{K_V F(p)}{p}\,\varepsilon(t)$$

$$\theta(t) = \frac{AKF(p)}{p}\{\sin(2\theta_0 - 2\theta(t) + d_{21} + d_{12}/2)\} \tag{7}$$

where d_{12} is the delay encountered by the signal from $1^{\underline{st}}$ node to $i^{\underline{th}}$ node.

To obtain the loop equation, we let

$$\phi \triangleq \text{loop phase error} = 2\theta_0 - 2\theta(t) + d_{21} + \frac{d_{12}}{2}$$

$$\phi = 2\theta_0 - 2\theta(t) + d_{21} + \frac{d_{21}}{2}$$

$$\phi = 2\theta_0 - \frac{2AKF(p)}{p}\sin(\phi) + d_{21} + \frac{d_{12}}{2}$$

Hence

$$\frac{d\phi}{dt} = \frac{2d\theta_0}{dt} - 2AKF(p)\sin\phi + \frac{d}{dt}(d_{21} + d_{12}/2) \tag{8}$$

$$\boxed{\frac{d\phi}{dt} = \frac{2d\theta_0}{dt} + \frac{d}{dt}\left(d_{21} + \frac{d_{12}}{2}\right) - 2AKF(p)\sin\phi}$$

In our case, since θ_0, d_{12} and d_{21} are constants,

$$\frac{d\phi}{dt} = -2AKF(p)\sin\phi \tag{9}$$

We are particularly interested in the steady state behavior of the system. Near the steady state, $\phi \to$ constant, i.e.

$$\lim_{t\to\infty}\left[\frac{d\phi}{dt}\right] \to 0$$

and

$$\lim_{t\to\infty} \phi(t) \to \phi_{ss}$$

From equation (9) we get with $F(p) = 1$,

$$\lim_{t\to\infty}\left[\frac{d\phi(t)}{dt}\right] = -2AK \lim_{t\to\infty}[\sin\phi(t)]$$

$$0 = -2AK\sin\phi_{ss}$$

$$\phi_{ss} = n\pi \qquad n = 0,1,2,\ldots$$

with n=0, we have

$$\phi_{ss} = 0 = 2\theta_0 - 2\theta_{ss} + d_{21} + \frac{d_{12}}{2}$$

$$\theta_{ss} = \theta_0 + \frac{1}{2}\left(d_{21} + \frac{d_{12}}{2}\right) \qquad (10)$$

Therefore local VCO output signal r(t) in s.s.

$$= K' \cos(\omega_0 t + \theta_{ss})$$

$$= K' \cos(\omega_0 t + \theta_0 + \frac{1}{2}(d_{21} + \frac{d_{21}}{2}) \qquad (11)$$

signal at the point P

$$= K' \cos(\omega_0 t + \theta_0 + \frac{1}{2}\left(d_{21} + \frac{d_{12}}{2}\right) - d_{21})$$

$$= K' \cos\left(\omega_0 t + \theta_0 + \frac{d_{12} - 2d_{21}}{4}\right) \qquad (12)$$

Now recall that d_{21} is the delay offered by the cable length at the frequency ω_0 while d_{12} is the delay due to the same cable length at $2\omega_0$. Assuming a linear characteristic of the cable delay with frequency, we can state

$$d_{12} = 2d_{21} \qquad (13)$$

Using (13) in (12) we get

$$\text{Signal at Point P} = K' \cos(\omega_0 t + \theta_0)$$

$$= \frac{A}{K'} s(t) .$$

If we assume unit amplitudes of all signals, the signal phase at point P is <u>exactly</u> the same as the phase of the master signal s(t).

Page Intentionally Left Blank

Table 1. COMPARISON OF PHASE CONTROL TECHNIQUES (ANALYSIS RESULTS)

PHASE CONTROL TECHNIQUE	COMMENT
MASTER SLAVE	● SYSTEM FREQUENCY CONTROLLED BY MASTER ● PHASE BUILD-UP DEPENDS ON THE PATH DELAYS, INSTABILITIES
MUTUAL SYNCHRONIZATION	● SYSTEM FREQUENCY DEPENDS ON DELAYS, INSTABILITIES ● PHASE BUILD-UP LESS SENSITIVE THAN MS
RETURNABLE TIMING AND EQUATIONAL TIMING	● SYSTEM FREQUENCY IS INDEPENDENT OF DELAYS! ● PHASE BUILD-UP MINIMIZED!

master frequency but suffers from the problem of phase build up. Even though this configuration enjoys the benefit of minimal cable length, the phase build-up may be excessive if the differential cable length does not remain small for all time. Furthermore, the oscillator instabilities, temperature gradients, etc. are not compensated for in this method.

The next configuration we discussed was the Mutual Synch Configuration. This system suffers from the fact that the steady state frequency depends on the delays; however, it minimizes phase build-up when compared with that of the Master Slave Configuration. The mutual synchronous configuration also suffers from the need for a large amount of cable length.

The Returnable Timing Configuration (RTC) has the advantage that the steady state frequency becomes independent of the path delays as long as the differential path delay is small and the number of PCCs is large. On the other hand, the phase build-up is comparable to that achieved with that of the mutual sync configuration. The RTC requires a huge cable length to implement.

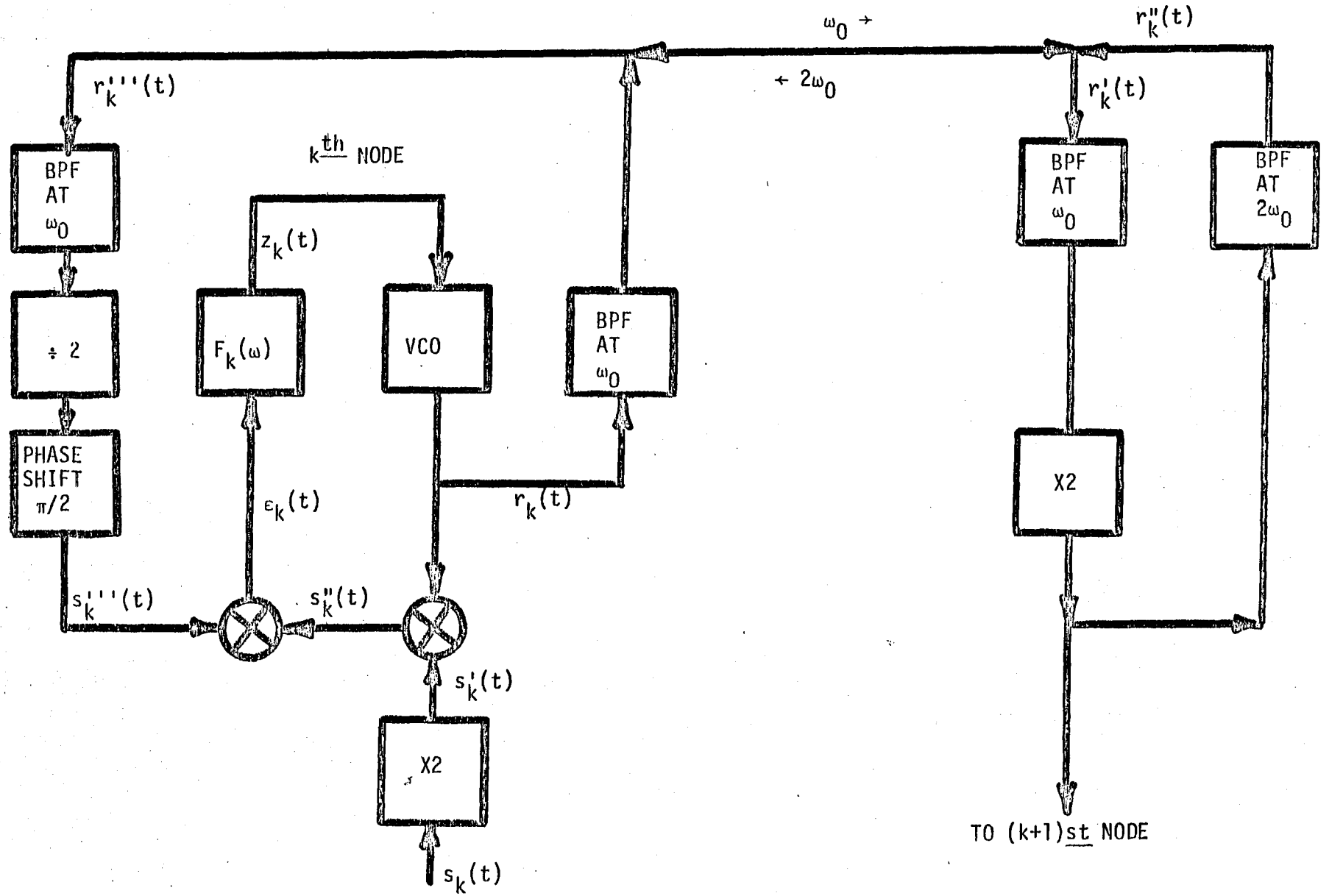

Figure 17. Phase Noise Analysis of MSRTC.

5.1 Phase Noise Analysis

The phase control centers in the antenna reference distribution system uses the phase locked loop. The theories developed above assume that the oscillators in the PLL are perfect. Now we wish to analyze the behavior of the system in the presence of the phase noise added by the oscillators in the configuration. Since the MSRTC is the most promising technique, we will develop the theory for that system only. Fig. 17 gives the particulars of the MSRTS system for phase distribution at the $k^{\underline{th}}$ PCC. Note that $\hat{x}(t)$ means the phase of the signal $x(t)$.

$$\hat{s}'_k(t) = 2\omega_0(t-\tau_{k,k-1}) + 2\theta_{k-1}(t-\tau_{k,k-1})$$

$$\hat{r}_k(t) = \omega_0 t + \theta_k(t)$$

$$\hat{s}''_k(t) = \omega_0(t-\tau_{k+1,k}) + \theta_k(t-\tau_{k+1,k})$$

$$\hat{r}'_k(t) = \omega_0(t-\tau_{k+1,k}) + \theta_k(t-\tau_{k+1,k})$$

$$\hat{r}''_k(t) = 2\omega_0(t-\tau_{k+1,k}) + 2\theta_k(t-\tau_{k+1,k})$$

$$\hat{r}'''_k(t) = 2\omega_0(t-\tau_{k+1,k}-\tau_{k,k+1}) + 2\theta_k(t-\tau_{k+1,k}-\tau_{k,k+1})$$

$$\hat{s}'''_k(t) = \omega_0(t-\tau_{k+1,k}-\tau_{k,k+1}) + \theta_k(t-\tau_{k+1,k}-\tau_{k,k+1})$$

$$\hat{\varepsilon}_k(t) = \text{lower sideband of } [\hat{s}'''_k(t) \times \hat{s}''_k(t)]$$

$$= 2\theta_{k-1}(t-\tau_{k,k-1}) - \theta_k(t) - \theta_k(t-\tau_{k+1,k}-\tau_{k,k+1}) - 2\omega_0\tau_{k,k-1} + \omega_0(\tau_{k+1,k}+\tau_{k,k+1}) \quad (1)$$

Assuming that the cable is nondispersive

$$\tau_{k,k+1} = \tau_{k+1,k}$$

and also assuming the linear regime of the phase locked loop operation, it is straightforward to obtain

$$\theta_k(\omega) = \frac{AKF_k(\omega)}{j\omega}\left[2\theta_{k-1}(\omega)e^{-j\omega\tau_{k,k-1}} - \theta_k(\omega)\{1 + e^{-2j\omega\tau_{k+1,k}}\} - 4\omega_0\pi(\tau_{k,k-1}-\tau_{k+1,k})\delta(\omega)\right] + \psi_k(\omega) \qquad (2)$$

where

τ_{ij} is the delay encountered by the signal flowing from $j^{\underline{th}}$ PCC to $i^{\underline{th}}$ PCC

$F_k(\omega)$ is the loop filter

$\psi_k(\omega)$ is the Fourier transformed phase noise added by the oscillator

One can solve for $\theta_k(\omega)$ from (2) which yields

$$\theta_k(\omega) = R_k(\omega)[\theta_{k-1}(\omega)\, e^{-j\omega\tau_{k,k-1}} - 2\omega_0\pi(\tau_{k,k-1}-\tau_{k+1,k})\delta(\omega)] + G_k(\omega)\psi_k(\omega) \qquad (3)$$

where

$$R_k(\omega) \triangleq \frac{2AKF_k(\omega)}{j\omega + AKF_k(\omega)\{1 + e^{-2j\omega\tau_{k+1,k}}\}}$$

and

$$G_k(\omega) \triangleq \frac{j\omega}{j\omega + AKF_k(\omega)\{1 + e^{-2j\omega\tau_{k+1,k}}\}}$$

Eq. (3) is a recursive relation for $\theta_k(\omega)$ and it could be solved for any general $\theta_N(\omega)$ with

$$R_k(\omega)e^{-j\omega\tau_{k\ k-1}} \triangleq H_k(\omega)$$

$$2R_k(\omega)\omega_0\pi(\tau_{k\ k-1}-\tau_{k-1\ k}) \triangleq P_k(\omega)$$

we get

$$\theta_N(\omega) = \left\{\prod_{i=1}^{N} H_i(\omega)\right\}\left[\theta_0(\omega) + \sum_{k=1}^{N}\left\{\frac{G_k(\omega)\psi_k(\omega)-P_k(\omega)\delta(\omega)}{\prod_{i=1}^{k} H_i(\omega)}\right\}\right] \quad (4)$$

Eq. (4) gives the output phase of $N^{\underline{th}}$ oscillator in the MSRTC. Let

$$\tilde{\theta}_N(\omega) = \theta_N(\omega) + \sum_{k=1}^{N}\left\{\prod_{i=k+1}^{N} H_i(\omega)\right\}P_k(\omega)\delta(\omega) \quad (5)$$

We would be interested in the mean and variance of the variable $\tilde{\theta}_N(\omega)$. Assuming that the phase noise added by each oscillator has zero mean, i.e.,

$$E[\psi_k(\omega)] = 0 \qquad \forall k=1,\ldots,N$$

we have from (4) and (5)

$$E[\tilde{\theta}_N(\omega)] = \left[\prod_{i=1}^{N} H_i(\omega)\right]\theta_0(\omega) \quad (6)$$

The spectral density on $\tilde{\theta}_N(\omega)$ is given by

$$S_{\tilde{\theta}_N}(\omega) = \left|\prod_{i=1}^{N} H_i(\omega)\right|^2\left[S_{\theta_0}(\omega) + \sum_{k=1}^{N}\left\{\frac{|G_k(\omega)|^2 S_{\psi_k}(\omega)}{\left|\prod_{i=1}^{k} H_i(\omega)\right|^2}\right\}\right] \quad (7)$$

This spectral density can be used to get the variance of $\tilde{\theta}_N(t)$

$$\sigma^2_{\tilde{\theta}_N} = \frac{1}{2\pi}\int_{-\infty}^{\infty}\left|\prod_{i=1}^{N} H_i(\omega)\right|^2\left[S_{\theta_0}(\omega) + \sum_{k=1}^{N}\left\{\frac{|G_k(\omega)|^2 S_{\psi_k}(\omega)}{\left|\prod_{i=1}^{k} H_i(\omega)\right|^2}\right\}\right]d\omega \quad (8)$$

Eq. (8) shows that the noise introduced by the master encounters all the loop filters ($H_i(\omega)$) but the noise introduced by each individual oscillator encounters only the filters in succession as is expected.

Limiting Cases

(1) Delays = 0 and $H_k(\omega) = 1 \quad \forall k \Longrightarrow G_k(\omega) = 0 \quad \forall k$ hence eq. (8) gives us

$$\sigma^2_{\theta_N} = \frac{1}{2\pi}\int_{-\infty}^{\infty} S_{\theta_0}(\omega)d\omega = \frac{1}{2\pi}\int_{-\infty}^{\infty} S_{\theta_0}(\omega)d\omega = \sigma^2_{master} \tag{9}$$

i.e. the variance of output of any oscillator in the MSRTC for this limiting case is the same as the master oscillator phase noise variance.

(2) Another limiting case arises when $H_k(\omega) = 0 \quad \forall k$ and with zero delays, $\Longrightarrow G_k(\omega) = 1$ and in this case (8) gives

$$\sigma^2_{\theta_N} = \frac{1}{2\pi}\int_{-\infty}^{\infty} S_{\psi_N}(\omega)\, d\omega \tag{10}$$

i.e. the variance of the output of $N^{\underline{th}}$ oscillator is due to its own phase noise only. Work on the phase noise accumulation for different kinds of filters is under way.

6. SUBARRAY LAYOUT

Since the location of the PCCs is intimately connected with the shape of the antenna, we will consider the structure of the antenna first. The total area proposed for the antenna is that of 1 km diameter circle. There are various ways of building this antenna, i.e. we may use square or rectangular building blocks. Such building blocks are called the subarrays.

6.1 The Square Geometry

In this case we assume a square building block or subarray of dimension 14x14 mt^2. size. As shown in Fig. 18, this subarray will have 7 radiating clusters, each having 14 dipoles or 14 slots on a radiating waveguide. As a matter of fact, we could consider any radiating element instead of a dipole. There are 4096 of these subarrays in the whole antenna. When the subarrays are stacked up, it has the shape of a square as shown in Fig. 19. This square will have length of one side to be 0.9 km. giving the area to be 0.81 km^2. The length of the diagonal is 1.27 km. Each radiating cluster in the subarray has a power amplifier and the phase control electronics necessary for the antenna operation.

6.2 Rectangular Geometry

In this case the basic building block is of rectangular geometry with dimensions 10x20 mt^2. This shape is shown in Fig. 20. There are 10 radiating clusters in each subarray and each radiating cluster

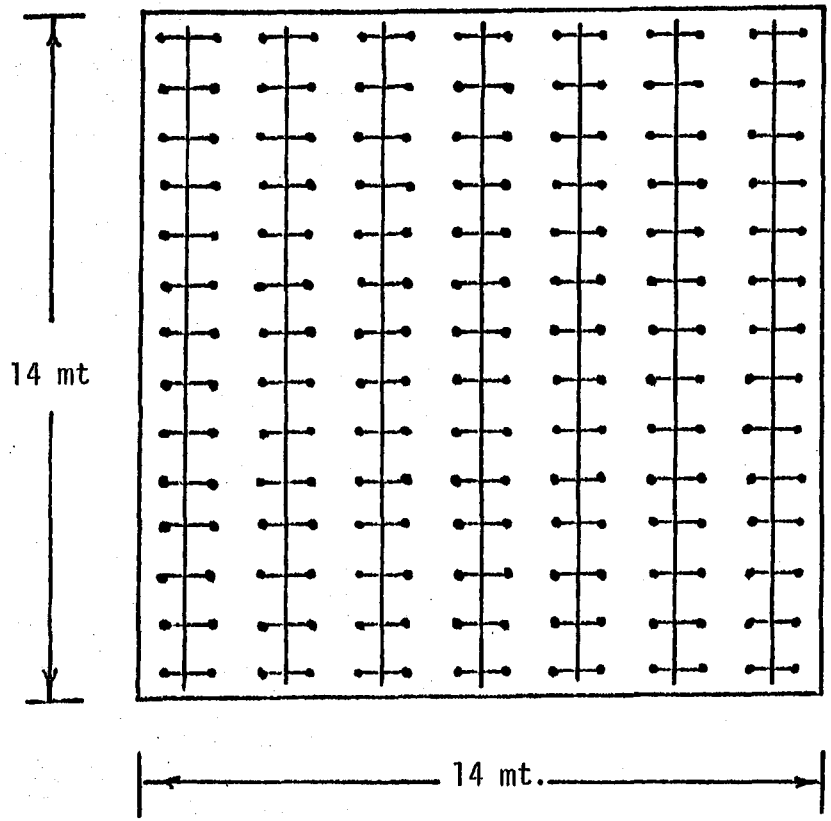

- SUBARRAY SIZE 14 x 14 mt.
- RADIATING CLUSTERS IN EACH SUBARRAY, 7
- RADIATING ELEMENTS--DIPOLES, SLOTTED WAVEGUIDE HORNS

Figure 18. Square Geometry.

Figure 19. PLAN FOR SQUARE GEOMETRY

LinCom

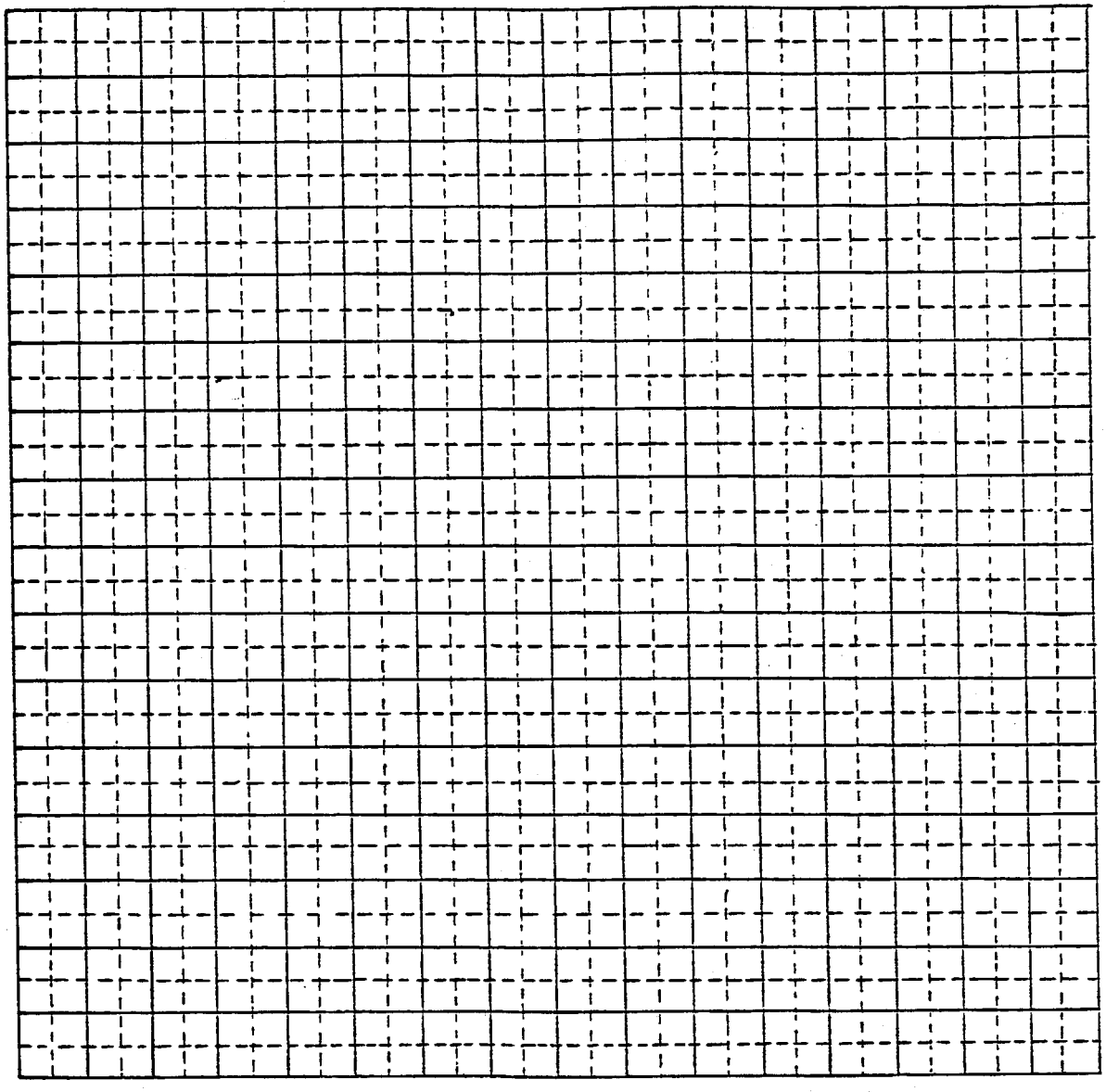

- TOTAL NUMBER OF SUBARRAYS = 4096
- TOTAL AREA = 808816 mt^2
- LENGTH OF SIDE = 896 mts.
- LENGTH OF DIAGONAL = 1.27 Km.

Figure 20. RECTANGULAR GEOMETRY

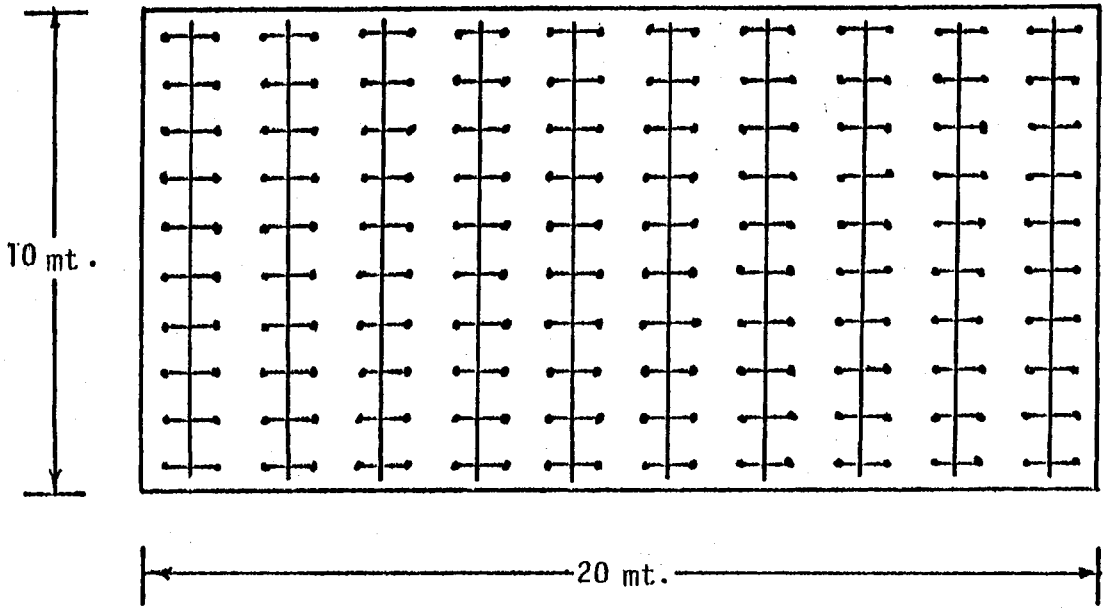

- SUBARRAY SIZE 10 x 20 mt.
- RADIATING CLUSTERS IN EACH SUBARRAY, 10
- RADIATING ELEMENTS - DIPOLES, SLOTTED WAVEGUIDES, HORNS

contains 10 radiating elements. These elements can be dipoles, slotted waveguide or any other kind of radiators. There are 4096 of these subarrays and they are arranged in a staggered fashion to give rise to the square antenna frame shown in Fig.21 . The area covered by this frame is 0.819 km^2.

We have also considered building the frame with hexagonal subarray building blocks; however, we do not report on the results here.

Figure 21. PLAN FOR STAGGERED RECTANGULAR GEOMETRY

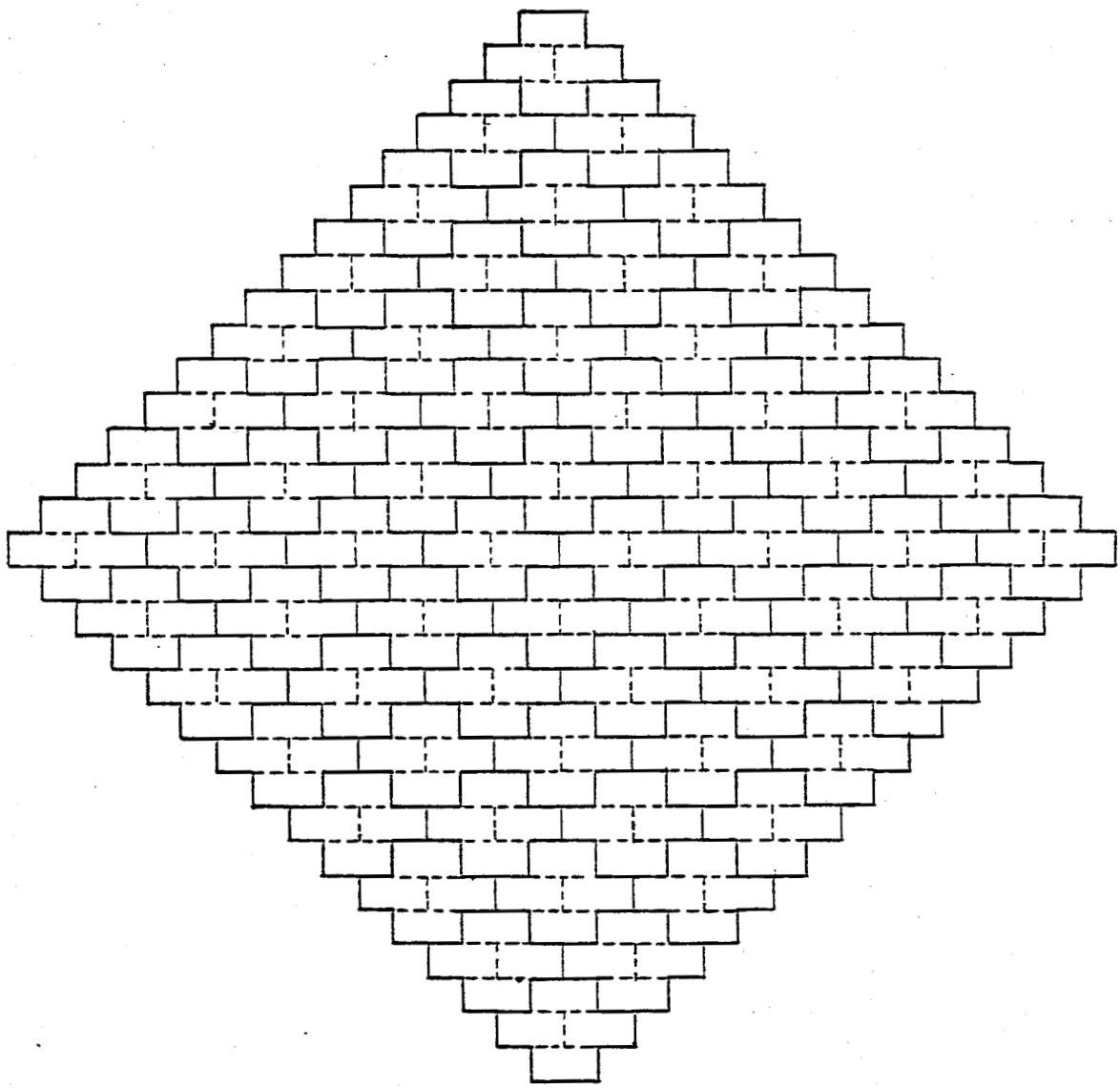

- TOTAL NUMBER OF SUBARRAYS = 4096
- TOTAL AREA COVERED = 819200 mt^2
- LENGTH OF DIAGONAL = 1.28 Km.

7.0 LOCATION OF THE PHASE CONTROL CENTERS PCCs

In the present SPS antenna configuration, there are approximately 30,000 radiating elements in which the radiated signal component should have equal phases to form a coherent wave front. One method of distributing the phase to the radiating elements is to "transmit" the phase from a master phase control center located at the center of the SPS antenna. Figure 22(a) shows this configuration. There are several disadvantages associated with this method. First of all, distribution of the phase from the master PCC to the radiating element via the power amplifiers (PAs) would require a large number of links. Normally, these links would be a cable, waveguide, etc. Since there are thousands of power amplifiers which must be phase controlled by the master PCC, an excessive amount of cable weight is required. In addition, the number of connections to the master PCC is prohibitive and any phase build-up would be uncompensated. Therefore, such an approach (direct phase distribution) is abandoned.

There exists another method of phase distribution from the master PCCs to the radiating elements which reduces the cable weight considerably. This method, termed the indirect phase distribution, distributes the phase of the master PCC via distribution PCCs. Figure 22(b) depicts this arrangement. In this particular case the ratio of cable length required for the direct to that required for the indirect connection approach is 1.42. This increase in cable length required for the direct connection is evident in Fig. 23. Here plots of the

Figure 22. DISTRIBUTION OF MASTER REFERENCE PHASE

(a) DIRECT

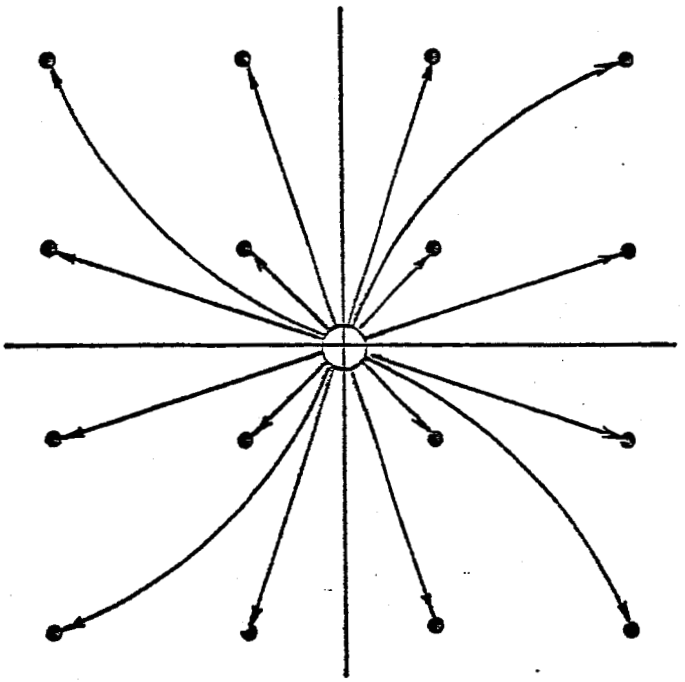

(b) INDIRECT

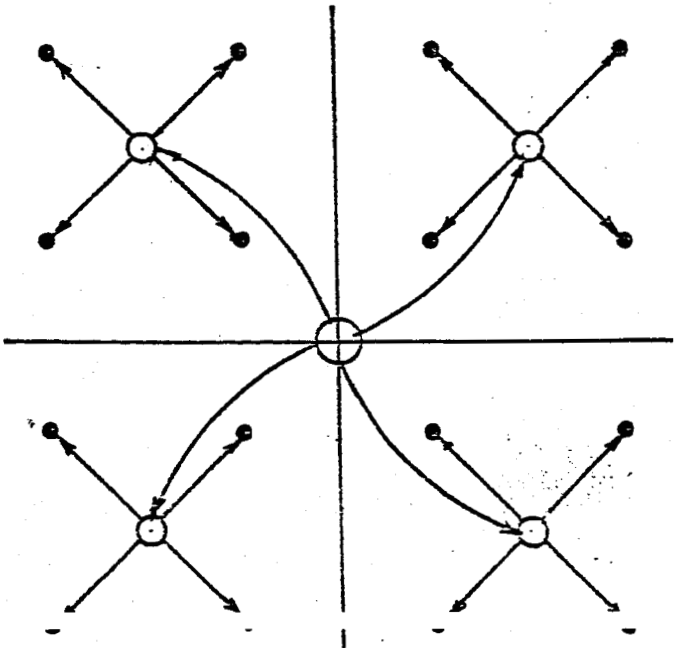

Figure 23. Cable Length Normalized to Antenna Coordinate System vs Number of Elements in Half Diagonal.

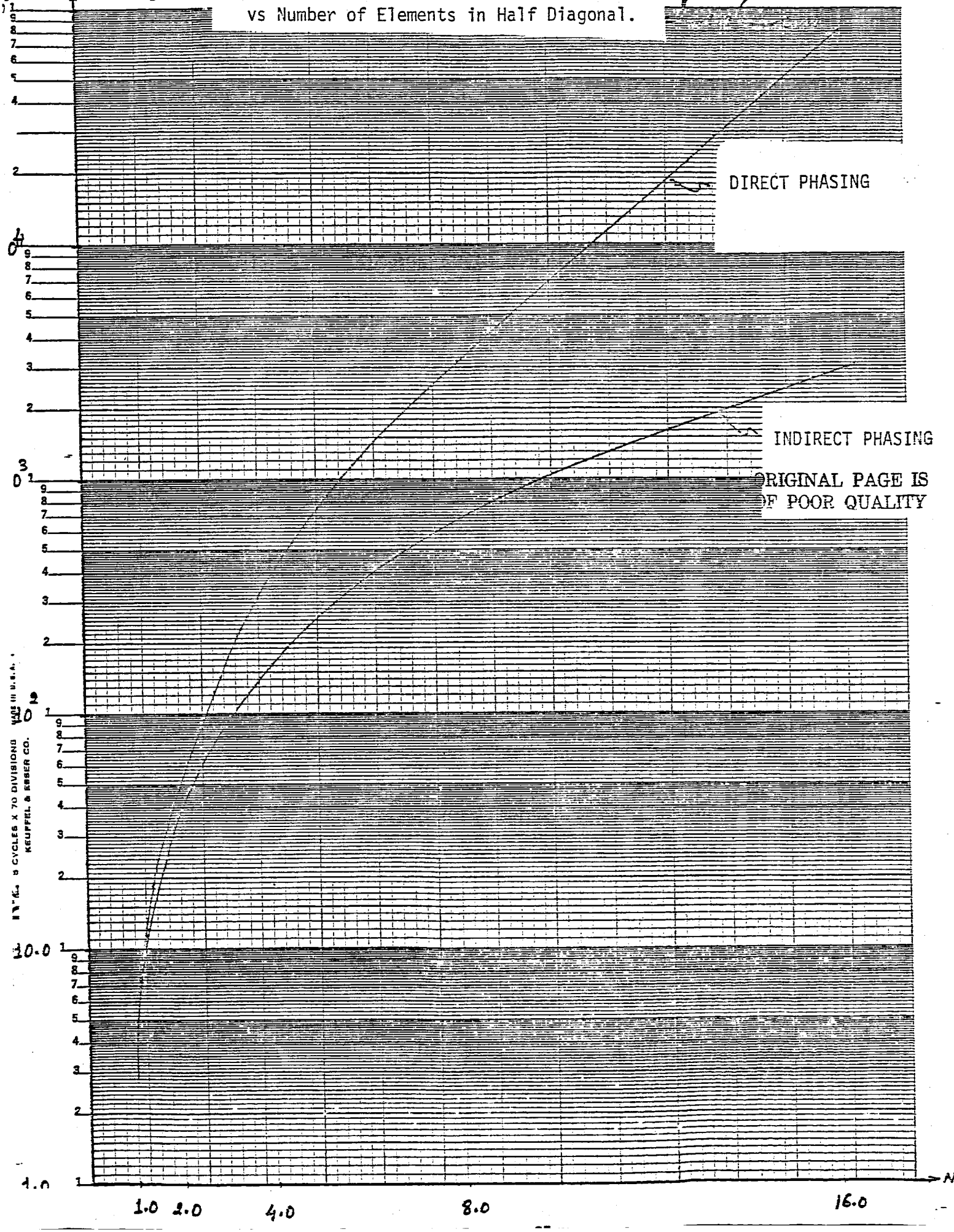

cable length normalized to subarray dimensions vs. the total number of radiating elements from the center of the antenna to the corner is depicted. Obviously the indirect method is more desirable.

7.1 Positioning of the Distribution PCCs

Now that we have established that the distribution PCCs are necessary for minimizing the cable length, the next question is where should they be located in the SPS antenna. Figure 24 shows the location of PCCs on the square geometry. There are 1364 PCCs plus the master PCC. Figure 25 shows the PCC position in the staggered rectangular geometry of the SPS antenna. Again there are 1364 PCCs plus one master PCC used in this configuration. Later we shall discuss the particular phase control configuration which minimizes phase build up.

Figure 24. Square Plan with PCC Layout.

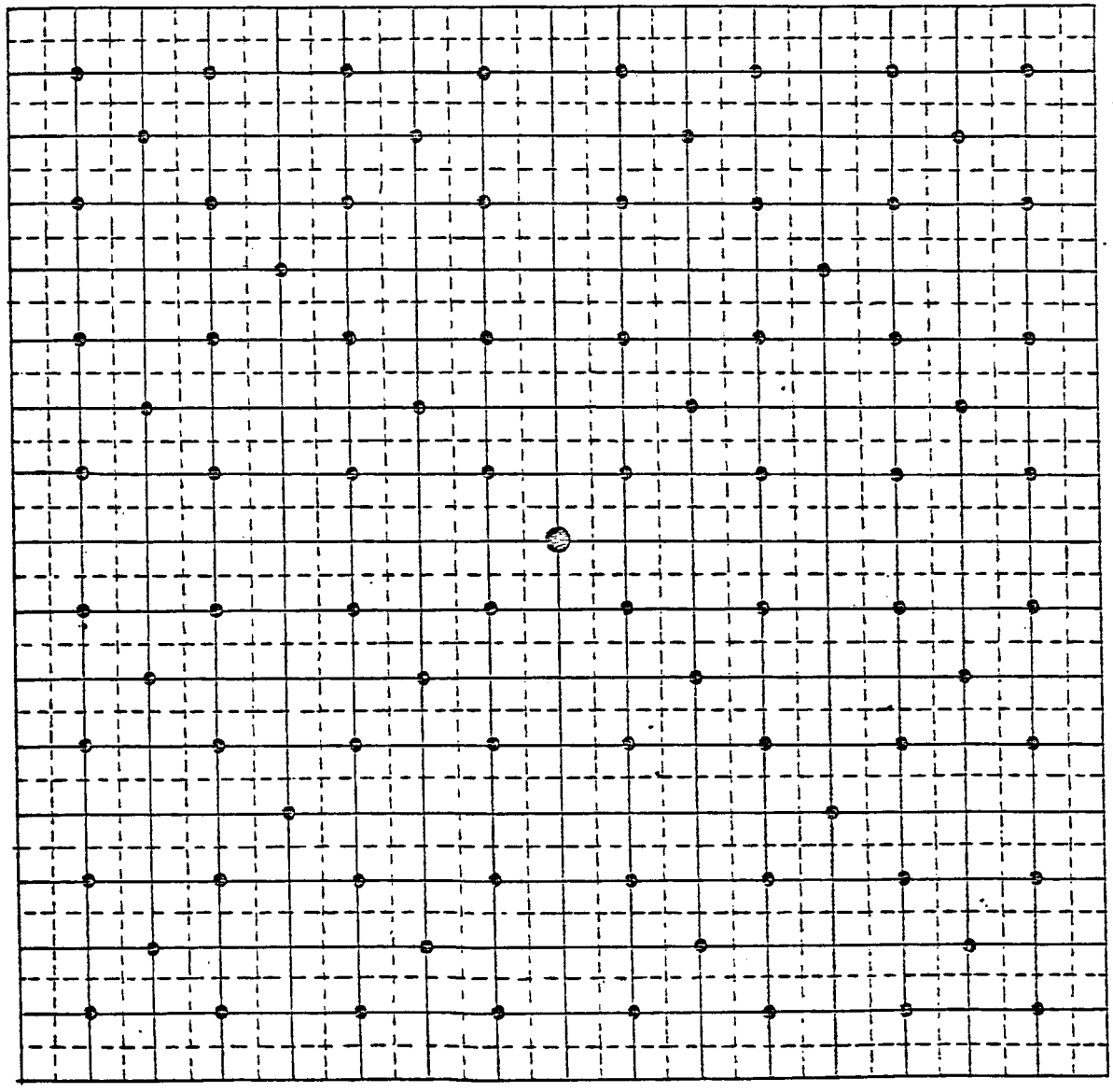

Figure 25. Staggered Rectangular Plan with PCC Layout.

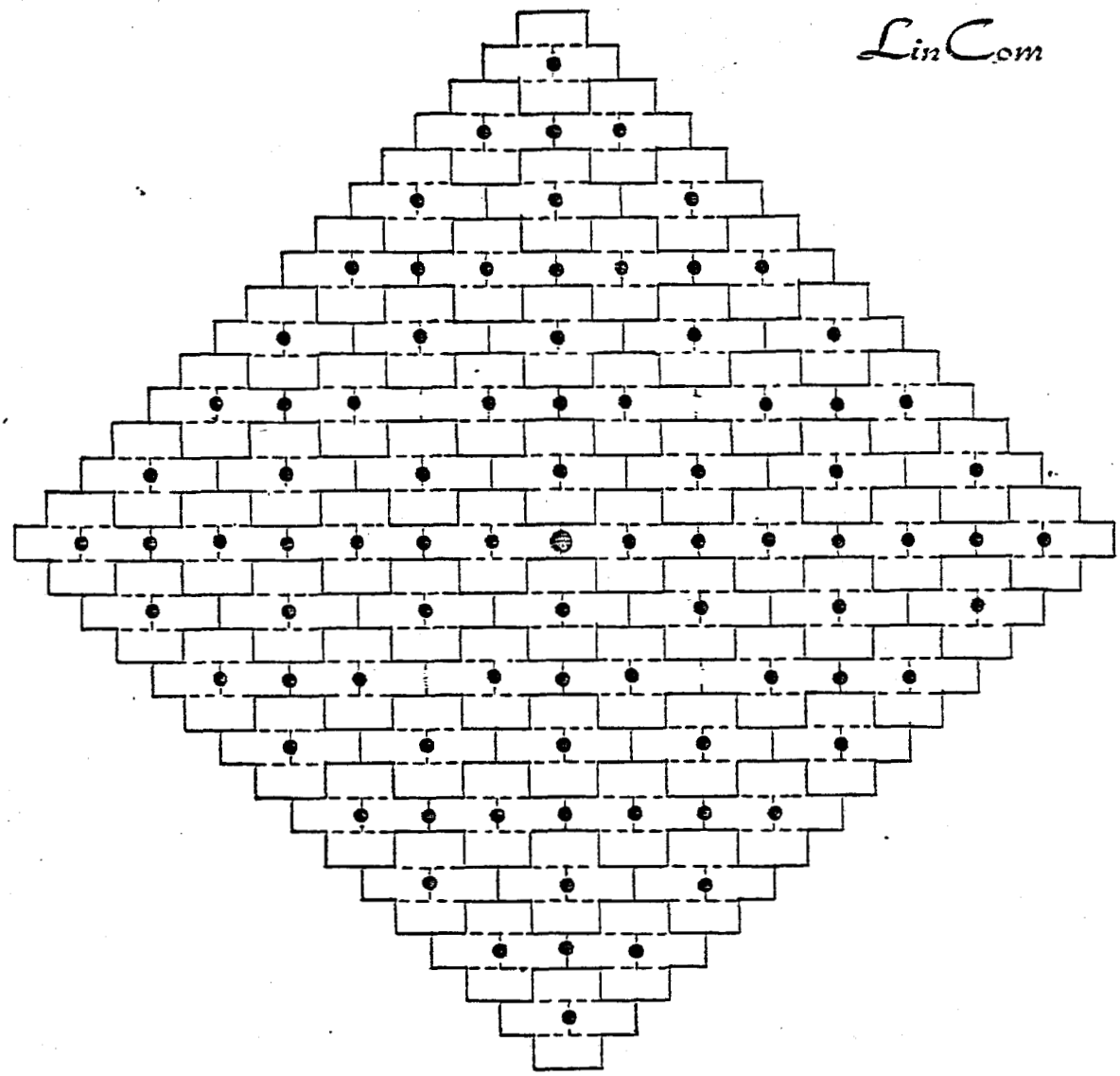

8.0 APPLICATION OF PHASE CONTROL FUNDAMENTALS TO SPS ANTENNA PHASE CONTROL

Once the PCCs are positioned on the antenna, the phase of the master PCC phase can be accomplished using any one of the phase control configurations discussed in Section 4.

8.1 Master Slave Phase Control

If the Master Slave phase control configuration is used, there are 1364 slave PCCs and one master. The master PCC distributes the phase to the first level of slave PCCs, see Fig. 26. Each of these four slave PCCs distribute their reference phase to four other PCCs in the next level of phase control and this continues until the PCCs are all exhausted. Note that the $n^{\underline{th}}$ level will have 2^{2n} PCCs. The master signal phase is conveyed to the last level of PCCs, termed terminal PCCs, via the connecting links. If the paths between two consecutive levels of slaves have the same length, then the phase and frequency of all the terminal PCCs would be identical. In what follows this Master Slave configuration will be abbreviated as MS.

8.2 Hierarchial Master Slave Phase Control in Groups of Four

This system is very similar to the one described above, see Fig. 27. The master PCC sends the phase and frequency to four first level slave PCCs. These four PCCs are connected in the Mutual Synchronous configuration described earlier. Each of these distribute their reference phase to four slave PCCs located in the next level of the hierarchy of PCCs. These groups of four PCCs are connected in the Mutual Synchronous configuration. This follows until we reach the terminal PCCs. Figure 27 shows such a connection.

Figure 26. MASTER-SLAVE PHASE CONTROL

LinCom

- Total Number of PCCs = 1365

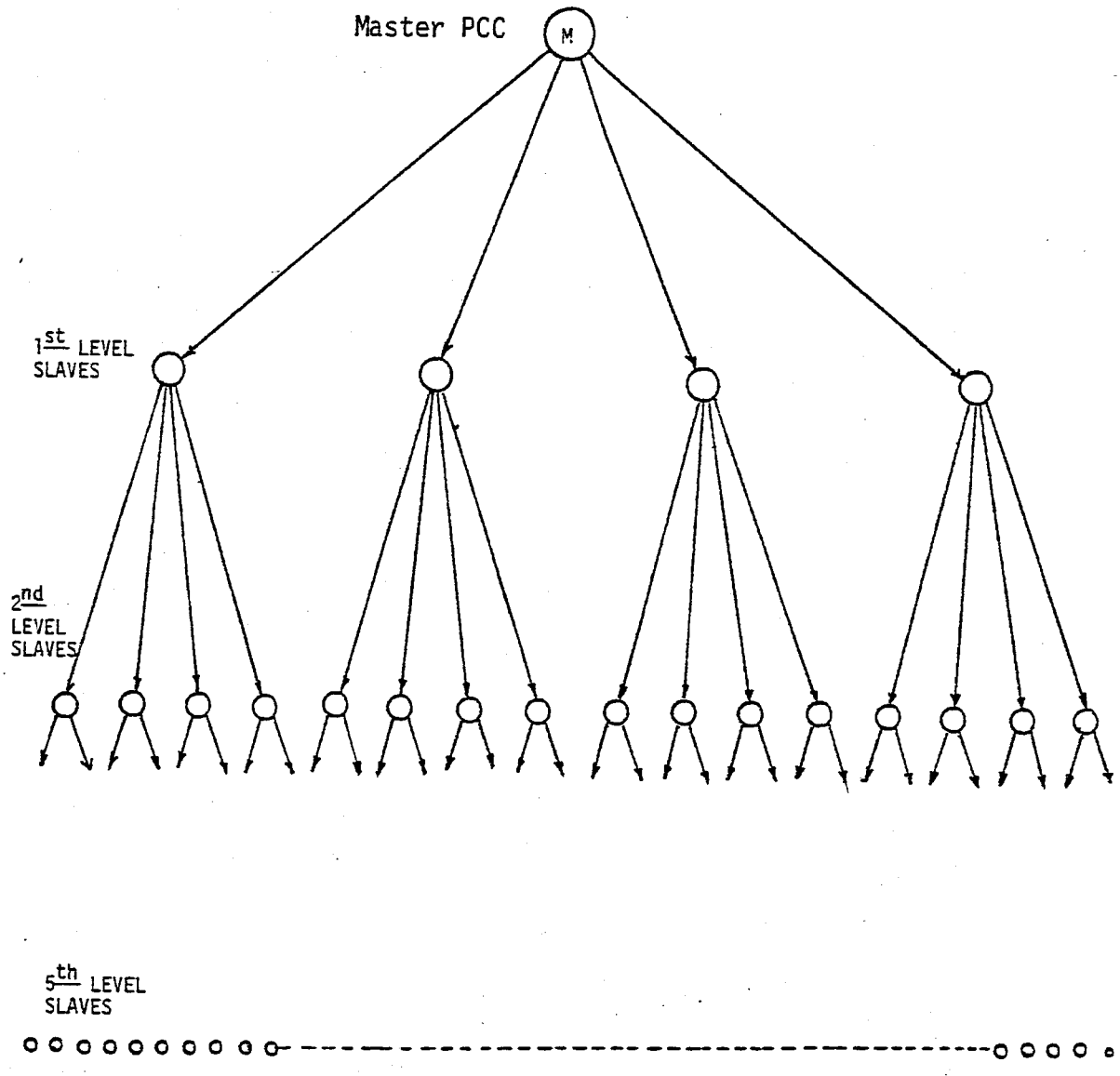

Figure 27. MASTER SLAVE HIERARCHIAL PHASE CONTROL IN GROUPS OF FOUR

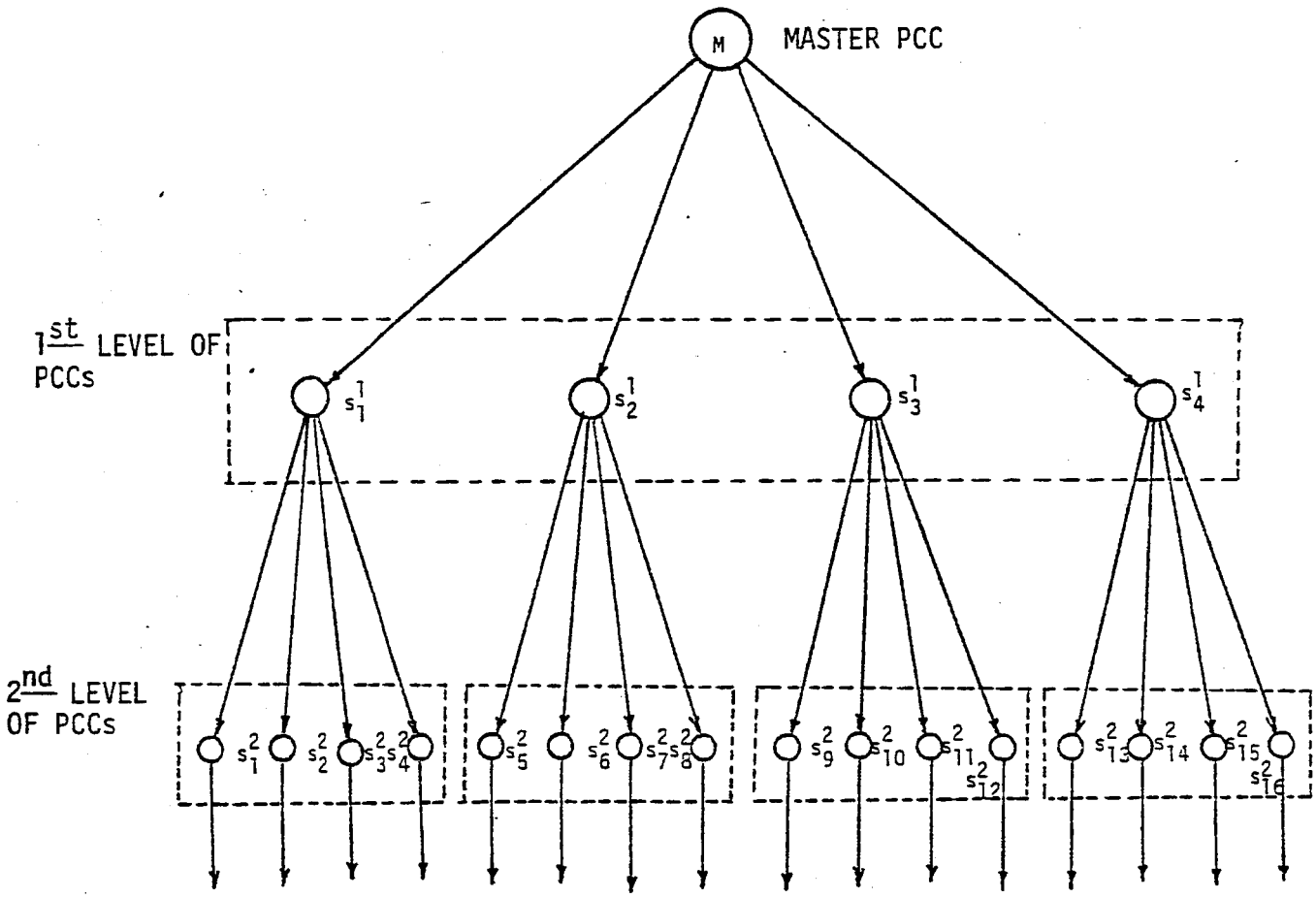

By imposing the Mutual Synchronous configuration on the groups of four PCCs, this configuration improves the system performance in terms of the differential phase build up at the cost of the increased cable length. Typical cable length calculations are presented in the next section. This system will be termed Hierarchial Master Slave Configuration 1 (HMS1).

8.3 Hierarchial Master Slave Phase Control in Groups of 4^n

As before, the master PCC distributes the reference phase to the four PCCs in the first level of slave PCCs, see Fig. 28. These four PCCs are connected in the Mutual Synchronous configuration. Each PCC in the 1^{st} level of the hierarchy distributes the phase and frequency to four PCCs in the next level. Thus there are $4^2 = 16$ PCCs in the second level. These 4^2 PCCs are connected in the Mutual Synchronous configuration. This goes on until we reach the terminal PCCs. Thus at the n^{th} level of the hierarchy of PCCs, there are 4^n PCCs and they are connected in the Mutual Synchronous configuration. This configuration increases the required cable length but the phase build up in the system is reduced considerably. Figure 28 depicts this configuration and we will find it convenient to refer to this configuration as the Hierarchial Master Slave Configuration 2 (HMS2).

It should be pointed out that instead of imposing the mutual synchronous connection on the groups of 4 PCCs on HMS1 and groups of 4^n PCCs in HMS2, we can impose the RTC also.

Figure 28. MASTER SLAVE HIERARCHIAL PHASE CONTROL IN GROUPS OF 4^n

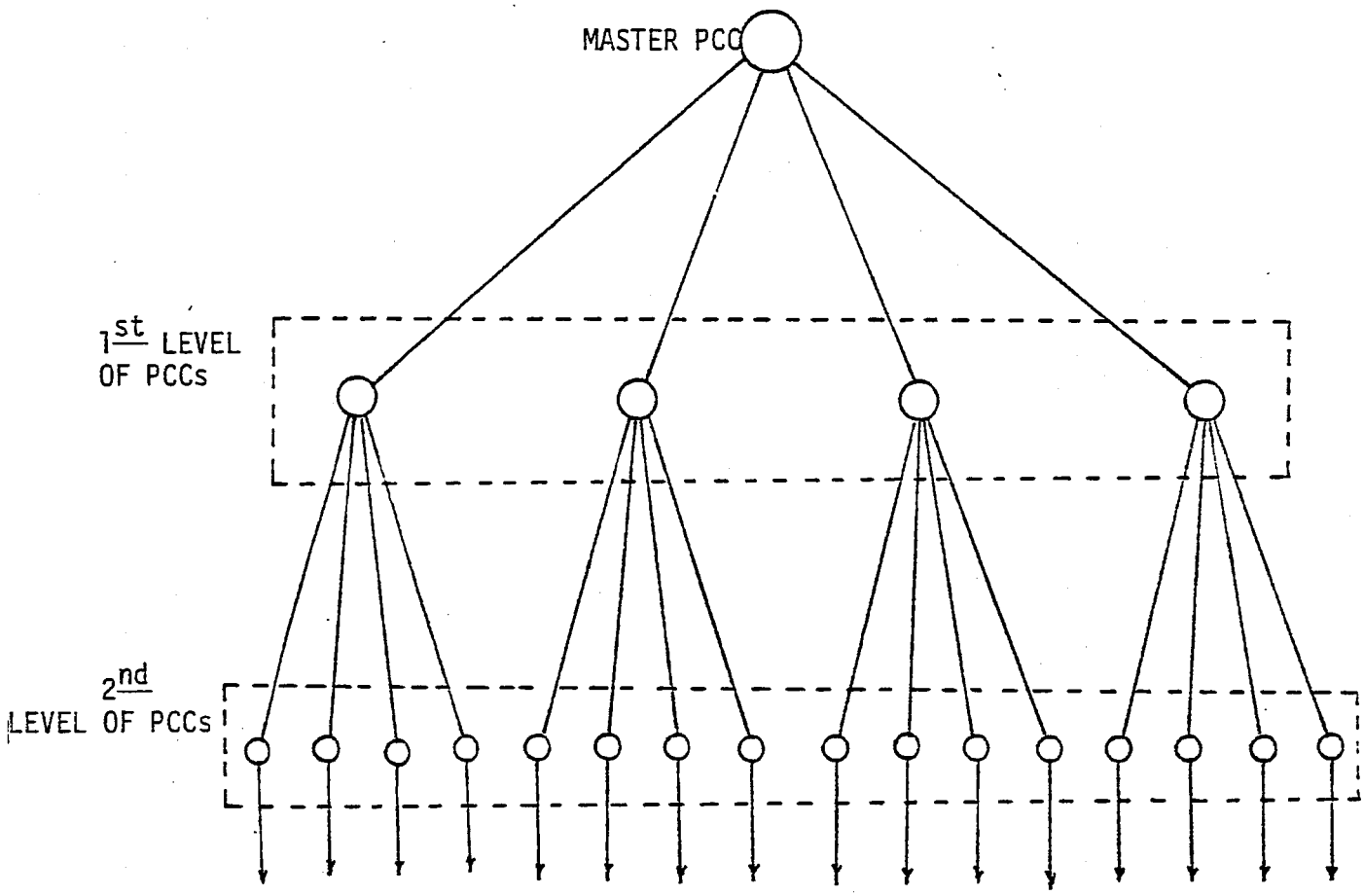

8.4 Master Slave Returnable Timing System Hybrid Configuration

The master PCC senses and locks on the incoming pilot phase. This phase is then sent to the next PCC by MSRTS which nullifies the path delay effects. The phase is used here for the conjugation circuits and then sent to the next PCC. This continues till all the subarrays are exhausted. In this system there is only one PCC per subarray to receive the incoming phase (signal) and there is no need for distribution PCCs. This type of feed is essentially a series feed. The operation of this system is independent of the path delays which means zero phase build up. Fig. 29 shows the MSRTS Hybrid building block.

There are two ways phasing of the antenna could be accomplished. (1) the master PCC could be placed at the center of the antenna and the aperture could be covered in a spiral fashion as shown in Fig. 30 distributing the phase to various PCCs. (2) The master PCC is placed at one of the corners of the rectangular antenna and then the antenna is scanned in parallel lines. This is shown in Fig. 31.

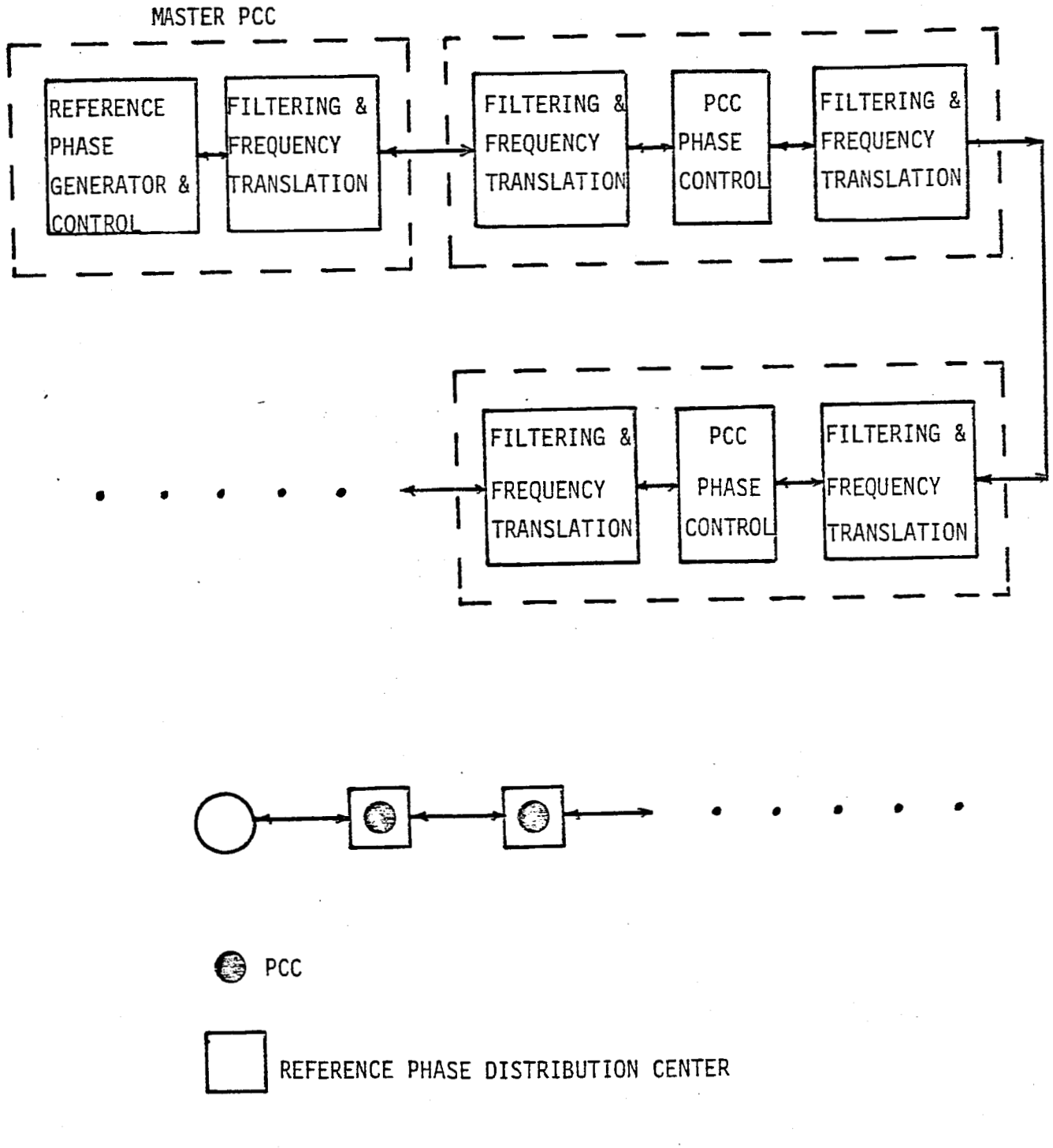

Figure 29. MSRTS Hybrid Building Block

Figure 30. MSRTC REFERENCE PHASE DISTRIBUTION SYSTEM FOR HEXAGONAL SUBARRAY LAYOUT

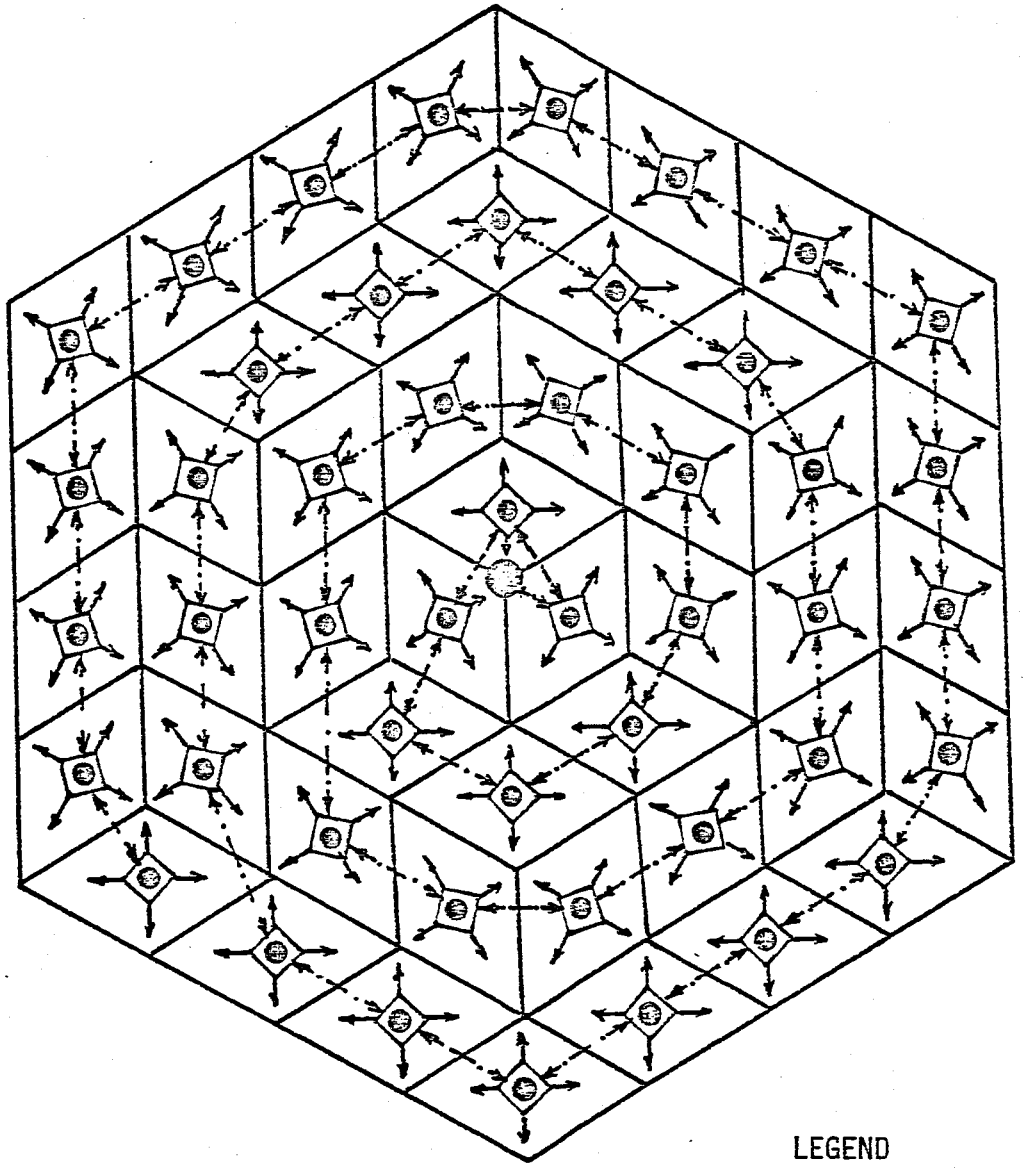

NUMBER OF PCCs = 2048

CABLE LENGTH ≅ 28 miles

LEGEND

● PCC

□ REFERENCE PHASE DISTRIBUTION CENTER

Figure 31. MSRTC REFERENCE PHASE CONTROL SYSTEM

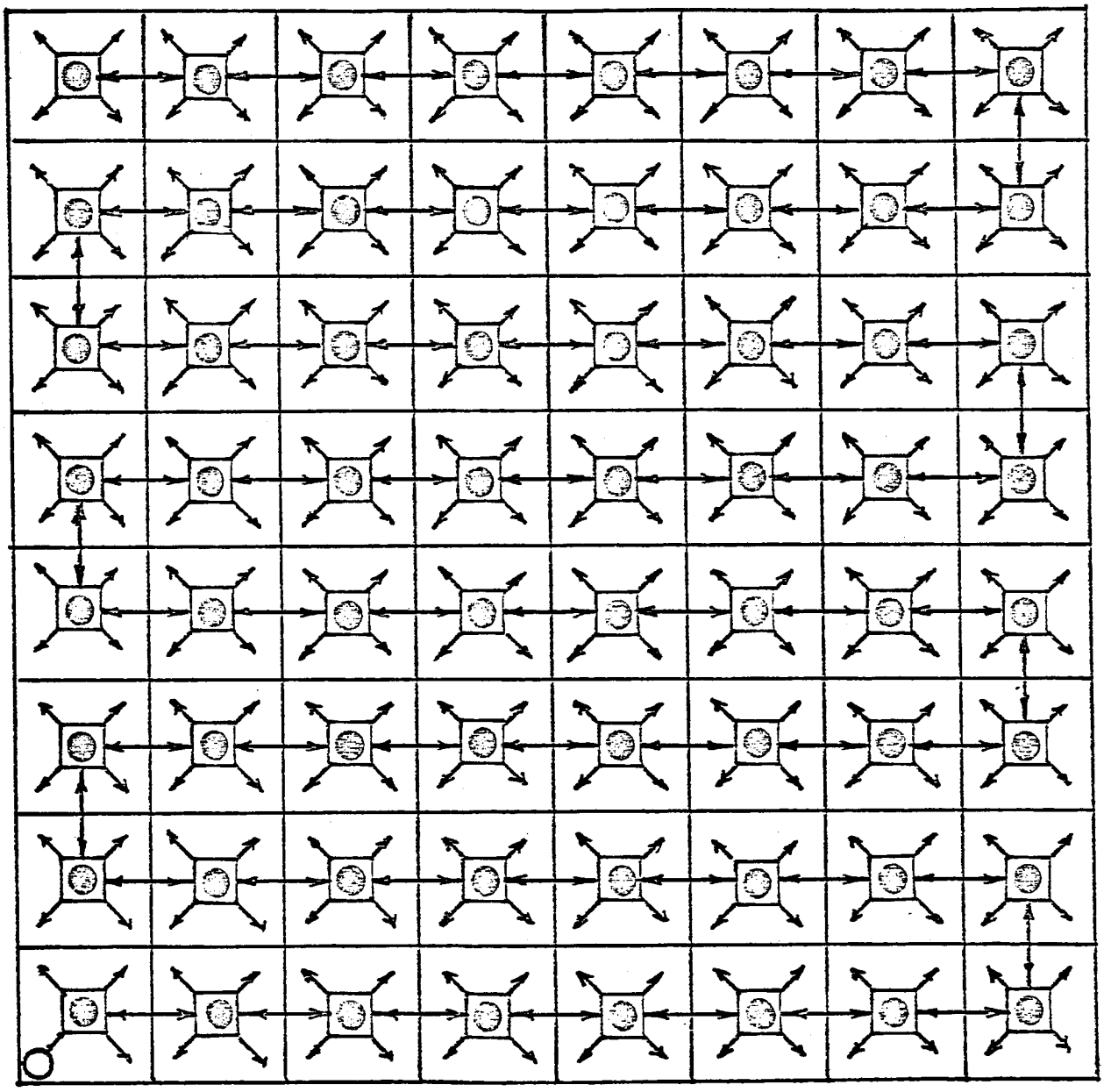

NUMBER OF PCCs = 1024

CABLE LENGTH REQUIRED ≅ 25 miles

LEGEND

● PCC

□ REFERENCE PHASE DISTRIBUTION CENTER

9.0 SYMMETRY REQUIREMENT AND PHASE BUILD UP

In a master slave configuration, eq. (3.1.1-3) suggests that a constant phase is distributed to the receiving PCC at any level when the path lengths between any two successive levels is the same. This implies symmetry to a certain extent. If the path lengths are not exactly identical between any two levels, a phase build up results. Using (3.1.1-3) we can compute this phase build up for the system.

In HMS1, (3.1.1-3) can be used to show that the phase build up will be negligible only if equality of path lengths is enforced on the links. The top half of Fig. 32 symbolizes this. On the other hand, using the RTC configuration instead of the mutual synchronous configuration in the HMS1 relieves the symmetry constraint to that illustrated in the bottom half of Fig. 32.

The phase build up can be computed using the theory given in Section 4. First we will compare the phase build-up of the MS with that of HMS1 with the RTC in groups of four. It can be shown that the phase build up for MS is worse than the HMS1 by a factor of 9 at the first level of PCC slaves, by a factor of 1.8 at the secondlevel of PCC slaves, by a factor of 1.42 times at the third level of PCC slaves, by a factor of 1.3 at the fourth level of PCC slaves and 1.22 times at the fifth level of PCC slaves.

Let us now investigate the HMS2 with the RTC connection at any level of slave PCCs rather than a mutual synchronous connection. Here, the phase build up for the MS configuration is worse than HMS2 by a factor of 9 at the first level of slave

Figure 32. SYMMETRY ESSENTIAL FOR A MUTUAL SYNCH. SYSTEM PHASE CONTROL

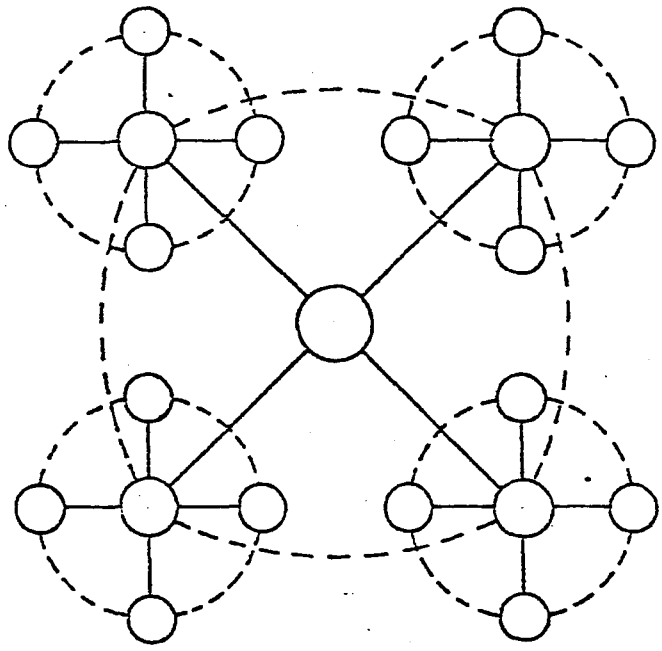

SYMMETRY UNESSENTIAL FOR HIERARCHIAL MASTER SLAVE RETURNABLE TIMING SYSTEM PHASE CONTROL

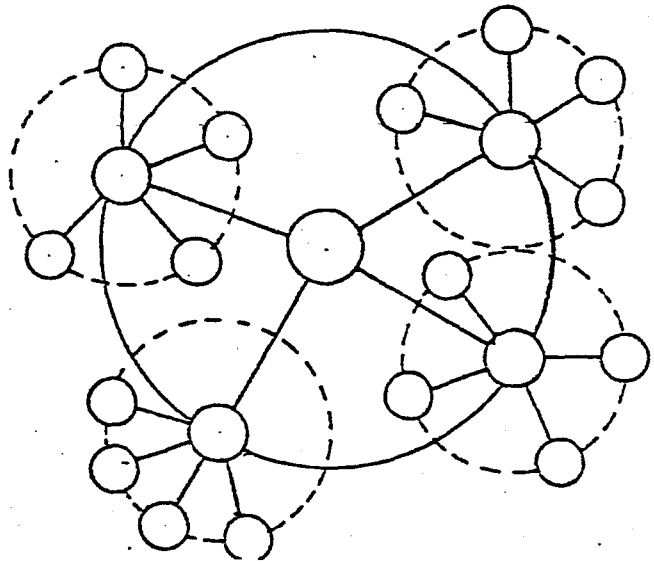

PCCs, by a factor of 66 at the second level of PCCs, by a factor of 387 at the third level, by the factor 4050 at the fourth level and by 10265 times at the fifth level.

Figs. 33 & 34 summarize this comparison. The actual connections of the PCCs is shown in Figs. 35 and 36. Here we have assumed a MS scheme, HMS1 and HMS2 schemes will just superimpose mutual synchronous connection or the RTC connection on the groups of four or groups of 4^n, respectively. The arrowheads show the direction of flow of the reference signal.

We saw above the HMS2 is quite superior to HMS1 and MS configuration when the phase build up is considered, but it needs an excessive amount of cable length, also it needs equal lengths of cable between two successive levels. The cable lengths necessary for MS, HMS1 and HMS2 from the master PCC to the terminal PCCs is shown in the table in Fig. 37 .

MSRTC which uses the Master Slave series feed with the returnable timing feature added does not need any symmetry. This system also has no phase build up associated with it. Thus it seems that MSRTC phase build up is by far the best phasing system for the antenna.

SPS REFERENCE PHASE DISTRIBUTION SYSTEM COMPARISONS		
SYSTEM CONCEPT	ADVANTAGES	DISADVANTAGES
MASTER SLAVE	MINIMIZES CABLE LENGTH	PHASE BUILD UP, PHASE JITTER
HIERARCHIAL MASTER SLAVE SYSTEMS	CONTROLS PHASE BUILD UP AND PHASE JITTER	USES MORE CABLE, PHASE BUILD-UP DEPENDS ON DIFFERENTIAL PATH DELAYS
MS RTS HYBRID	CONTROLS PHASE BUILD UP AND PHASE JITTER, MINIMIZES CABLE LENGTH	

Figure 33. SPS Reference Phase Distribution System Comparisons.

Figure 34. PHASE BUILD UP COMPARISONS

Δ CABLE LENGTH (cms)	∇ PHASE FOR MASTER SLAVE		∇ PHASE FOR HMS 1		∇ PHASE FOR HMS 2	
	f 2.45×10^9	f 70×10^6	f 2.45×10^9	f 70×10^6	f 2.45×10^9	f 70×10^6
0.2	29.4°	0.42°	24.17°	0.345°	0.002869°	4.09×10^{-5}
4.0	588°	16.8°	483°	13.81°	0.05739°	1.639×10^{-4}
10.0	1470°	42°	1208°	34.53°	0.14348°	4.099×10^{-3}
70.0	10290°	294°	8460°	241°	1.0043°	0.0287°
90.0	13230°	378°	10878°	310°	1.2913°	0.03689°
2500	367500°	10500°	302166°	8633°	35.8°	1.02°

∇Phase for MSRTC = 0°

Figure 35. MASTER SLAVE PHASE CONTROL IN SQUARE LAYOUT

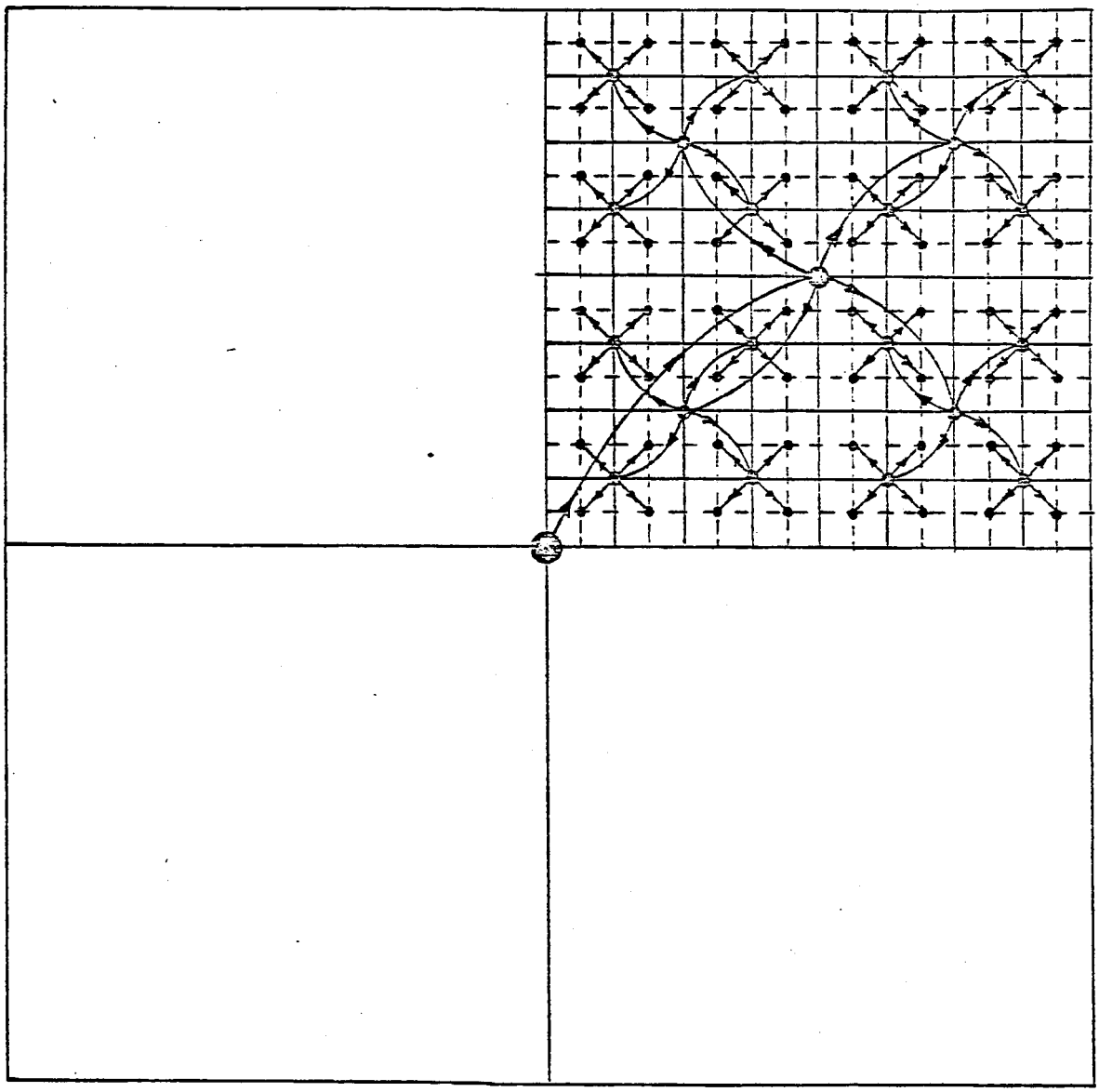

Figure 36. MASTER SLAVE PHASE CONTROL IN STAGGERED RECTANGULAR LAYOUT

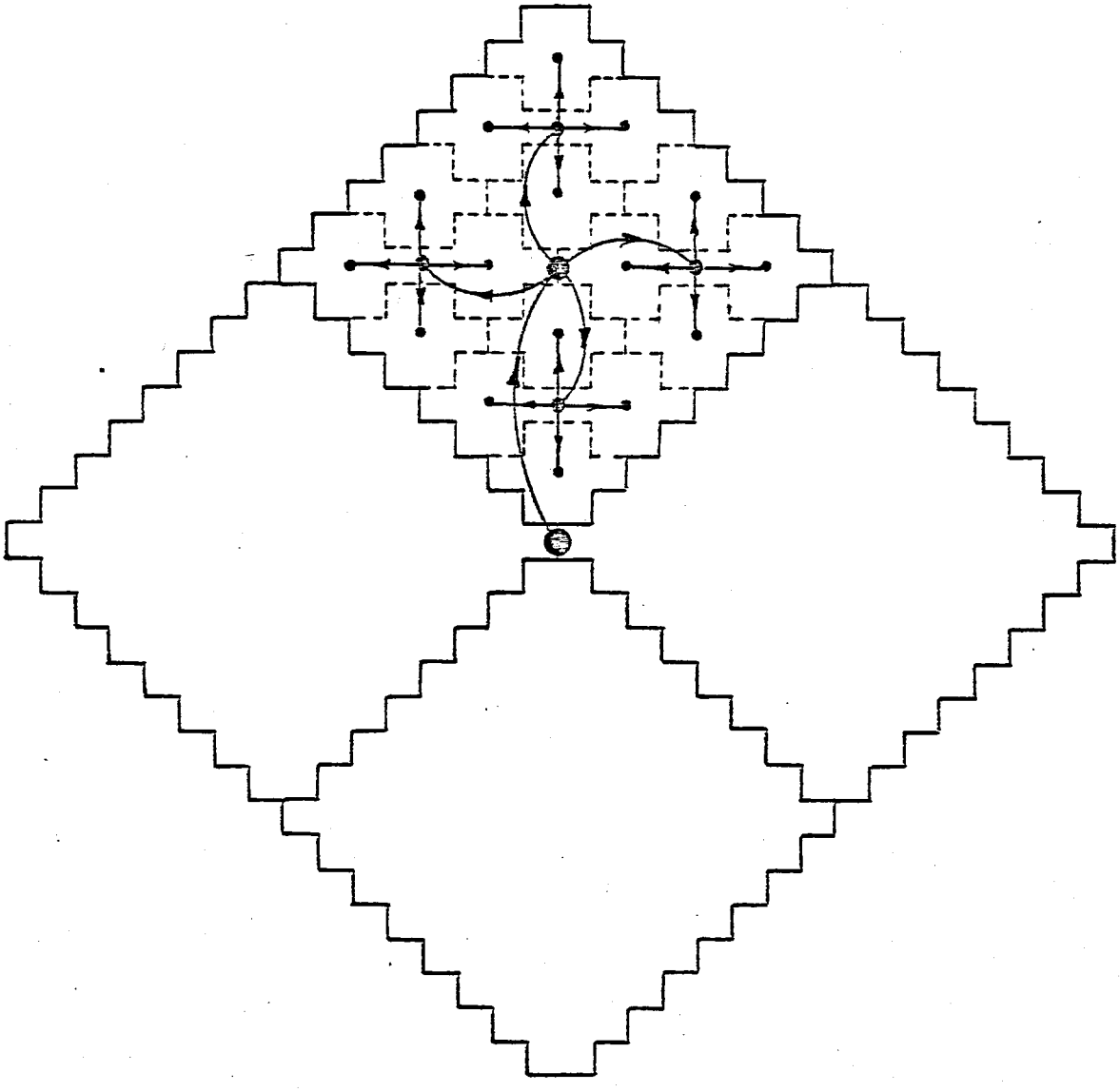

CABLE OR WAVEGUIDE LENGTH (MILES) TO TERMINAL PCC			
LEVEL	MS	HMS1	HMS2
1	0.05	0.17	0.17
2	0.3	0.77	3.8
3	1.4	3.3	122
4	5.9	13.5	3,905
5	24	55.1	124,740

MSRTC (Square): 25 Miles
(Spiral): 28 Miles

Figure 37. Cable or Waveguide Length to Terminal PCCs.

10. PHASING OF THE POWER AMPLIFIERS

The power amplifiers add their own instabilities to the phase of the signal they are amplifying. This is accomplished through their AM-AM and AM-PM characteristics. If left unattended, this phase noise effect reduces the power transfer efficiency by producing a phase jitter on the transmitted beam caused by the received beam to wander randomly over the aperture of the rectenna.

One way of phasing the power amplifier is to connect the power amplifiers using one of the phase control configurations described in Sections 3 and 4. If the Master Slave Configuration is used then the power amplifier layout around the point of reference (the terminal PCC) should be symmetric in order to minimize the phase build up. This is shown as the dashed circle in Figure 38 for the rectangular and square layout. If the RTC is used to connect the power amplifiers, the symmetry requirement can be largely avoided and the power amplifiers placed at the base of the radiating elements. The cable length associated with the power amplifier layout is shown in Table 1 of Fig. 39 and Table II gives the total length of the cable for MS, HMS1 and HMS2 reference phase distribution configuration plus the power amplifier layout.

proposed to be used in the system have a considerable phase jitter. Since mutual coupling reduces the phase jitter of oscillators, the same technique could be used for reducing the phase jitter of the amplifiers. The mutual synchronization could be applied at different levels resulting in Fig. 41 , and Fig. 42.
Although the figures shown assume the MS, mutual synch or RTC mode of reference distribution, it can be made applicable to MSRTC equally well.

Figure 38. LAYOUT OF POWER AMPLIFIERS

● RECTANGULAR LAYOUT

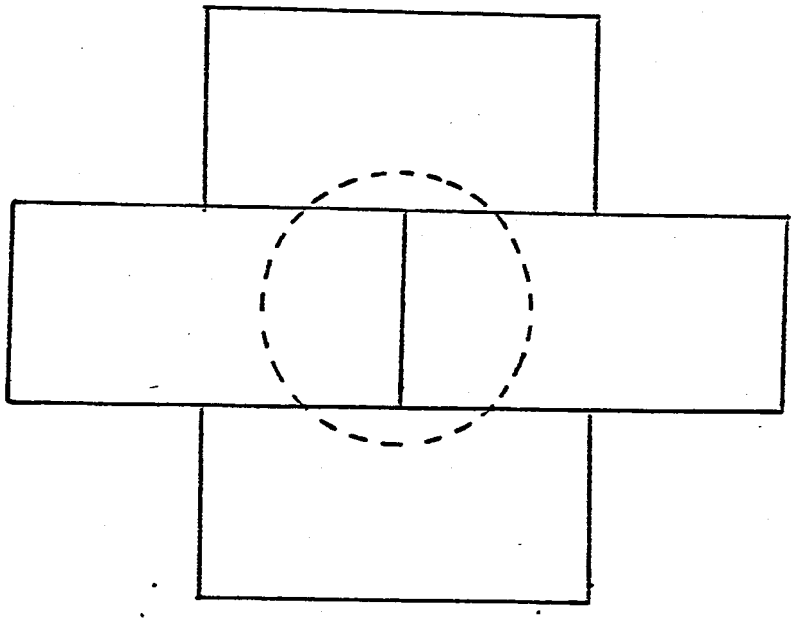

● SQUARE LAYOUT

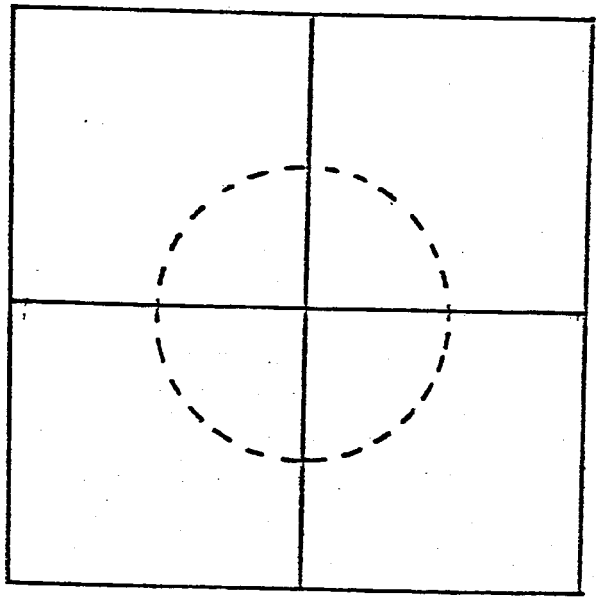

CABLE OR WAVEGUIDE LENGTH (MILES) TO PAs	
1	0.49
2	1.95
3	7.8
4	31.2
5	124.7

Table I.

CABLE OR WAVEGUIDE LENGTH (MILES) TO PCCs PLUS PA PHASING			
LEVEL	MS	HMS1	HMS2
1	0.53	0.66	0.6
2	2.2	2.7	5.8
3	9.2	11	130
4	37	45	3,936
5	149	180	124,864*

*Equals Five Times Earth's Circumference

Table II.

Figure 39. Cable or Waveguide Length to PCCs Plus PA Phasing.

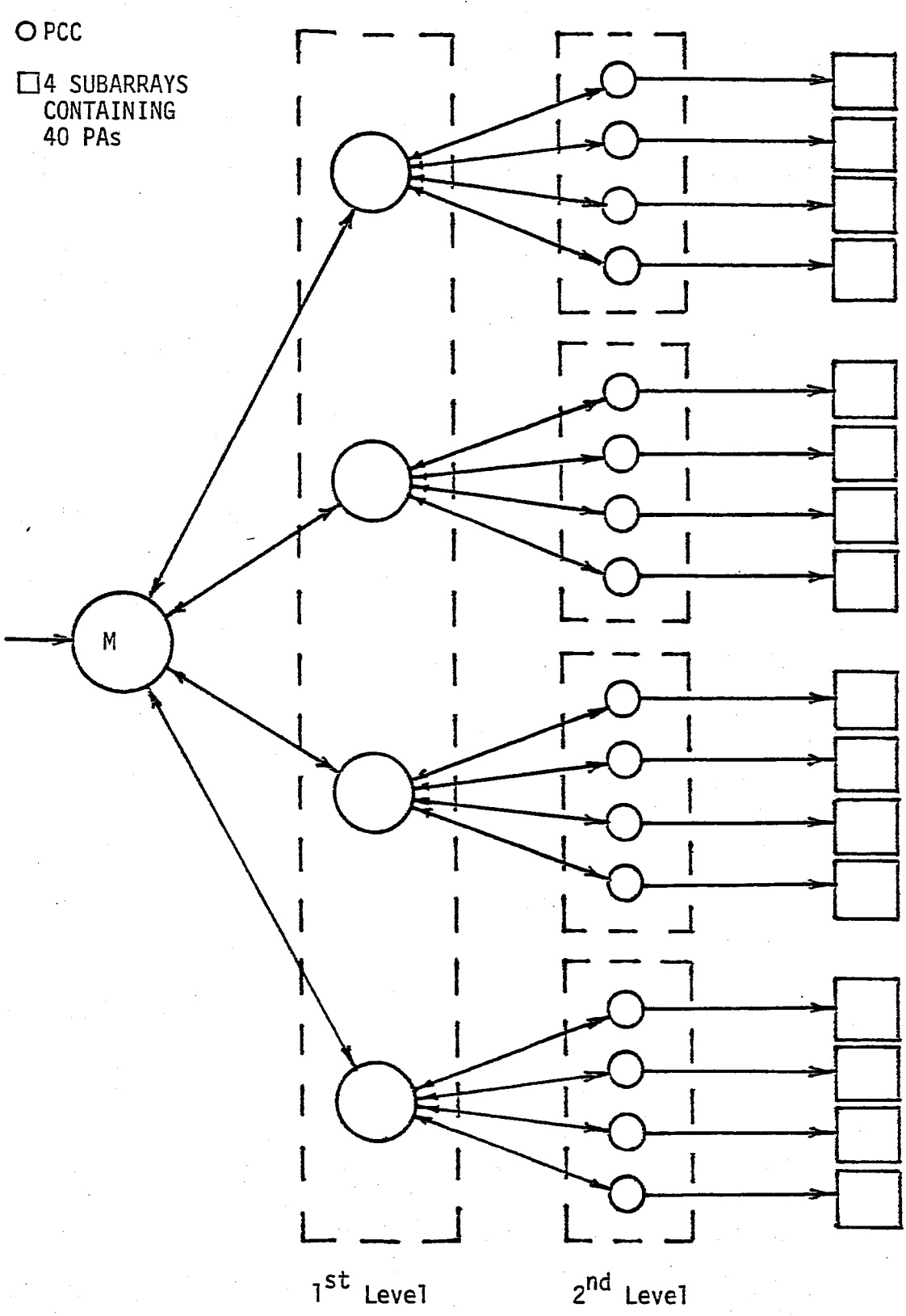

Figure 40. Converter of PA's in Subarrays.

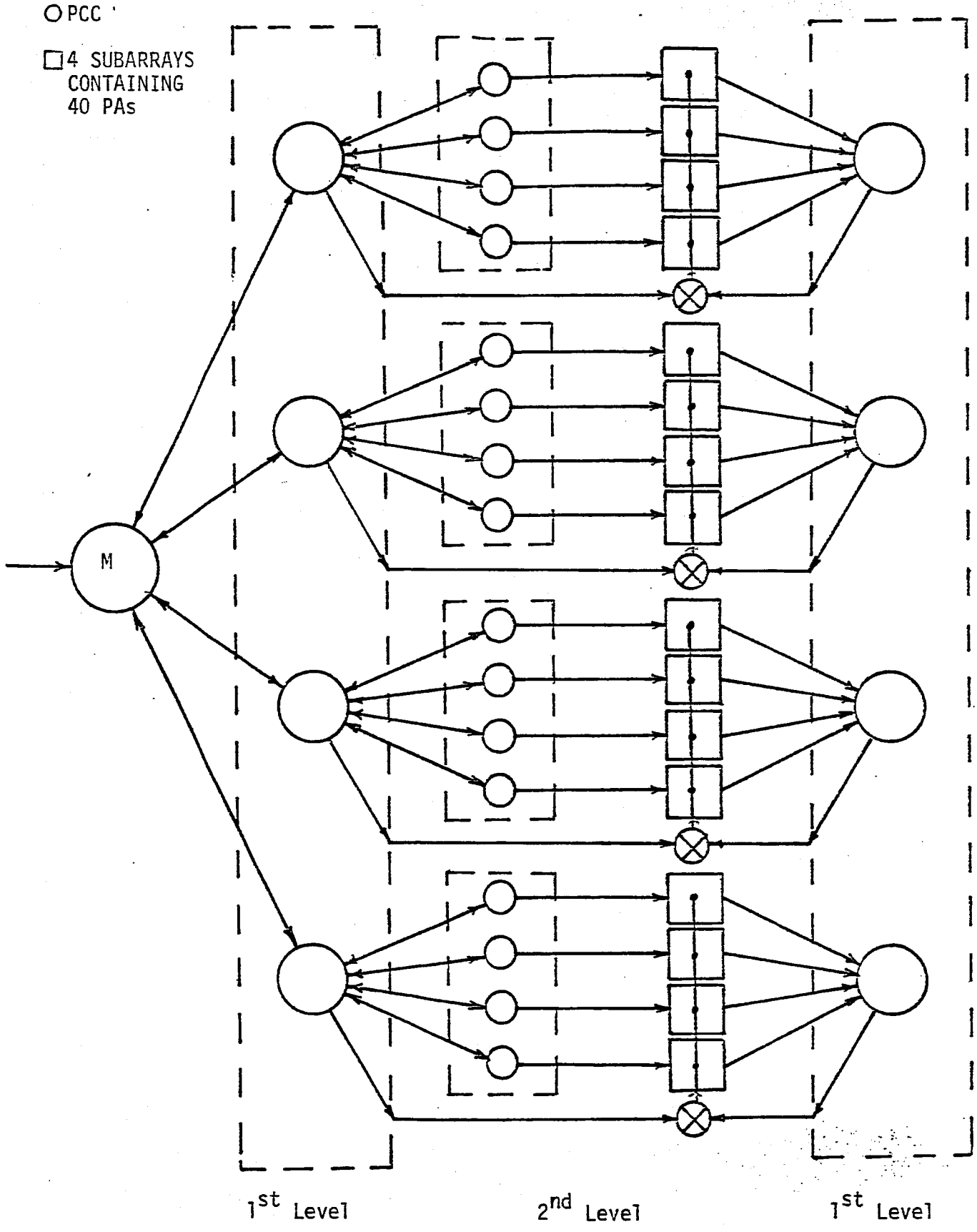

Figure 41. Mutual Synch Imposed on 1st Level of PAs.

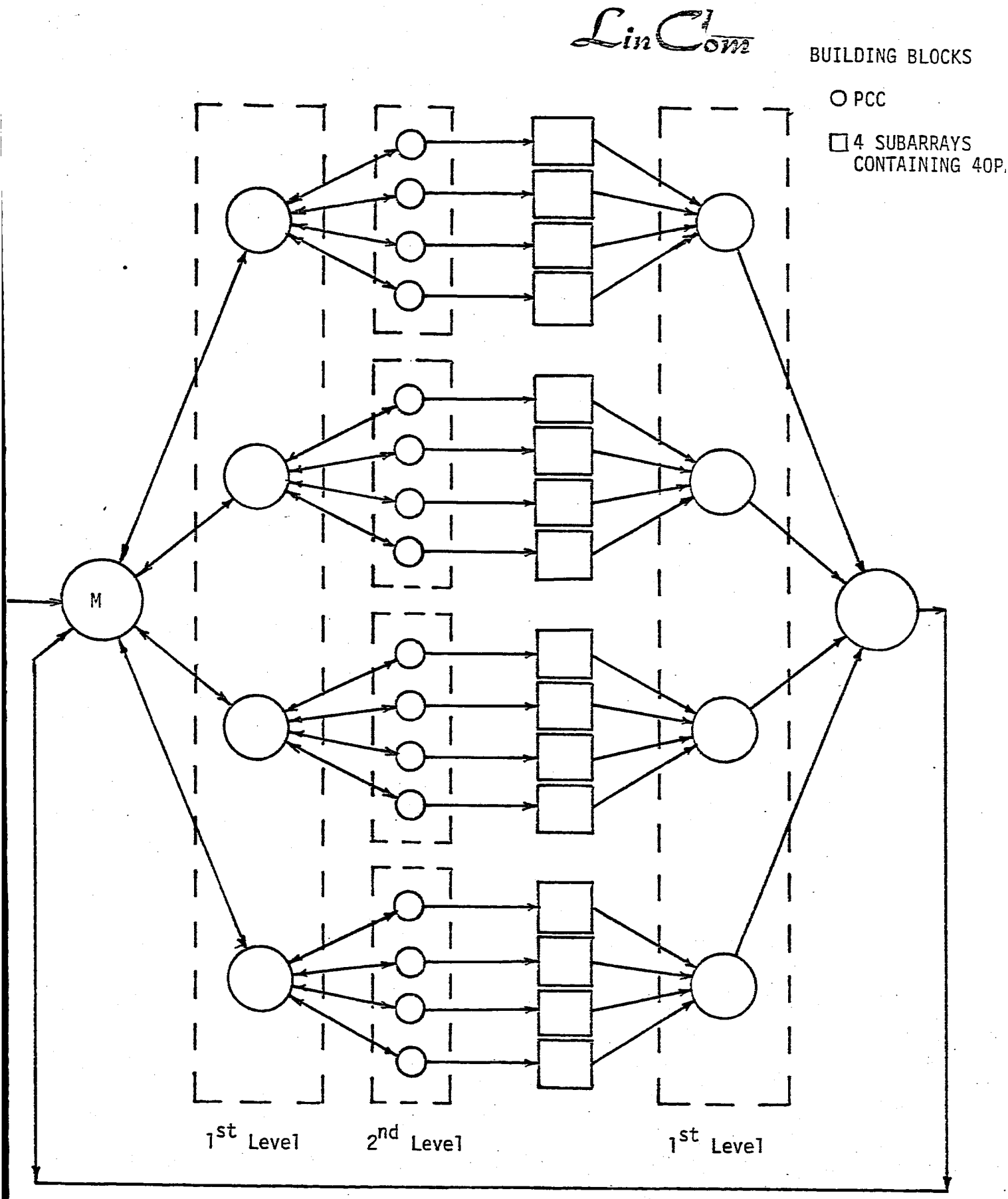

Figure 42. Mutual Synch Imposed on the PAs for Two Levels.

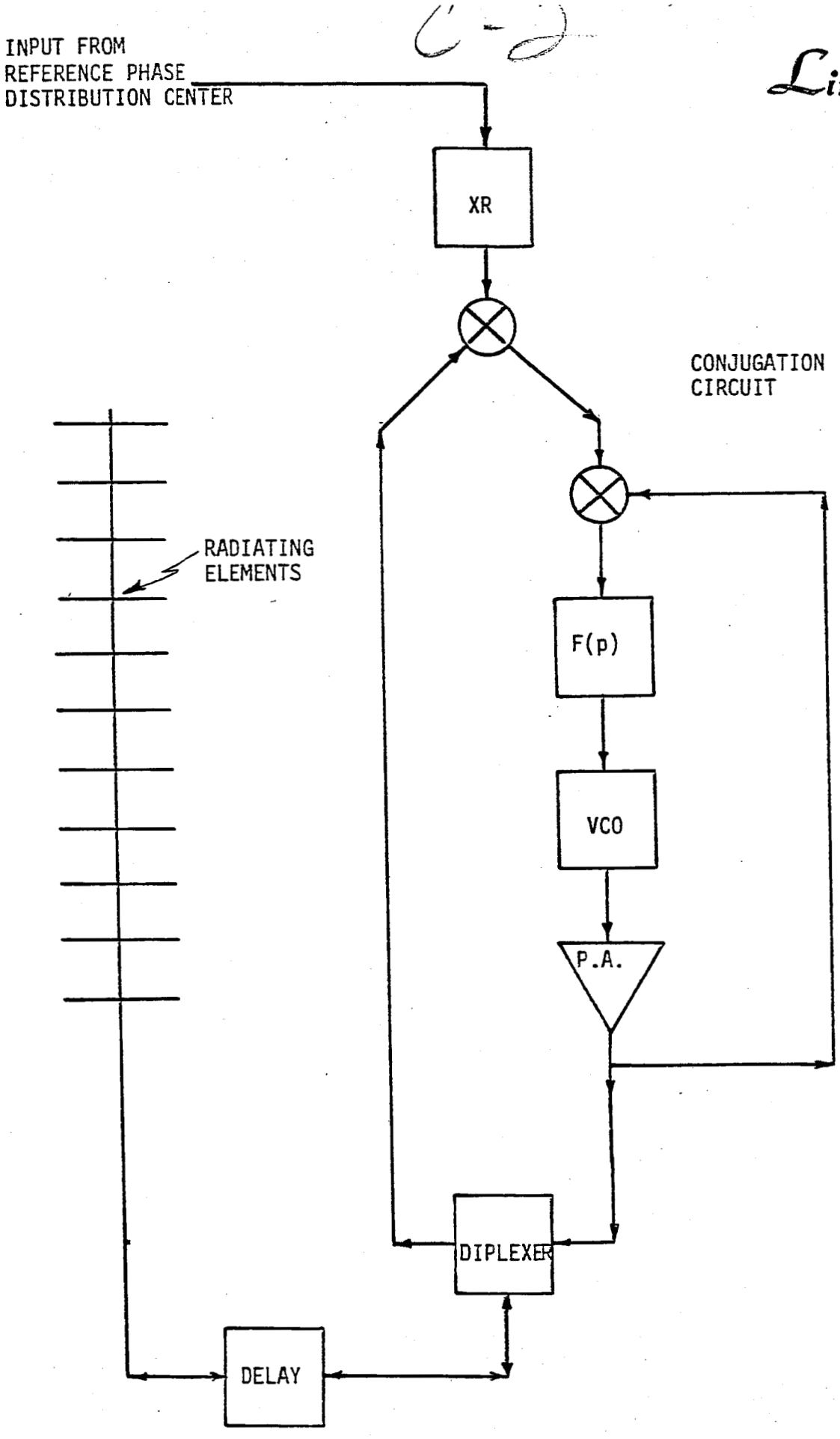

Figure 43. FUNCTIONAL DIAGRAM OF POWER AMPLIFIER PHASING AND CONJUGATION CIRCUIT

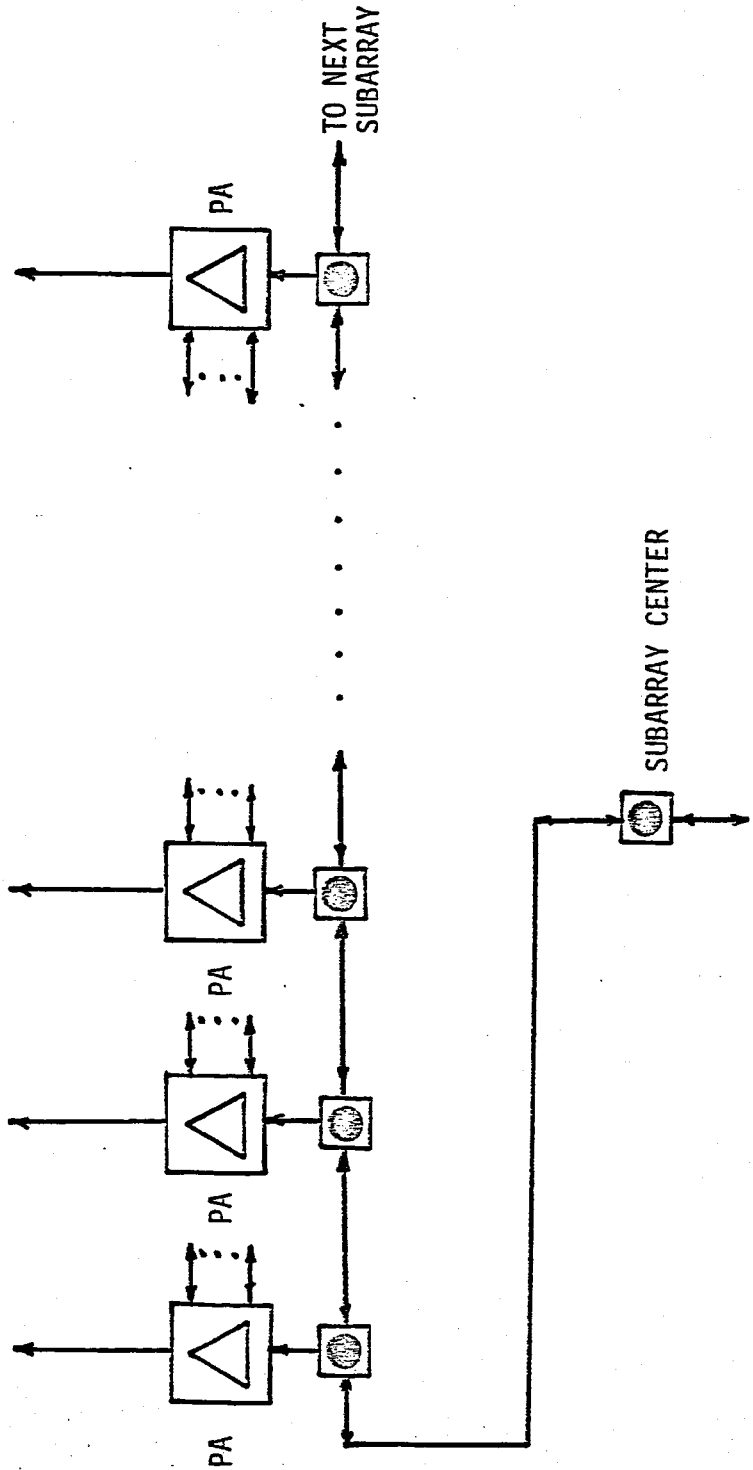

Figure 44. CONNECTIONS OF PAs IN A SUBARRAY

11. ANTENNA BEAM STEERING

As was pointed out in Sections 3.1 and 3.2 there are two different ways of forming and steering the SPS antenna beam. (1) On-board phase control via phase conjugation and (2) SPS beam forming and steering via the ground station. In this section we will try to develop the theory for these two methods and enumerate the advantages and disadvantages they have.

11.1 On-Board Phase Control and Beam Steering via Phase Conjugation

Assume that the reference phase distribution system distributes a constant phase characteristic to each PCC. This reference is used to phase the power amplifiers. If the PAs output signals are coherent, beam pointing can be accomplished using the phase conjugation scheme. The idea is: "The phase of transmitted signal from any element in a retrodirective array must bear a conjugate relationship to the phase of the received signal at that element when compared with the common reference in the power amplifier outputs." Assuming a pilot signal is sent from the rectenna center which illuminates the antenna, the master PCC located on the SPS antenna phase locks to the incoming pilot. This phase and frequency is distributed to all the PCCs which in turn distribute the phase to the PAs. At each radiating element, the received pilot phase would be conjugated by using the constant phase supplied at the PA outputs. If done properly, a coherent beam is formed which will be automatically focused at the rectenna because of the retrodirective property created. Figure 45 is a conceptual representation of such a system. One simplified conjugation

Figure 45. ON BOARD PHASE CONTROL AND BEAM STEERING USING RETRODIRECTIVE ACTIVE PHASED ARRAY CONCEPT

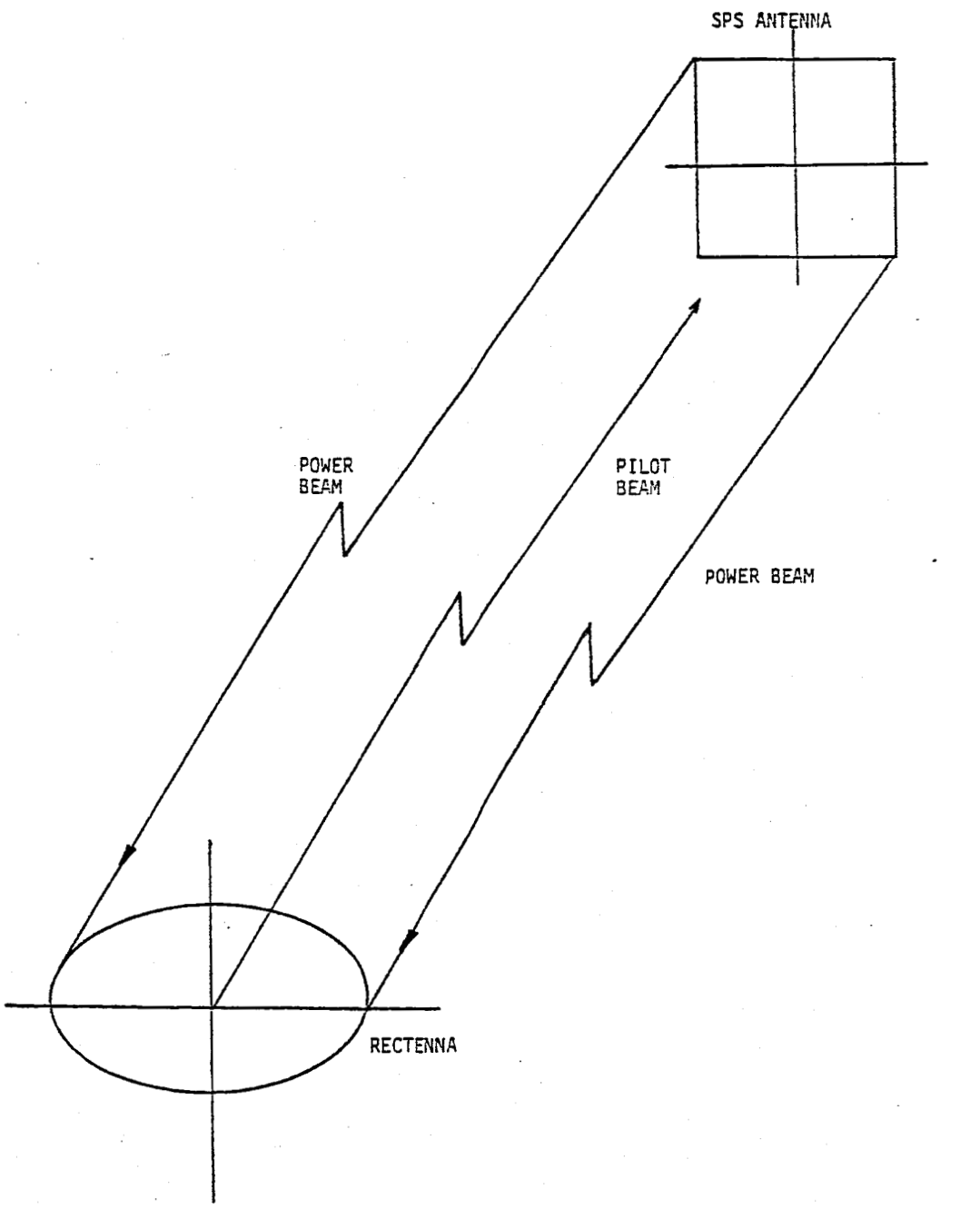

scheme is defined in Fig. 46, the line delay between the radiating element and the diplexer does not degrade performance due to the fact that after conjugation, the same path is traversed and the delay effects cancel.

The conjugation will work very well as long as the up and downlink signals have the same frequency. This is impossible because if the downlink signal, having a high power density, is at the same frequency as the uplink, the uplink will get totally annihilated and hence continuous operation of the SPS antenna is not possible. Thus a frequency separation between the uplink and downlink seems necessary to reduce the interference between the signals. This frequency separation causes a problem, viz., the frequency shift introduces a shift in the beam pointing direction, see Fig. 47. Thus to point the beam in the correct direction other phase control equipment is required. In what follows the beam shift and beam pointing problems are discussed below.

11.1.1 Frequency Separation and Beam Pointing

Figure 48 shows the geometry of the system to be used. The incident wave has a wave number K_r and a direction (α_r, β_r). The wave received by the $i^{\underline{th}}$ element is equal to

$$\frac{AW_i}{R_i} \quad e^{j(\psi - K_r R_i)} \qquad (11.1.1\text{-}1)$$

where A is a constant, W_i is an amplitude factor and R_i is the distance between the $i^{\underline{th}}$ element and the pilot source

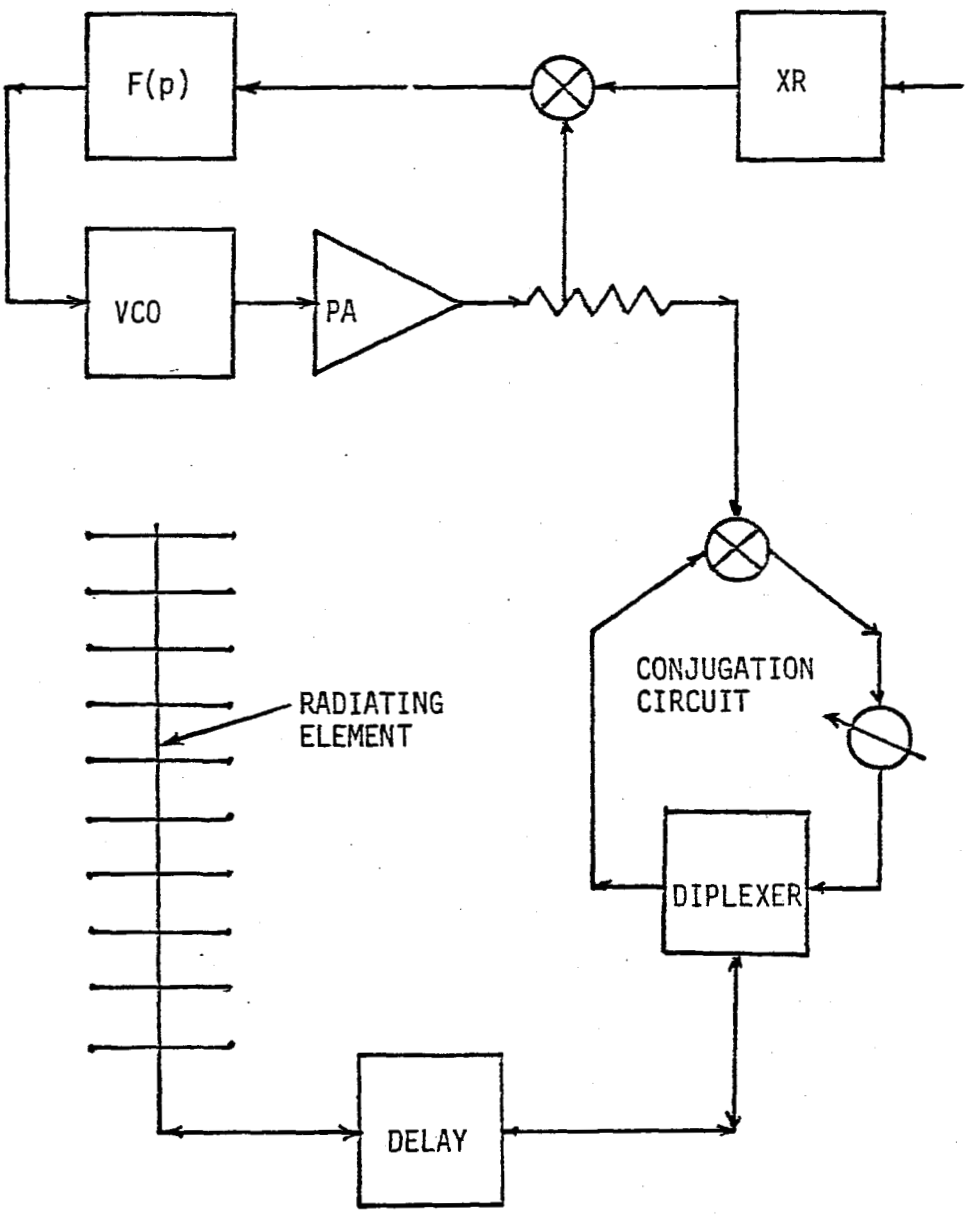

Figure 46. Functional Diagram of Power Amplifier Phasing and Conjugation Circuit.

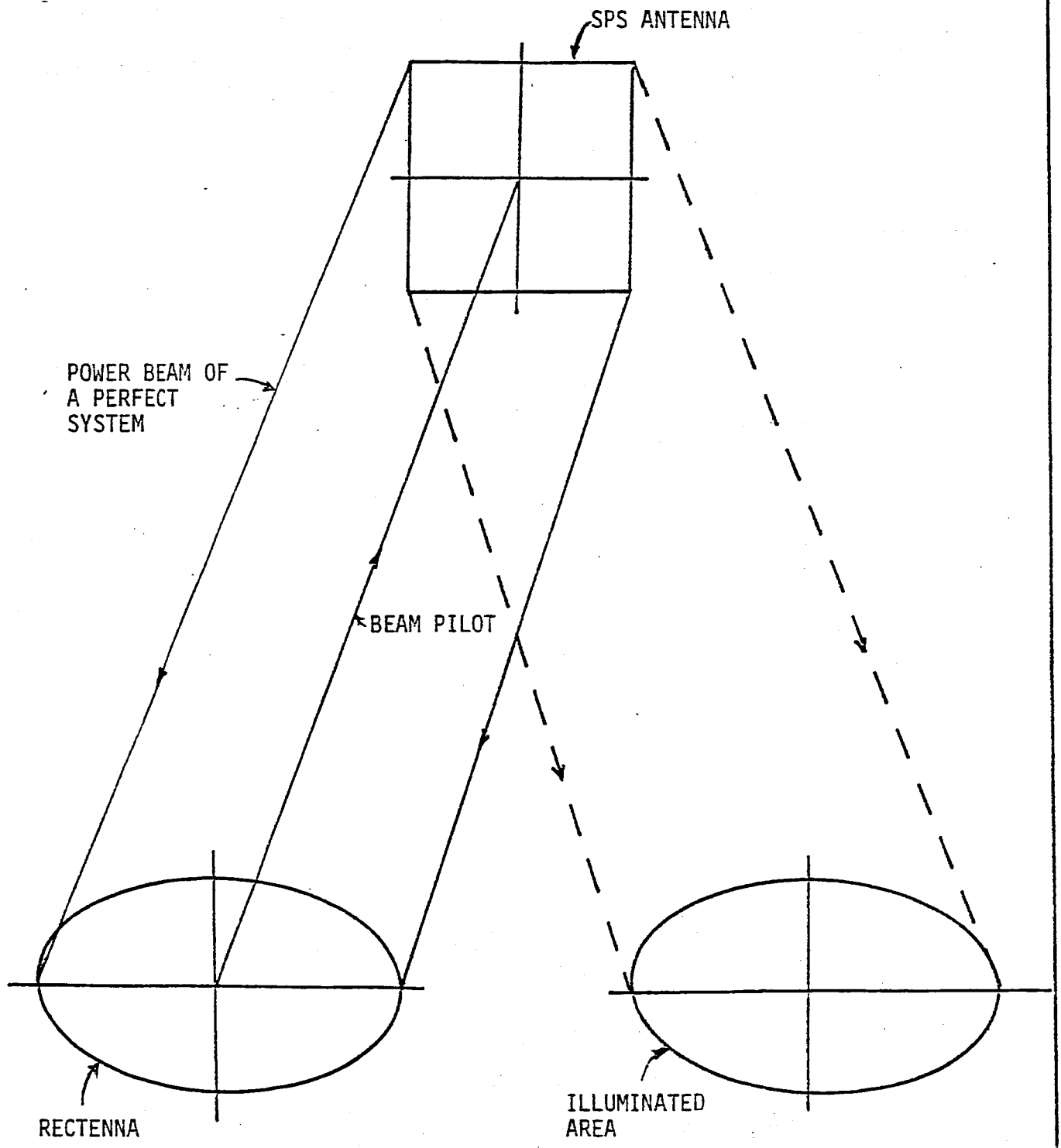

Figure 47. Effect of Frequency Separation.

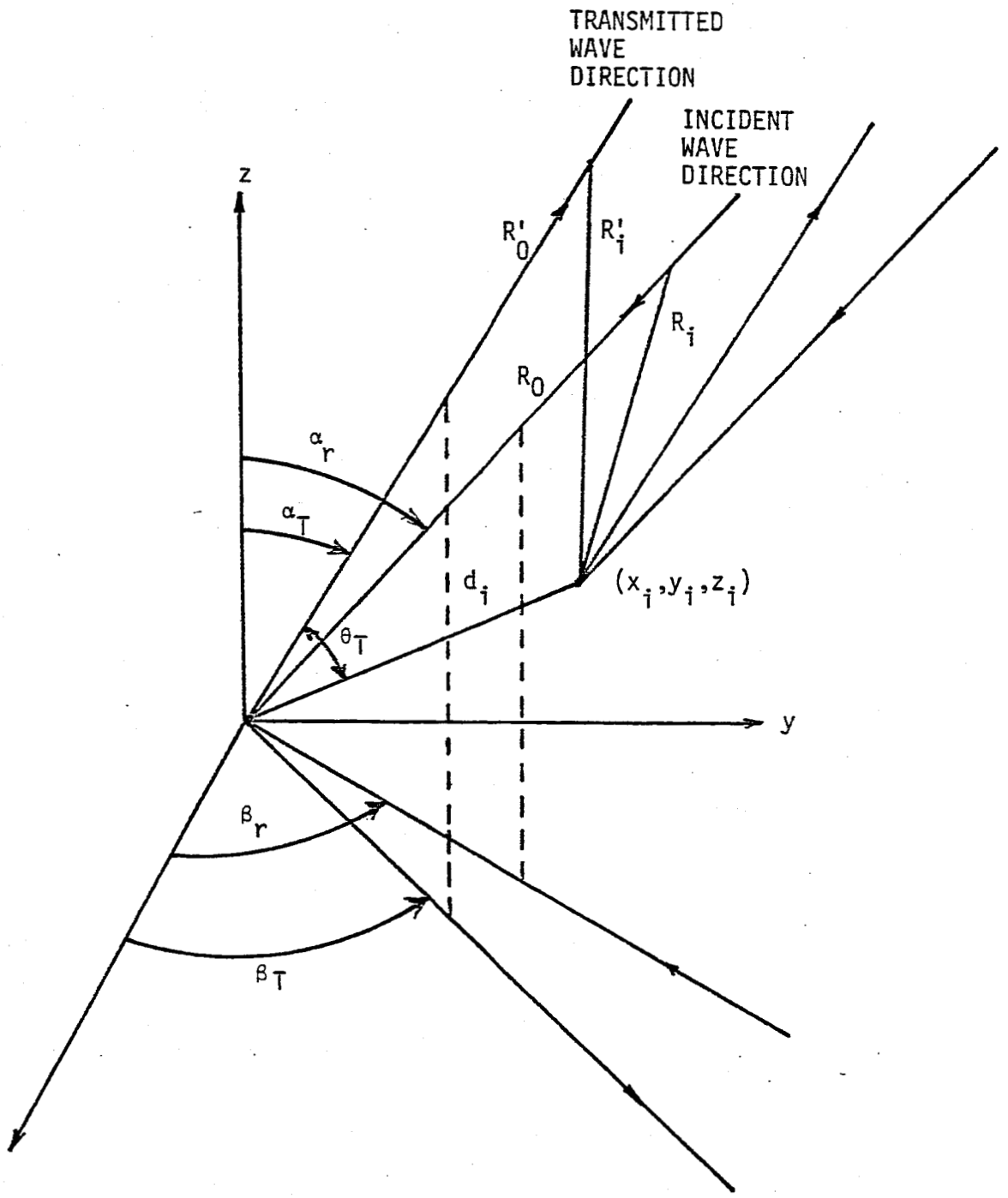

Figure 48. The System Geometry.

$$\frac{AW_i}{R_i} e^{j(\psi - K_r R_i + K_r R_0 - K_r R_0)}$$

$$Ae^{-jK_r R_0} \frac{W_i}{R_i} e^{j[\psi - K_r(R_i - R_0)]} \qquad (11.1.1\text{-}2)$$

where ψ is the arbitrary phase shift associated with the pilot source.

The phase of this received wave is conjugated in the conjugation circuit, amplified and retransmitted at a different frequency having the wave number K_T. This wave has the form $(AW_i/R_i)e^{-j[\psi - K_r(R_i - R_0)]}$ where R_0 is the distance between the pilot source and the antenna center. Depending on the frequency separation, this retransmitted wave will travel in a different direction than the direction of the incoming pilot wave. The re-radiated wave at a point R_i' from the $i^{\underline{th}}$ element would have the form

$$Ae^{-jK_T R_0'} \frac{W_i}{R_i} e^{-j[\psi - K_r(R_i - R_0)] - jK_T(R_i' - R_0')}$$

Hence the total wave would be

$$Ae^{-j(K_T R_0' + \psi)} \sum_{i=1}^{N} \frac{W_i}{R_i} e^{+j[K_r(R_i - R_0) - K_T(R_i' - R_0')]}$$

The retransmitted wave has the direction (α_T, β_T) and it comes to focus at R_i' which is not equal to the rectenna or the pilot source point. When the beam gets into focus at R_0', we can state that

$$K_r(R_i - R_0) = K_T(R_i' - R_0') \qquad (11.1.1\text{-}3)$$

It could be seen easily that this condition is the same as the one achieved by the bandwidth consideration. Since

$R_i' \neq R_i$ and $R_0' \neq R_0$, the beam has missed the rectenna. Hence we would like to add a phase to the radiated wave such that the beam will scan back to the rectenna.

11.1.2 Calculations of Phase Shifts Necessary

From Fig. 39 we can say that

$$R_i' = [(R_0')^2 + d_i^2 + 2d_i \cdot R_0']^{1/2}$$

$$= R_0' \left[1 + \left(\frac{d_i}{R_0'}\right)^2 - 2\left(\frac{d_i}{R_0'}\right) \cos \theta_T\right]^{1/2} \qquad (11.1.1\text{-}4)$$

θ_T and d_i are defined in Fig. 39. Expanding (11.1.1-4) in a power series gives

$$R_i' = R_0' - d_i \cos \theta_T + \frac{d_i^2 \sin^2 \theta_T}{2R_0'} + \frac{d_i^3 \sin^2 \theta_T \cos \theta_T}{2(R_0')^2}$$

Therefore

$$R_i' - R_0' = -d_i \cos \theta_T + \frac{d_i^2 \sin^2 \theta_T}{2R_0'} + \frac{d_i^3 \sin^2 \theta_T \cos \theta_T}{2(R_0')^2}$$

from the geometry of Fig. 39 we can say that

$$d_i \cos \theta_T = x_i \sin \alpha_T \cos \beta_T + y_i \sin \alpha_T \sin \beta_T + z_i \cos \alpha_T \qquad (11.1.1\text{-}5)$$

Using the far-field approximation,

$$R_i' - R_0' = -d_i \cos \theta_T$$

$$= -[x_i \sin \alpha_T \cos \beta_T + y_i \sin \alpha_T \sin \beta_T + z_i \cos \alpha_T]$$

Now we can rewrite the wave radiated from the antenna to be

$$Ae^{-j(K_T R_0' + \psi_s)} \sum_{i=1}^{N} \frac{W_i}{R_i} e^{+j[\phi_i - K_T(R_i' - R_0')]} \qquad (11.1.1\text{-}6)$$

where

$$\phi_i = K_r(R_i - R_0) \qquad (11.1.1\text{-}7)$$

from (11.1.1-6) we know that the wave focuses at

$$\begin{aligned}\phi_i &= K_T(R_i' - R_0') \\ &= -K_T[x_i \sin\alpha_T \cos\beta_T + y_i \sin\alpha_T \sin\beta_T + z_i \cos\alpha_T]\end{aligned} \qquad (11.1.1\text{-}8)$$

Now we want to scan the beam from (α_T, β_T) direction to (α_r, β_r) direction then the phase shift to be added to the $i^{\underline{th}}$ element would be (up to first order)

$$\Delta\phi_i = \frac{\partial\phi_i}{\partial\alpha_T}\Delta\alpha + \frac{\partial\phi_i}{\partial\beta_T}\Delta\beta \qquad (11.1.1\text{-}9)$$

Therefore

$$\begin{aligned}\Delta\phi_i = &-K_T[x_T \cos\alpha_T \cos\beta_T + y_i \cos\alpha_T \sin\beta_T - z_i \sin\alpha_T]\,\Delta\alpha \\ &+ K_T[x_i \sin\alpha_T \sin\beta_T - y_i \sin\alpha_T \cos\beta_T]\Delta\beta\end{aligned} \qquad (11.1.1\text{-}10)$$

We know that we want the beam to be directed in (α_r, β_r) direction hence

$$\phi_i + \Delta\phi_i = K_T(R_i - R_0) \qquad (11.1.1\text{-}11)$$

Therefore

$$\begin{aligned}\Delta\phi_i &= K_T(R_i - R_0) - \phi_i \\ &= K_T(R_i - R_0) - K_r(R_i - R_0) \\ &= (K_T - K_r)(R_i - R_0)\end{aligned} \qquad (11.1.1\text{-}12)$$

with far field approximation we get

$$-\Delta\phi_i = (K_T - K_r)[x_i \sin\alpha_r \cos\beta_r + y_i \sin\alpha_r \sin\beta_r + z_i \cos\alpha_r] \qquad (11.1.1\text{-}13)$$

Thus if the $i^{\underline{th}}$ element receives the phase shift $-\Delta\phi_i$ the beam will shift back to (α_r, β_r) direction. It should be noted that the beam points towards (α_r, β_r) direction but it has a different frequency than the uplink signal.

For later use we should compute $\Delta\alpha$ and $\Delta\beta$ defined in (11.1.1-10). We already know that (see Fig. 49)

$$\Delta\beta = \beta_r - \beta_T$$

Using (11.1.1-10), (11.1.1-13) and the above equation gives us $\Delta\alpha$ in terms of $\Delta\beta$

$$\Delta\alpha = \Big[\Big(1 - \frac{K_T}{K_r}\Big)\{x_i \sin\alpha_r \cos\beta_r + y_i \sin\alpha_r \sin\beta_r + z_i \cos\alpha_r\} + \{x_i \sin\alpha_T \sin\beta_T - y_i \sin\alpha_T \cos\beta_T\}\Delta\beta\Big] / [x_i \cos\alpha_T \sin\beta_T + y_i \cos\alpha_T \sin\beta_T - z_i \sin\alpha_T] \qquad (11.1.1\text{-}14)$$

Thus to compute $\Delta\alpha$ we need (α_r, β_r) as well as (α_T, β_T) once we calculate $\Delta\alpha$ and $\Delta\beta$ we have

$$\Delta\theta = [(\Delta\alpha)^2 + (\Delta\beta \sin\alpha_T)^2]^{1/2}$$

and this $\Delta\theta$ gives us the beam pointing error.

11.1.3 Effect on Pointing Due to Measurement Error in the Position

We have $\Delta\beta = \beta_r - \beta_T$ but $\Delta\alpha$ depends on the coordinates. If the coordinates with error are (x_i', y_i', z_i') then the $\Delta\alpha'$ could be obtained by replacing x_i by x_i', y_i by y_i' and z_i by z_i', $\Delta\beta$ by $\Delta\beta'$ in equation (11.1.1-14). Then

$$\Delta\theta' = [(\Delta\alpha')^2 + (\Delta\beta' \sin\alpha_T)^2]^{1/2}$$

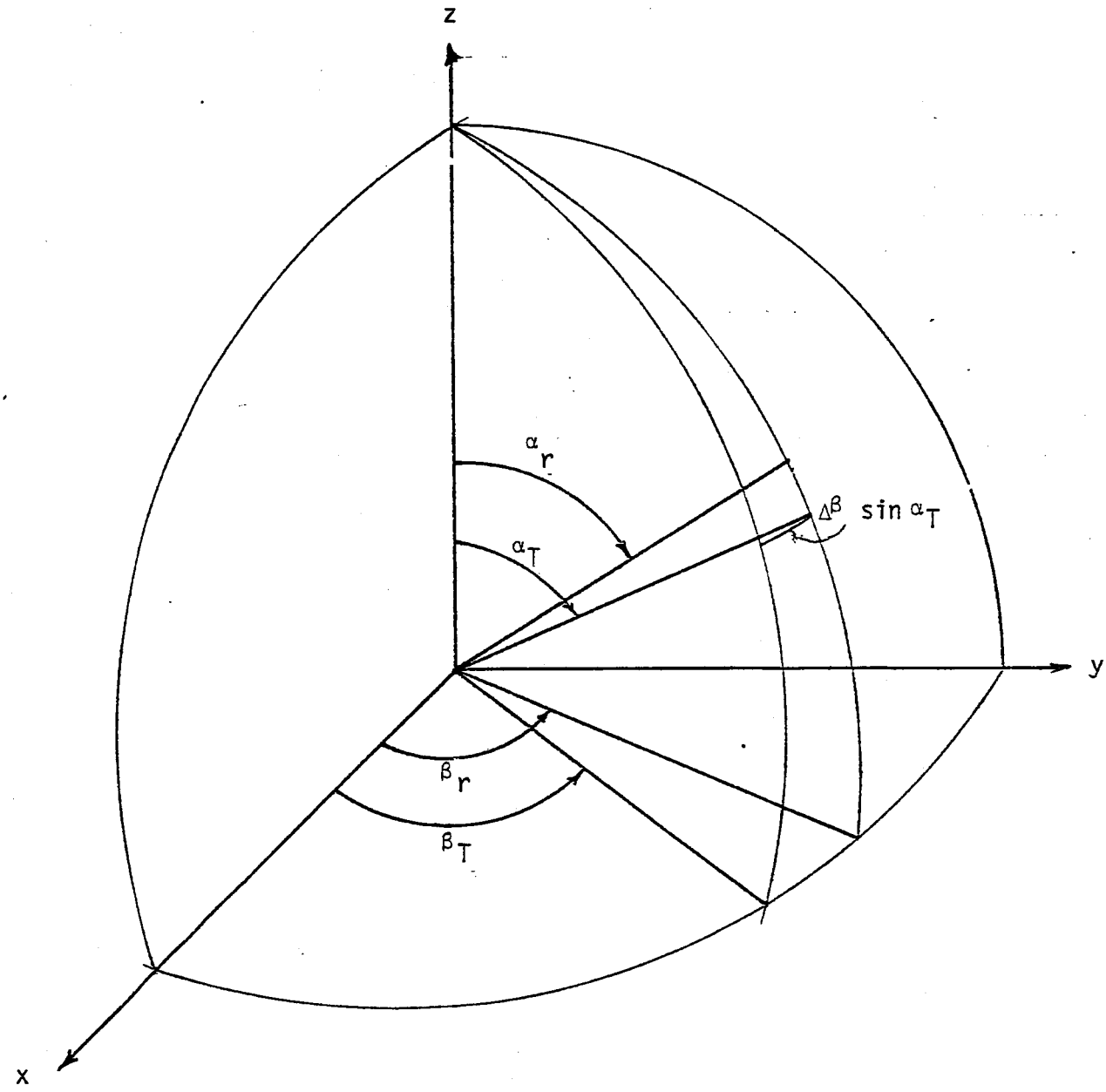

Figure 49. Scanning Geometry.

and

$$\delta\theta = \Delta\theta - \Delta\theta'$$

Figure 50 shows the amount of compensation necessary. Thus for two different frequencies we conclude that the conjugation scheme will work if proper steps are taken to avoid the effects of the uplink-downlink frequency separation.

Summarizing the above: (1) The scheme needs a conjugating circuit at each radiating element which automatically conjugates the incoming wave. (2) A correction phase is necessary to steer the beam back to the desired direction. This correction phase depends upon the position coordinates of the elements of the antenna and the incoming wave parameters. The values of α_r and β_r could perhaps be obtained, to the desired accuracy, by using a monopulse tracking system. These values of α and β, the position coordinates, and accurate values of λ_r can be used in principle to compute the phase correction required at each element.

The above concepts can be implemented as illustrated in Fig. 51. Due to the flexing of the SPS antenna, it is divided into groups of subarrays. In each subarray there are M radiating elements and, along with each radiating element, there is a power amplifier and a conjugating circuit. This conjugating circuit accepts the input from the reference distribution system of the antenna. The pilot wave received at each element is phase conjugated using the reference phase supplied to the conjugation circuit and is amplified by the power amplifier. Before this

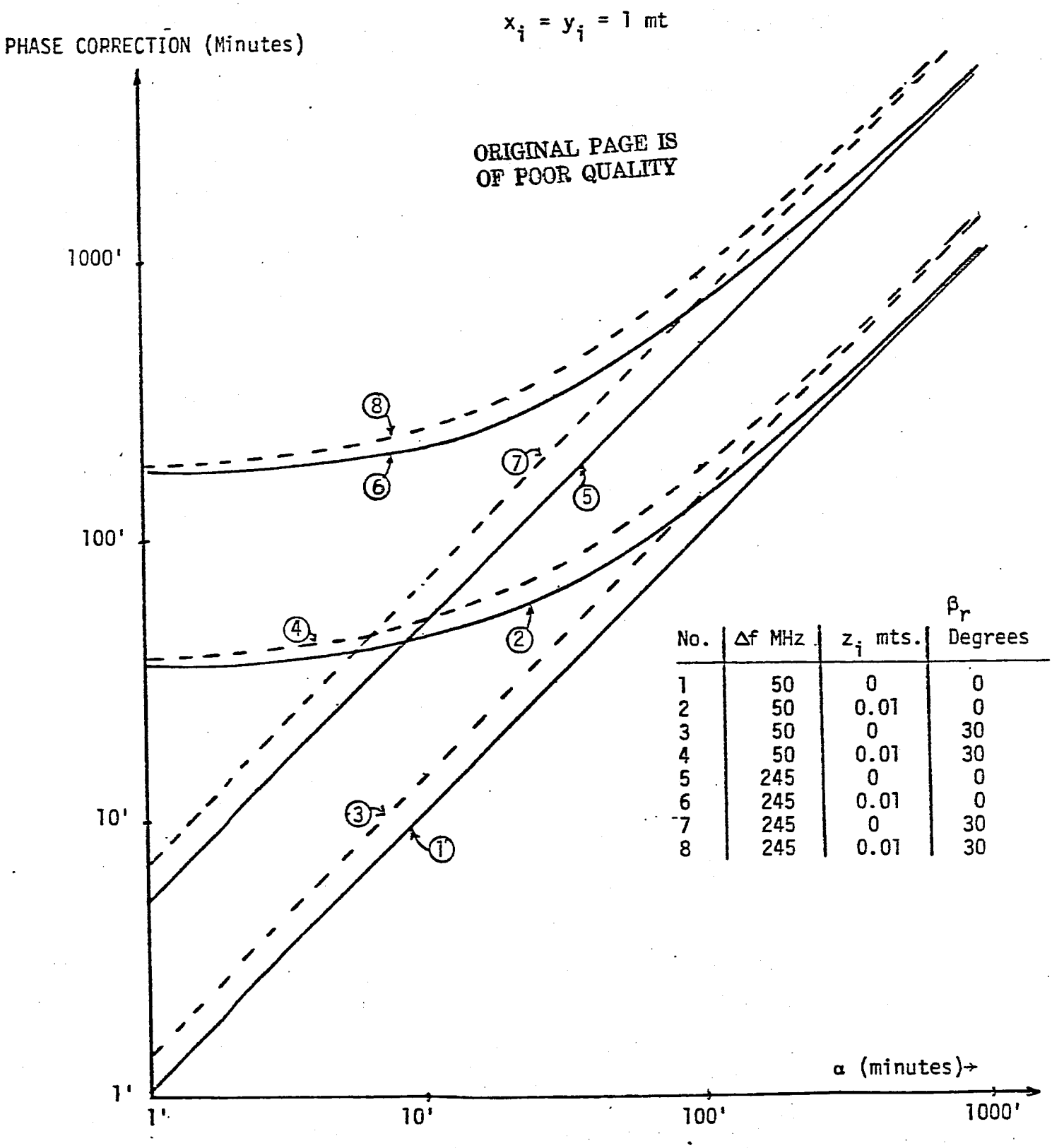

Figure 50. Phase Correction vs Angle of Incidence.

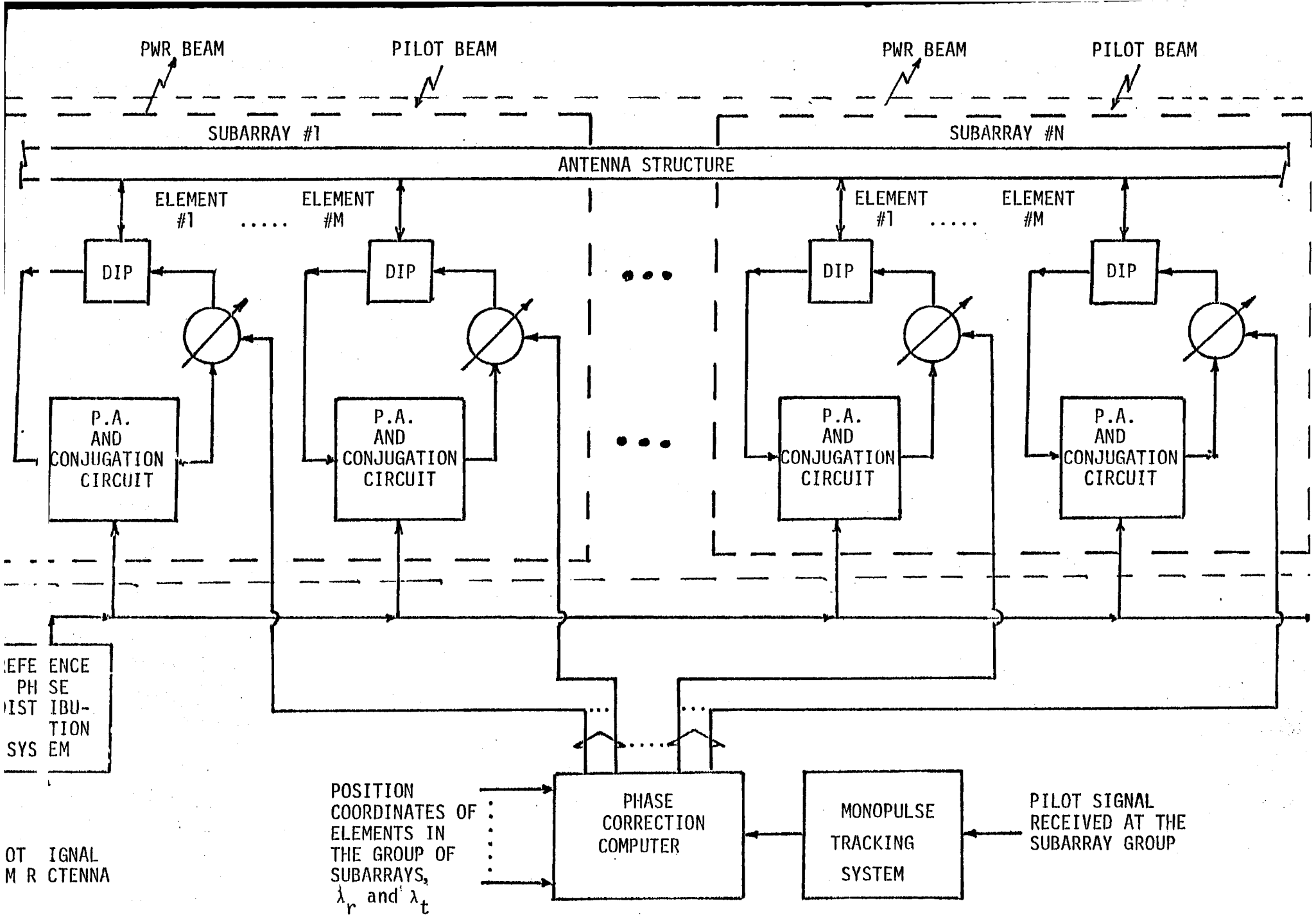

Figure 51 Beam Steering by Phase Conjugation

wave is radiated, its phase is adjusted to take care of the beam pointing error introduced by the frequency separation of the uplink signal from the downlink signal. This adjustment is done by a phase shifter which receives the phase correction term from the phase correction computer. There are two inputs to this computer: the input from the monopulse tracking system producing azimuth and elevation angles of the arriving pilot beam and the other position coordinates of all the radiating elements in the group of subarrays. This system is completely automatic in operation. The number of subarrays in the group is determined by several factors, e.g., antenna flexing, plane waves approximation of a spherical wave.

11.2 SPS Beam Forming and Steering via a Ground Station

One main disadvantage associated with the phase conjugation method is the pointing error introduced due to the uplink-downlink frequency separation requirement. Another major problem is that this method is difficult to secure (power rob) and easy to jam unless additional measures are taken.

An alternate approach to beam forming, pointing and steering is illustrated in Fig. 52. Here we see that various points in the rectenna are selected for the placement of sensors, see Figs. 52 and 53. The purpose of these sensors is to receive the power signal from the satellite. A portion of the received signal at each sensor serves as the input to the signal processor, Fig. 52. The signal processor receives two inputs. (1) The signals from sensors, and (2) the input from the Satellite Orbit Determination Computer, (SOD). The signal

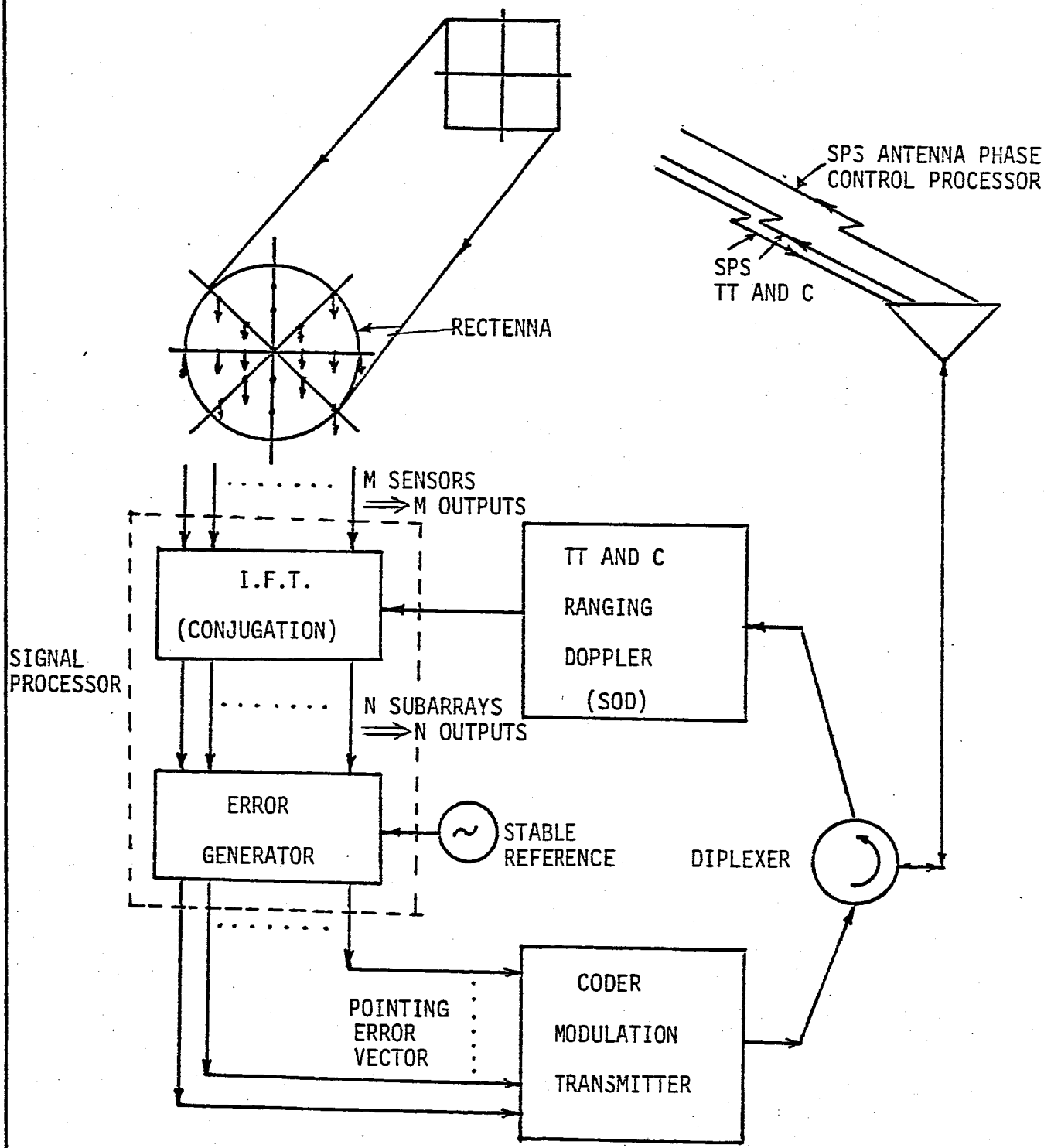

Figure 52. SPS Beam Forming and Steering via Ground Station.

Figure 53 PHASE CONTROL FROM GROUND STATION

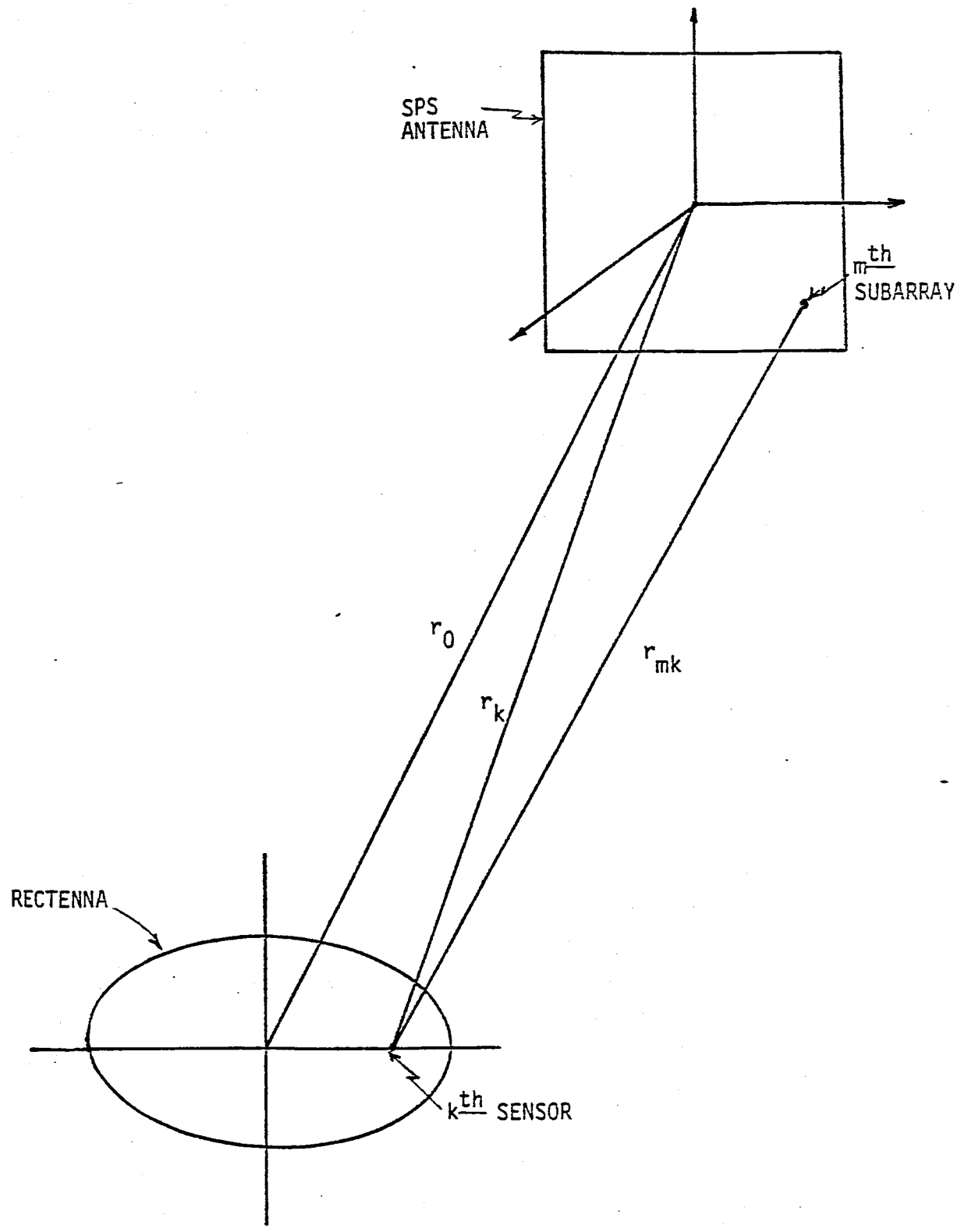

processor processes these inputs and computes the angle of arrival of the beam radiated by each subarray in the transmitting antenna. When this is compared with the desired angle of arrival, of the signal, the beam pointing error in the transmitting antenna is generated for each subarray. Thus the output of the signal processor is a vector of beam pointing errors. This error vector is transmitted to the satellite by a separate communications link, see Fig. 52. The error vector is distributed at the antenna to the proper subarray . The process of nulling the vector error signal results in focusing the subarrays radiated signals towards the center of the rectenna.

There are two approaches to evaluating the components of the beam pointing error vector. One approach is to evaluate the error components serially. This approach is illustrated in Fig. 54. The alternate approach is to evaluate the error components in parallel, see Fig. 55. While parallel processing requires more hardware in its implementation, it has the distinct advantage of producing an error vector much faster. Hence, if the medium is not sufficiently stable parallel processing may be required over that of serial processing.

One of the problems with this approach is that to start the beam pointing process, some energy has to be incident on the sensors. Hence, the transmitted beam may have to be swept back and forth over the rectenna before it hits some of the sensors. This problem could be solved by a combination of retrodirective and ground control methods. The retrodirective method will radiate the beam more or less

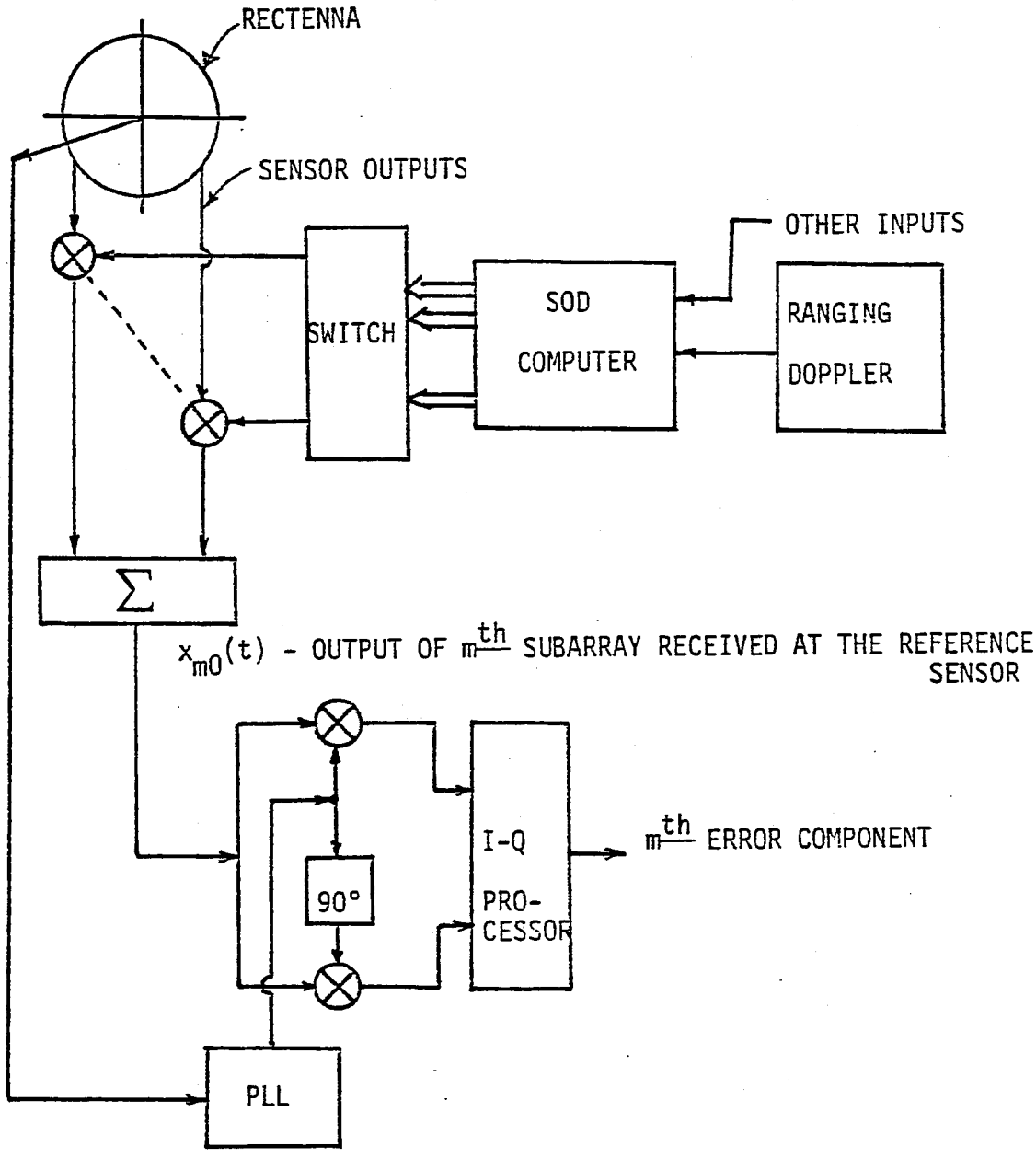

Figure 54. SPS Feedback Control Via Ground Telemetry and Command.

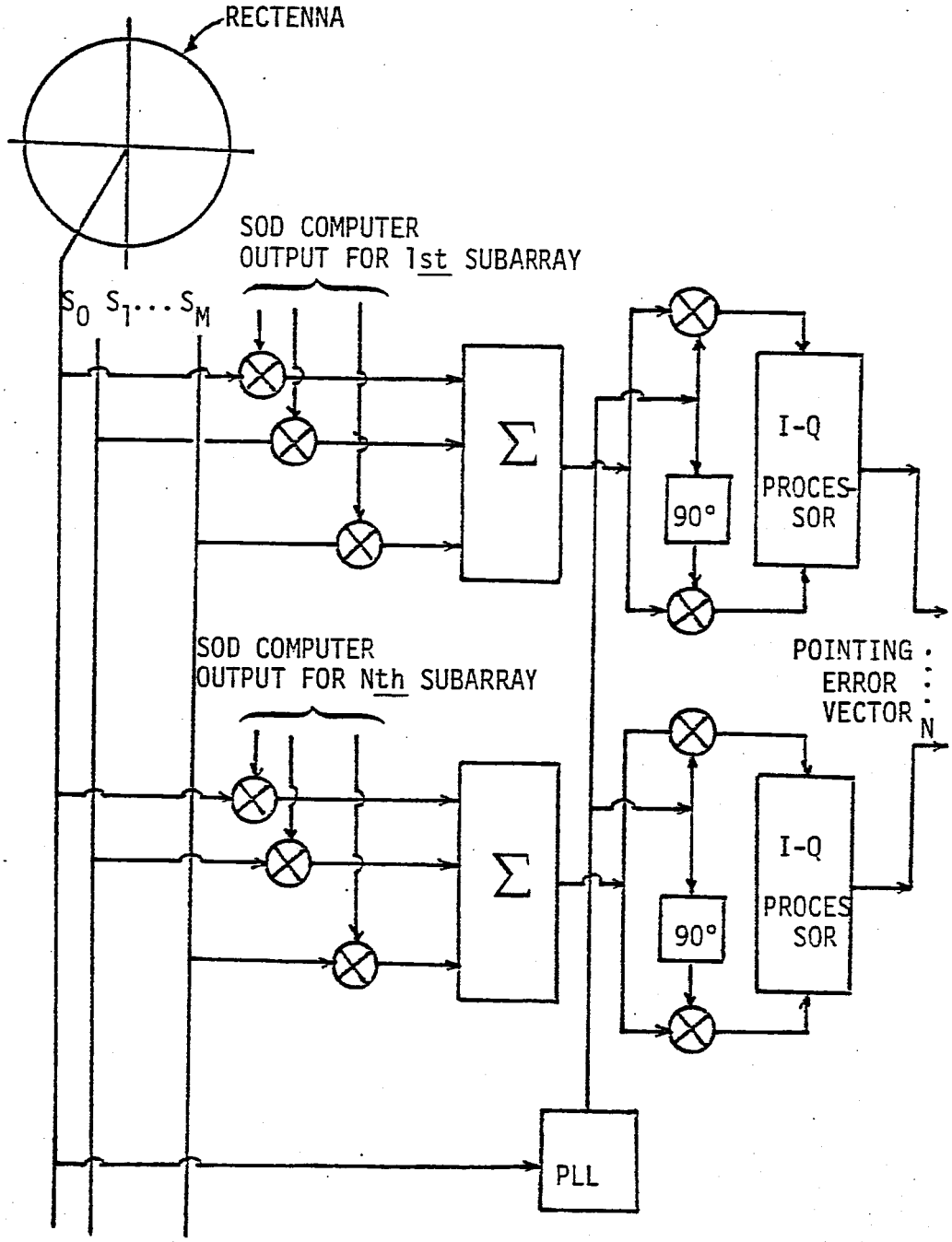

Figure 55. SPS Feedback Control via Ground Telemetry and Command.

in the direction of the pilot beam and the error correction for the frequency separation and other effects could be done by ground sensing. Figures 56 and 57 summarize the advantages and disadvantages of the retrodirective as well as the ground control scheme. Further work on understanding this method and its performance is currently under way.

Fig. 56 . ADVANTAGES AND DISADVANTAGES OF SPS RETRODIRECTION SELF FOCUSING ARRAY BY PHASE CONJUGATION

ADVANTAGES	DISADVANTAGES
●MINIMIZES SYSTEM COMPLEXITY ●PROVIDES AUTOMATIC BEAM FORMING AND STEERING ●DIFFICULT FOR LIGHTNING BOLT TO DESTROY	●ELABORATE PHASE CONTROL AND TRANSFER SYSTEM IS REQUIRED TO SUPPLY A CONSTANT PHASE TO THE RADIATING ELEMENTS ●SEPARATE CIRCUITS APPEAR TO BE NECESSARY FOR PA PHASING AND FOR THE CONJUGATION PROCESS NEEDED FOR BEAM STEERING ●DIFFICULT TO SECURE AND POWER ROBBING

Fig. 57.. ADVANTAGES AND DISADVANTAGES OF FEEDBACK VIA GROUND TELEMETRY AND COMMAND SYSTEM

ADVANTAGES	DISADVANTAGES
●SIGNAL PROCESSING TRANSFERRED TO GROUND ●CONJUGATION CIRCUITS ARE NOT NECESSARY ●SYSTEM CAN BE MADE SECURE ●REDUCED SATELLITE HARDWARE COMPLEXITY	●REQUIRES ACCURATE RANGE AND RANGE RATE MEASUREMENTS TO SATELLITE SUBARRAYS ●REQUIRES ERROR DISTRIBUTION AND PHASE CORRECTION SYSTEM ON THE SATELLITE ANTENNA ●REQUIRES LARGE NUMBER OF SENSORS TO ESTABLISH PHASE REFERENCE

12.0 POWER TRANSMISSION EFFICIENCY CALCULATION

Since the power transmission efficinecy is directly related to the beam forming and the beam pointing ability of the antenna, there are two different effects that degrade the power transmission efficiency. They are:

(1) The random effects:

  (a) Temperature and antenna flexing induced fluctuations in the path delays of the reference phase distribution system.

  (b) Power amplifier instabilities.

  (c) Instabilities associated with the phase control centers used in the reference phase distribution system.

(2) The nonrandom effects:

  (a) Uncompensated path delays in the reference phase distribution system.

  (b) Beam squinting due to frequency separation of the uplink and downlink signals.

The combination of random effects has a mean value and a variance. This mean value of the random effects combined with the nonrandom effects produces the beam pointing error. In what follows, we will investigate the effect of the random and nonrandom parameters described above on the power transmission efficiency.

12.1 Problem Formulation

We consider the transmitting antenna to be a planar array of radiating elements in the xy plane. There will be 2N+1 rows of elements, each row parallel to y axis with a common spacing

is d_x units between the rows. Each row will contain 2N+1 radiating elements whose common spacing is d_y units. Thus any element position can be described by (m,n) where $-N \leq m \leq N$ and $-N \leq n \leq N$. The normalized current in the $(m,n)^{th}$ element will be denoted by $I_{mn} = I_m \cdot I_n$.

The complex radiation pattern for this antenna in the absence of errors (random or otherwise) described above is obtained as

$$f(\alpha,\beta) = \sum_{m,n=-N}^{N} I_m \cdot I_n e^{jK[md_x \sin\alpha\cos\beta + nd_y \sin\alpha\sin\beta]} \quad (1)$$

where α and β are the polar coordinates of the point under consideration and $\sin\alpha\cos\beta$ and $\sin\alpha\sin\beta$ are the projections of this point onto the equitorial plane. The factor in the exponent in equation (1) is due to the position of the radiating element, better known as the array factor while the remaining terms form the element factor of the array.

The antenna will be phased up to make the main lobe of the pattern point in the direction of the rectenna (conjugation scheme). The phasing system will introduce the random and nonrandom errors described above. As a result of conjugation and the mean part of random errors and the deterministic (nonrandom) errors, the beam will point in the direction (θ_0,ϕ_0) in polar coordinates. Besides squinting the beam off the broadside, the random effects introduce a phase jitter on the beam. Considering these effects, (1) becomes

$$f(\alpha,\beta) = \sum_{m,n=-N}^{N} I_m \cdot I_n e^{j(\delta\phi_m + \delta\phi_n)} e^{jK[md_x(\sin\alpha\cos\beta - \sin\theta_0\cos\phi_0) + nd_y(\sin\alpha\sin\beta - \sin\theta_0\sin\phi_0)]} \quad (2)$$

where $\delta\phi_m$ and $\delta\phi_n$ are the zero mean random variables. We also assume that $\delta\phi_m$ and $\delta\phi_n$ are independent random variables with normal distribution. We are basically interested in the power transmitted by the beam to the rectenna hence it would be quite useful to obtain the average power pattern (APP) for the antenna.

$$\text{APP} \triangleq E[f(\alpha,\beta)\cdot f^*(\alpha,\beta)] = P(\alpha,\beta) \tag{3}$$

where $f^*(\alpha,\beta)$ is the complex conjugate of the radiation pattern $f(\alpha,\beta)$ and the expectation operation is carried out over the random variables $\delta\phi_m$ and $\delta\phi_n$. Since $\delta\phi_m$ and $\delta\phi_n$ are assumed Gaussian random variables,

$$E[e^{j\delta\phi_m}] = e^{-\sigma_x^2} \quad \forall m$$

and

$$E[e^{j\delta\phi_n}] = e^{-\sigma_y^2} \quad \forall n \tag{4}$$

The above is true because all the $\delta\phi_m$ ($\delta\phi_n$) come from the same population with mean 0 and variance σ_x^2 (σ_y^2). Using equations (1)-(4) we obtain an equation for $P(\alpha,\beta)$.

$$P(\alpha,\beta) = \sum_{m,n=-N}^{N} I_m^2 \cdot I_n^2 + e^{-\sigma_x^2}\left\{\sum_{n=-N}^{N} I_n^2\right\}\left\{\sum_{\substack{m,m'=-N \\ m\neq m'}}^{N} I_m \cdot I_{m'} e^{jKd_x(m-m')(\sin\alpha\cos\beta - \sin\theta_0\cos\phi_0)}\right\}$$

$$+ e^{-\sigma_y^2}\left\{\sum_{m=-N}^{N} I_m^2\right\}\left\{\sum_{\substack{n,n'=-N \\ n\neq n'}}^{N} I_n \cdot I_{n'} e^{jKd_y(n-n')\sin\alpha\sin\beta - \sin\theta_0\sin\phi_0)}\right\}$$

$$+ e^{-(\sigma_x^2+\sigma_y^2)}\left\{\sum_{\substack{m,m'=-N \\ m\neq m'}}^{N} I_m \cdot I_{m'} e^{jKd_x(m-m')(\sin\alpha\cos\beta - \sin\theta_0\cos\phi_0)}\right\}$$

$$\left\{ \sum_{\substack{n,n'=-N \\ n\neq n'}}^{N} \sum I_n \cdot I_{n'} e^{jKd_y(n-n')(\sin\alpha \sin\beta - \sin\theta_0 \sin\phi_0)} \right\} \tag{5}$$

Thus the power pattern $P(\alpha,\beta)$ is a function of α and β. To obtain the power transmitted to the rectenna, $P(\alpha,\beta)$ should be integrated over α and β covering the rectenna region. θ_0 and ϕ_0, the beam pointing direction is the parameter. The main beam power transmission efficinecy is defined as follows:

$$\text{Main Beam Power Transmission Efficiency} = \frac{\iint_{\text{Rectenna}} P(\alpha,\beta)\overline{ds}}{\iint_{\text{Rectenna}} P'(\alpha,\beta)\overline{ds}} \tag{6}$$

where $P'(\alpha,\beta)$ is the $P(\alpha,\beta)$ with no errors (random or otherwise), i.e., with the beam ideally pointed towards the rectenna.

Numerical computation techniques were employed to evaluate equation (6). In the computations carried out, it was assumed that the satellite is directly above the rectenna center, i.e., the antenna sees the rectenna as a perfect circle. Thus ϕ_0 can be set to zero because the integral value is independent of ϕ_0. The value of θ_0 was incremented in steps of 20% of θ_n, where

$$\theta_n = \tan^{-1}\left[\frac{\text{Rectenna Radius}}{\text{Distance Between Antenna and Rectenna}}\right]$$

This computation also incorporates the effect of 10 dB taper on the currents feeding the radiating elements. Results of this computation is shown in Fig. 58. As this figure shows, even with

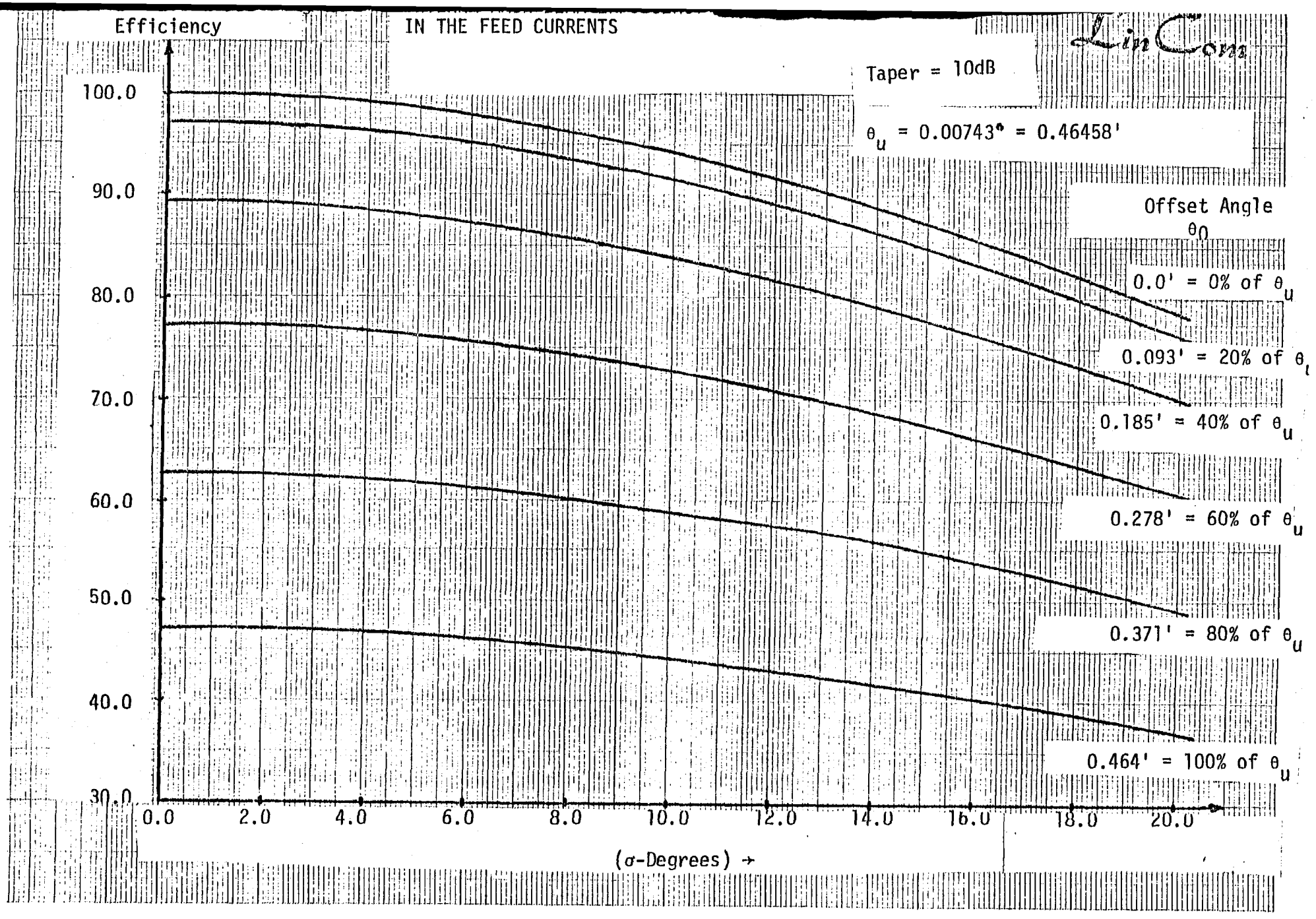
Efficiency
IN THE FEED CURRENTS
Lin Com
Taper = 10dB
θ_u = 0.00743° = 0.46458'
Offset Angle
θ_0
0.0' = 0% of θ_u
0.093' = 20% of θ_u
0.185' = 40% of θ_u
0.278' = 60% of θ_u
0.371' = 80% of θ_u
0.464' = 100% of θ_u
100.0
90.0
80.0
70.0
60.0
50.0
40.0
30.0
0.0
2.0
4.0
6.0
8.0
10.0
12.0
14.0
16.0
18.0
20.0
(σ-Degrees) →

$\phi_0 = 0$, i.e., perfectly aligned beam, to obtain the power transmission efficiency of 96%, the phase jitter introduced by the phasing system should be below 6 degrees.

One important thing to note in this computation is that we have assumed that the satellite sees the rectenna as a perfect circle, i.e., antenna is directly above the rectenna center. When this is not true, the antenna sees the rectenna as an ellipse, and in such a case the efficiency depends on ϕ_0. Current work is extending the above results to include this case.

12.2 Two Frequency Technique for Retrofire Arrays

This is an alternate technique for pointing a retrofire array. Ideally, a retrofire or Van Atta array returns a signal in the same direction as any signal incident on the array. In practice, heterodyning techniques are used to provide frequency separation between the incident signal and the returned signal. Unfortunately this frequency separation introduces a pointing error for signals that are not exactly broadside incident on the array, i.e., the returned signal direction is not exactly equal to the incident signal direction. This problem may be circumvented by a two frequency technique. This technique has the advantage that frequency isolation is provided between the uplink and return link yet the return signal direction is exactly equal to the incident signal direction. The disadvantage is an increase in complexity since more hardware is required at each antenna. Since the circuit is the same for each antenna in the array the additional hardware may be built using film technologies resulting in modest cost increase. Probably the main consideration is reliability since increased complexity necessarily implies a higher likelihood of failure. The two frequency method can be implemented simply and current work is under way to exploit this aspect of the system.

REFERENCES

[1] Lindsey, W. C., Synchronization Systems in Communication and Control, Prentice-Hall, 1972, Englewood Cliffs, N.J.

[2] Hansen, R. C., Microwave Scanning Antennas, Parts I and III, Academic Press, New York, 1966.

[3] Skolnik, M. I., Radar Handbook, McGraw-Hill, New York, 1970.

[4] Titschmarsh, F. C., Introduction to the Theory of Fourier Integrals, Oxford University Press, New York, 1937.

Page Intentionally Left Blank

Page Intentionally Left Blank